PART I
SYNTHESIS AND CHARACTERIZATION

PART I

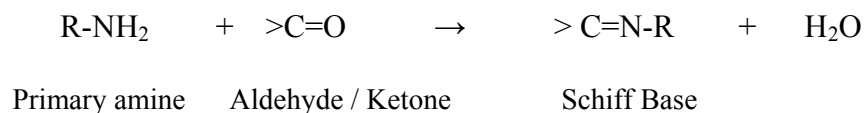# SYNTHESIS AND CHARACTERIZATION

CHAPTER 1

INTRODUCTION AND REVIEW

Coordination chemistry is the rapid growing branch of chemistry and deals with the interaction between the metal and ligand. It was Werner, a Swiss chemist who first recognized such a class of compounds and awarded Nobel Prize in chemistry in 1913 for his invaluable contribution to coordination chemistry. Metal complexes possess wide variety of applications in pharmaceutical, agricultural and various industrial fields. Cis–platin is a platinum based chelate and acts as a well known anti cancer drug due to the high DNA binding capacity of the metal chelate. Oxygen has inevitable role in the life of every living organism and it is carried by haemoglobin present in blood, which is an iron complex. Right from textile to petroleum industry numerous metal chelates have got wide range of applications.

Schiff Bases

Among the metal chelates studied, Schiff base complexes have got great attention. A Schiff base is a compound with a functional group that consists of an azomethine linkage or an imino group. It is formed by the condensation reaction between an aldehyde or a ketone with a primary amino group as shown below.

$$\text{R-NH}_2 \quad + \quad >\text{C=O} \quad \rightarrow \quad >\text{C=N-R} \quad + \quad \text{H}_2\text{O}$$

Primary amine   Aldehyde / Ketone   Schiff Base

where R may be an alkyl or aryl group. Schiff bases possessing aryl groups are easier to synthesize due to their extra stability through conjugation effect. Comparatively less stable alkyl Schiff bases may polymerize or decompose to their parent compounds in the presence of moisture. The formation of Schiff base

from an aldehyde or ketone is a reversible process and takes place generally in the presence of acidic or basic or neutral media. In the first part of the mechanism, the amine reacts with the aldehyde or ketone to give an unstable addition compound called carbinolamine. The carbinolamine loses water by either acid or base catalyzed pathways. In the second step carbinolamine undergoes acid catalyzed dehydration. The second step is the rate determining step of the process which is catalyzed by acid. But too much acid concentration will adversely affect the nucleophilicity of amine and hence the synthesis is to be best carried out in mild acidic condition. Many Schiff bases may be hydrolyzed back to their parent compounds in the presence of acid or base. In some cases it is better to remove the water formed during the reaction by distillation using azeotrope forming solvent [1].

In most cases, especially the condensation between the aromatic aldehyde or ketones with various amines are not reversible and the resultant Schiff bases can be easily separated from the reaction mixture. The mechanism for the formation of Schiff base is depicted in Figure 1.1.
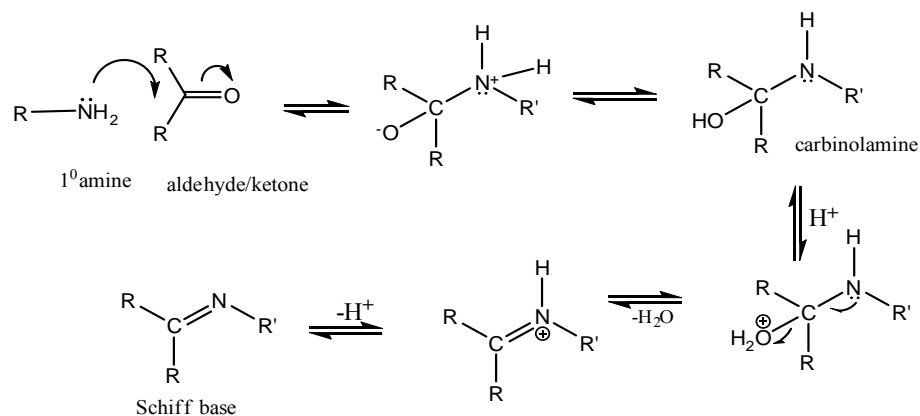
Figure 1.1 Mechanism of Schiff base formation

The name Schiff base is given to these classes of compounds after the German chemist Hugo Schiff (1864). Schiff bases are very popular in coordination chemistry due to their potential chelating ability to the metal ions through azomethine moiety. A variety of methods including direct synthesis, template methods, microwave assisted synthesis etc were developed by scientists for the synthesis of Schiff bases [2].

The amazing capacity of several Schiff base molecules in participating chelation process is due to the easiness of providing the lone pair of electron on nitrogen atom which in turn arises due to the low electronegative nature of nitrogen atom. Metal chelates having five or six membered ring system acquires high stability. The stability of metal chelates depends on the strength of the azomethine linkage, basicity of the imino group and sterric factors due to the other groups present in the ligand. Because of the relative easiness of preparation, synthetic flexibility and the peculiar binding nature of the azomethine linkage make the Schiff bases excellent chelating molecules [3]. Schiff bases and their metal chelates can be synthesized by different ways. Important methods are discussed below.

1) *Direct synthesis*

This method involves the condensation reaction between carbonyl compound and amino compound in alcohol or a mixture of alcohol and water. Azeotropic distillation followed by the treatment with molecular sieves ensure the complete removal of water molecules from the reaction mixture [4,5]. Dehydrating solvents such as tetramethyl orthosilicate or trimethyl orthoformate can also be used for

the removal of water [6,7]. The synthesized Schiff base can be separated and purified by suitable techniques. The purified Schiff base is then allow to react with the metal salts in aqueous or alcoholic medium to obtain chelates. The main advantage of this method is that the minimization of impurities during the metal chelate synthesis.

It is clear from the mechanism of formation of Schiff bases that the efficiency of direct condensation involves the presence of highly electrophilic carbonyls and strongly nucleophilic amino compounds, which can be accelerated by the use of compounds that act as Brönsted-Lowry or Lewis acids, to activate the carbonyl group, accelerating the nucleophilic attack by amines and dehydrate the system by removing water. Brönsted-Lowry or Lewis acids used for the synthesis of Schiff bases include $ZnCl_2$, $TiCl_4$, $Ti(OR)_4$, alumina, H_2SO_4, $NaHCO_3$, $MgSO_4$, $Mg(ClO_4)_2$, CH_3COOH, $Er(OTf)_3$, P_2O_5/Al_2O_3 and HCl [8-16].

2) *In situ method*

This method is employed only if the recovery of the Schiff base from the reaction mixture is tedious. At first the parent aldehydes or ketone is allow to react. After the completion of the reaction, metal salts in aqueous or alcoholic solution are added and reflux the mixture for a particular period.

2) *Template synthesis*:

In situ one-pot template condensation reactions lie at the heart of macrocyclic chemistry. Therefore, template reactions have been widely used for the synthesis of macrocyclic complexes, in which transition metal ions are generally used as the

template agent [17-19]. For instance, D. Singh et al have synthesized a novel series of complexes of the type $M(C_{28}H_{24}N_4)X_2]$, where $M = Co(II)$, $Ni(II)$, $Cu(II)$, $Zn(II)$ and $Cd(II)$, $X = Cl^-$, NO_3^-, CH_3COO^- and $C_{28}H_{24}N_4$ corresponds to the tetradentate macrocyclic ligand, were synthesized by template condensation of 1,8-diaminonaphthalene and diacetyl in the presence of divalent metal salts in methanolic medium [20]. The reaction pathway is depicted in Figure 1.2.
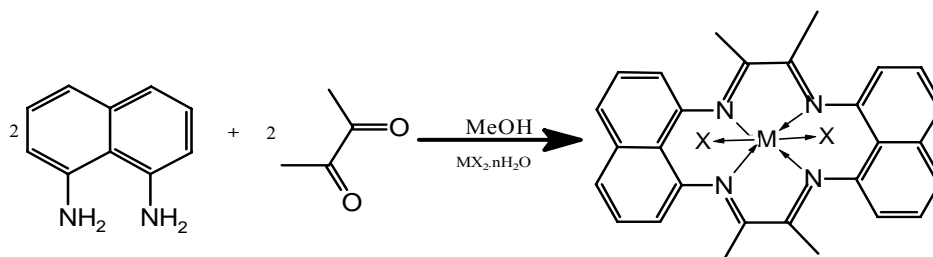

Fig. 1.2 Example for template synthesis

Applications of Schiff Bases and Their Metal Chelates

Many Schiff base and its metal chelates possess wide variety of application in the pharmaceutical field, catalysis reactions, analytical field and anti corrosion compounds. The subsequent paragraphs describe few examples.

Schiff base ligands containing various donor atoms (like N, O, S, etc.) show broad biological activities and are of special interest due to variety of ways in which they can bond to metal ions. It is known that the existence of metal ions bonded to biologically active compounds may enhance their activities [21]. Schiff bases derived from sulfane thiadiazole and salicyladehyde and thiophene-2-aldehyde and their metal chelates exhibit toxicities against insects [22-23]. Zhu et al have reported that fluorination of the aldehyde part of the Schiff base enhance activity against insects [24]. Many thiazole, benzothiazole, pyran and quinazole

derived Schiff bases posses effective antifungal activity and the efficiency is enhanced when groups such as methoxy, halogen and naphthyl are attached [25-27].

Several Schiff bases derived from furan and their transition metal chelates found to be very efficient against fungi such as *A. niger, A. solani* etc [28,29]. Large number of heterocyclic and non heterocyclic Schiff bases and their metal complexes display antibacterial activity. Schiff bases derived from furfural, pyridine aldehydes, salicylaldehyde, thiazole, amino acids, taurine, glucosamine, aminopyridine, aminothiazole, pyrazolone, indole and benzaldehyde and their metal chelates are found to be efficient inhibitors towards the growth of different bacteria [30-41]. A lot of Schiff bases acquire anti-inflammatory, allergic inhibitors reducing activity, radical scavenging and anti-oxidative action. Thiazole and furan based Schiff base and their metal chelates display analgesic activity [42-45]. Several Schiff bases exhibit anti-cancer activity and sometimes the activity enhanced upon complexation with transition metal ions. It is reported that Schiff bases derived from quinoline, pyridine, nitrophenols, vanillin and benzene sulfonanilide, anthracene carboxaldehyde and their metal complexes show significant anti-cancer activity [46-50].

Many Schiff bases containing aromatic ring system and their metal chelates are found to catalyze various reactions such as oxygenation, hydrolysis, reduction and decomposition reactions [51,52]. It was reported by S. Forster et al [53] that some cobalt Schiff base complexes can catalyze the oxidation of anilines with tert-butyl hydroperoxide to give nitrobenzenes. A selective chromogenic

chemosensor was designed by M. X. Liu et al using a novel 5-mercapto triazole derived Schiff base. The sensing of Cu^{2+} by this sensor was found to be reversible, with the Cu^{2+-}induced color being lost upon addition of EDTA [54].

Copper(II) and iron(III) chelates were synthesized from 4-formyl-3-hydroxy benzamidine or 3-formyl-4-hydroxy benzamidine and various L- or D-amino acids and their inhibitory activities for bovine alpha-thrombin were explored by E. Toyota et al [55]. Amine terminated liquid natural rubber(ATNR) on reaction with glyoxal yield poly Schiff base [56], which improves aging resistance of rubber. Organocobalt complexes with tridentate Schiff base act as initiator of emulsion polymerization and co-polymerization of dienyl and vinyl monomers [57]. It has been reported that Zinc(II) complexes with Schiff bases type chelating ligands can be used as an effective emitting layer [58]. Amino acid Schiff base complexes derived from 2-hydroxy-1-naphthaldehydes are important due to their use as radiotracers in nuclear medicine [59]. Many organic molecules containing hetero atoms and compounds containing azomethine linkage (C=N) were reported to act as good corrosion inhibitors for carbon steel, aluminum, copper and zinc in acidic media. A detailed survey regarding the corrosion inhibition capacity of the Schiff bases is given in Part II.

Schiff Bases Derived From Pyridine and Their Metal Chelates- A Review

Novel potential Schiff bases derived from acetylpyridine and their transition metal chelates have been synthesized by various researchers and characterized. Some of them have got properties including pharmaceutical agents. A series of Schiff bases derived from 2-acetylpyridne and 4-(2-

aminoethyl)morpholine, and 4-(2-aminoethyl)piperazine and their transition metal complexes were synthesized and characterized by N. S. Gwaram et al using elemental analysis, NMR, FT-IR and UV-Vis spectral studies. Zn (II) complex displayed square pyramidal geometry while Cd(II) complexes exhibited polymeric structure. Ni(II) complexes possessed an octahedral geometry [60].

R.H. Prince and D. A. Stotter [61] reported of a series of metal(II) complexes of a quinquidentate ligand produced in situ or by complexation with the Schiff-base, condensation-product of two moles of 2-acetylpyridine with 3,3′-iminobispropylamine. From the *in situ* synthesis of the Ni(II) compound only a quadridentate, mono-Schiff-base complex with coordinated acetyl-pyridine is isolable. Analytical data, infra-red studies, magnetic moments and solution-spectra of the complexes were described, and the interconversion of the two types of Ni(II) complex investigated. Binuclear Schiff base complexes derived from glycine (Gly) and 3-acetylpyridine (3-APy) in the presence of $M(OAc)_2$ [M = Co(II), Ni(II), Cu(II), Zn(II) and Cd(II)] have been synthesized by N. A. Nawar [62]. The role of pH in promoting the condensation of glycine and 3-acetylpyridine, as well as the substitution of acetates by hydroxide ion, has been discussed. The reaction of glycine with 3-acetylpyridine in the presence of MCl_2 [M = Co(II) and Ni(II)] and MCl_3 [M = Fe(III) and Cr(III)] yields mono- and/or binuclear complexes containing both of glycine and 3-acetylpyridine without condensation. Both types of complex were isolated and characterized by chemical analysis, conductance, spectral, magnetic and thermal measurements.

Recently, N. M. Hosny et al [63] synthesized metal chelates of Cu(II), Co(II), Ni(II), Cr(III) and Fe(III) chlorides with a Schiff base ligand derived from 2-acetylpyridine and leucine. The IR spectra show that the Schiff base can act as a neutral tridentate ligand to Cu(II), Co(II) and Ni(II) through the pyridyl nitrogen, azomethine nitrogen and carbonyl oxygen. Another mode of chelation has been established that the Schiff base can act as mononegative tridentate ligand to Fe(III) and Cr(III) through pyridyl nitrogen, azomethine nitrogen and the carbonyl oxygen after the displacement of hydrogen from hydroxyl group. The synthesized metal chelates were subjected to elemental, spectral, thermal, magnetic and molar conductance studies. The results suggest that Co(II) and Ni(II) metal chelates posses tetrahedral geometry while Fe(III) and Cr(III) acquire octahedral geometry. A square planar geometry was assigned to Cu(II) complex. Semi empirical calculation of the complexes was also performed.

In 2007, N. M. Hosny [64] synthesized Schiff-base complexes $[ML(H_2O)_2(Ac)]nH_2O$ (M=Co(II), Ni(II) and Zn(II); L= novel heterocyclic Schiff-base ligand derived from 2-acetylpyridine and alanine and n= 1–3/2) were synthesized and characterized by elemental analysis, spectral (FTIR, UV/Vis, MS, [1]Hnmr), thermal (TGA), conductance and magnetic moment measurements. The results suggest octahedral geometry for all the isolated complexes. IR spectra show that the ligand coordinates to the metal ions as mononegative tridentate through pyridyl nitrogen, azomethine nitrogen and carboxylate oxygen after deprotonation of the hydroxyl group. Semi-empirical calculations PM3 and AM1

have been used to study the molecular geometry and the harmonic vibrational spectra to assist the experimental assignments of the complexes.

A new Cd(II) complex with a tridentate Schiff base derivative of gallic hydrazid with 2-acetylpyridine has been prepared by A. A. Alhadi [65]. The structure of the ligand 3,4,5-trihydroxybenzoic acid[1-(pyridyl)-ethylidene]hydrazone (GAPy) was confirmed using the X-ray structure analysis. The elemental analysis, FTIR, UV-Vis, [1]Hnmr spectral studies and thermal analysis indicate that the Schiff base ligand GAPy is a tridentate ligand which is coordinated with the Cd(II) complex through N, N and O atoms. They confirm that acetate ion is a bidentate ligand which is coordinated with the metal ion through two O atoms. A series of new Zn(II) complexes of 2-acetylpyridine thiosemicarbazone/semicarbazone Schiff base complexes have been synthesized and characterized by elemental analysis, IR, electronic and ^{1}H NMR spectral studies by R. Manikandan et al [66]. The thiosemicarbazone/semicarbazone ligand coordinates to zinc as tridentate N, N and S/O donors. Based on the analytical and spectral results, tetrahedral geometry has been tentatively proposed by them for all the complexes.

V. R. Souza [67] reported the synthesis and spectroscopic/electrochemical properties of iron(II) complexes of polydentate Schiff bases generated from 2-acetylpyridine and 1,3-diaminopropane, 2-acetylpyrazine and 1,3-diaminopropane, and from 2-acetylpyridine and L-histidine. The complexes exhibit bis(diimine) iron(II) chromophores in association with pyrazine, pyridine or imidazole groups displaying contrasting pi-acceptor

properties. In spite of their open geometry, their properties are much closer to those of macrocyclic tetraimineiron(II) complexes. An electrochemical/spectroscopic correlation between E degrees (FeIII/II) and the energies of the lowest MLCT band has been observed, reflecting the stabilization of the HOMO levels as a consequence of the increasing backbonding effects in the series of compounds. They also reported the Mössbauer data which confirm the similarities in their electronic structure, as deduced from the spectroscopic and theoretical data.

[Cu(2AcPh)Cl]2H_2O, [Cu(2AcpClPh)Cl]2H_2O, [Cu(2AcpNO$_2$Ph)Cl], [Cu(2BzPh)Cl], [Cu(2BzpClPh)Cl] and [Cu(2BzpNO$_2$Ph)Cl] complexes were synthesized and characterized by A. Angel et al [68], with 2-acetylpyridine-phenylhydrazone (H$_2$AcPh), 2-acetylpyridine-para-chloro-phenylhydrazone (H$_2$AcpClPh), 2-acetylpyridine -para-nitro-phenylhydrazone (H$_2$AcpNO$_2$Ph), 2-benzoylpyridine-phenylhydrazone(H$_2$BzPh), 2-benzoylpyridineparachloro-phenyl hydrazone (H$_2$BzpClPh) and 2-benzoylpyridine-para-nitro-phenylhydrazone (H$_2$BzpNO2Ph) .

Schiff Bases Derived From Furan-2-Aldehyde and Thiophen-2-Aldehyde and Their Metal Chelates - A Review

Many researchers have synthesized and characterized Schiff bases derived from furan-2-aldehyde and thiophene-2-aldehyde. The chelating ability of the newly synthesized Schiff bases was exploited and different transition chelates were prepared and characterized.

Synthesis and characterization of some thiocarbohydrazone Schiff bases derived from pyrole, thiophene and furan carbaldehyde and their complexes with

Cu(II), Ni(II), Zn(II), Co(II) and Fe(II) were done by F. Esmadi et al [69]. The prepared Schiff bases are bis(pyrrole-2-carboxaldehyde)thiocarbohydrazone (Pytch), bis(thiophene-2-carboxaldehyde)thiocarbohydrazone (Thtch) and bis(furfuralthiocarbohydrazone (Futch). They found that Futch ligand produced tetracoordinate complexes of the general formual [MLCl$_2$] where they act as neutral bidentates bonding through the two imine nitrogens. Thtch ligand acted as neutral bidentate producing a tetracoordinate complex of the formula [Fe(Thtch)Cl$_2$] or as monobasic tridentate producing tetracoordinate [Zn(Thtch)Cl] complex or as monobasic bidentate forming tetracoordinate [M(Thtch)$_2$] complexes where M = Co, Ni and Cu.

Complexes of Co(II), Ni(II), Cu(II), Zn(II) and Mn(II) of a Schiff base derived from o-phenyldiamine and furfural were synthesized and characterized by F. Dianzhong et al [70] using various physical and chemical methods. Electronic spectra, magnetic moment studies, EPR and XPS studies revealed that these metal chelates have octahedral geometry. The non-electrolytic nature of the complexes was verified by the molar conductance measurements.

In 2009, P. Mittal et al [71] have synthesized and characterized novel Schiff bases derived from furan-2-aldehyde and thiophene-2-aldehyde with vinyl aniline. The chelating ability of these Schiff bases were screened by preparing the transition metal chelates of metal ions such as Co(II), Ni(II), Cu(II) and Mn(II). They verified the octahedral geometry of these complexes with various physico-chemical methods. The complexes were also screened for their antimicrobial activity.

New two nickel(II) and copper(II) complexes of two Schiff base ligands formed by condensation of furfural and benzil with S-benzyldithiocarbazate have been synthesized and characterized by elemental analysis, magnetic and spectroscopic measurements by M. A. Ali et al [72]. The geometries of nickel(II) complexes, were square planar and octahedral, respectively. Cu(II) complexes acquired dimeric/polymeric structure due to low magnetic moment values.

A new series of transition metal complexes of Mn(II), Co(II), Ni(II), Cu(II) and Zn(II) were synthesized from the Schiff base ligand derived from 4-aminoantipyrine, furfural and o-phenylenediamine by M. S. Suresh et al [73]. The structural features were derived from their elemental analyses, infrared, UV-visible spectroscopy, NMR spectroscopy, thermogravimetric analyses, ESR spectral analyses and conductivity measurements. The data suggested square planar geometry for the complexes having metal ions with primary valency two.

In 2013, Y. Harinath et al [74] have synthesized a new Schiff base bidentate ligand (L), 5-methyl thiophene-2-carboxaldehyde carbohydrazone and its metal [Cu(II), Cd(II), Ni(II) and Zn(II)] complexes with general stoichiometry $[M(L)_2X_2]$ (where X=Cl). The ligand and its metal complexes were characterized by elemental analyses, IR, ^{1}Hnmr, ESR spectral analyses, and molar conductance studies. The molar conductance data revealed that all the metal chelates are non-electrolytes. IR spectra showed that ligand (L) is coordinated to the metal ions in a bidentate manner with N and O donor sites of the azomethine-N, and carbonyl-O. ESR and UV-Vis spectral data showed that the geometrical structure of the complexes are orthorhombic.

Scope and Objectives of the Present Investigation

The quest for novel Schiff bases and their metal chelates is the perpetual phenomenon for the chemists and scientists. By the exploration of the chelating ability of the Schiff bases, a novel class of metal complexes may be opened, which may possess potential applications in industrial, pharmaceutical and catalytic fields. By elucidating the structures of the metal chelates and ligands using advanced tools and techniques, a proper correlation can be made with the structure and activity. Even though large number of Schiff bases was prepared and chelating efficacy of the compounds was exploited, still remain wide scope for the synthesis of novel Schiff bases which possesses hetero atoms and their metal chelates. Literature survey showed that Schiff bases which are primarily derived from heterocyclic compounds such as acetylpyridines, furan-aldehydes and thiophene-aldehydes and their metal chelates were not much explored and reported.

In the present course of investigation it is proposed to synthesize and characterize novel heterocyclic Schiff bases derived from 3-acetylpyridine, furan-2-aldehyde and thiophene-2-aldehyde using various spectroscopic techniques such as IR, UV-vis, NMR and mass. It is also proposed to synthesize new transition metal complexes of these Schiff bases by exploiting their chelating ability. The geometry and structure of the metal chelates are to be recognized by analytical tools like as spectral, magnetic, electrical and elemental analyses.

CHAPTER 2

MATERIALS AND METHODS

This chapter includes the brief description of the common reagents used for the preparation of Schiff bases and their transition metal complexes. The methods employed for the purification of the samples and different analytical techniques accepted for the characterization of the Schiff bases and the metal complexes are also listed.

Reagents

All Schiff bases were synthesized using analar grade samples. 3-acetyl pyridine, furan-2-aldehyde and thiophene-2-aldehyde were purchased from Fluka. Other reactants such as semicarbazide hydrochloride, thiosemicarbazide and phenylhydrazine hydrochloride were obtained from E. merck. Samples from Qualigens such as p-aminobenzoic acid, and m-aminobenzoic acid were also utilized for the Schiff base synthesis.

Metal salts used for the analysis were the acetates of copper, chromium, manganese, nickel and zinc. Ferric chloride was used for the synthesis of Fe(III) chelates while nitrates of cadmium and silver where used for the preparation of Cd(II) and Ag(I) chelates. All metal salts were purchased from Qualigens or E. mecrk

All the metal chelates were synthesized in ethanol medium. The ethanol used for this purpose was first distilled and dried over $CaSO_4$.

C H N S Analysis

Percentage of carbon, hydrogen nitrogen and sulphur of the Schiff base ligands and their metal complexes were determined by microanalysis using Elementar make Vario EL III model CHN analyzer.

Estimation of Metals

Estimation of metals was mainly done by pyrolitic, volumetric, colourimetric and gravimetric analysis. As a preliminary examination, pyrolytic method was followed for the determination of the metal content. About 0.2 g of the metal chelate was strongly heated for 2 hours in a previously weighed silica crucible for the complete decomposition. After cooling, the mass of the metal oxide left behind was measured. From this, the percentage of metal was estimated.

For conducting other analyses, a known amount of the metal chelates were digested for 1 hour with a mixture of concentrated nitric and perchloric acid. The decomposition of the metal complexes takes place at this stage. After the digestion, the mixture was further extracted with concentrated HCl. The resultant solution was then quantitatively transferred into a volumetric flask. A definite volume of the solution was taken and different analyses were carried out for finding out the percentage of the metal.

Iron and chromium were estimated by photometric method using the colouring agents such as potassium thiocyanate and diphenyl carbazide respectively. The percentage of nickel and zinc was determined by complexometric titration in which EDTA as the complexing agent and murexide and eriochrome black-T as the indicators for nickel and zinc respectively. Cobalt

was also estimated by EDTA titration using xylenol orange as the indicator. Back titration method was employed for the estimation of manganese with EDTA as the titrant and eriochrome black-T as the indicator [75-78].

The percentage of copper was determined by iodometric titration using sodium thiosulphate as the titrant and starch as the indicator.

Physicochemical Techniques

The structure of the Schiff base ligands were confirmed by various spectroscopic techniques such as mass, ^{1}Hnmr, ^{13}Cnmr, infrared and UV-visible [79-81]. To explicate the structure and geometry of the metal chelates, physicochemical techniques such as, magnetic susceptibility measurements, molar conductance studies and spectral studies like UV-Visible, ^{1}Hnmr and infrared have been performed.

Molar conductance studies

To predict the ionic nature of the metal chelates, molar conductance studies were conducted in DMSO solvent at a concentration of 10^{-3}M at $30 \pm 2°C$. ELICO conductivity meter was used for the molar conductance measurement. By using the relation $\Lambda_m = K/C$, the molar conductance of the complexes (Λ_m) can be calculated, where C is the molar concentration of the metal complex solutions. Cell constant was maintained as 1 in all investigations [82].

Magnetic moment studies

Magnetic susceptibility was measured by Sherwood, UK (Mark 1). The corrected (for diamagnetism) gram susceptibilities (χ_g) of the chelates were determined by Gouy method using Hg[Co(NCS)$_4$] as calibrant. On multiplication

of χ_g with the molar mass gave molar susceptibility.

$\chi_M = \chi_g \, M$

The effective magnetic moments were calculated from the molar susceptibilities using the equation

$\mu_{eff} = 2.84 \, \chi_M$

where χ_M was the molar susceptibility corrected for diamagnetism [83,84].

Infrared spectra

KBr pellet method was used for recording the infrared spectra of ligands and complexes in the range 4000-400cm^{-1} on a Shimadzu model FT-IR Spectrometer (Model: IR affinity). Significant stretching frequencies in the infrared spectrum were very useful in predicting the functional groups present on them. Comparison between the infrared spectrum of the ligand and the metal chelates were very valuable in predicting the coordinating sites of the Schiff base to the metal ion.

Electronic spectra

Electronic spectra of the ligands and complexes were recorded with the help of a Shimadzu UV-visible-1800 Spectrophotometer using DMSO as solvent. Electronic spectral studies gave supplementary evidence for the structure of the ligand and the geometry of the complexes.

Mass spectra

Before performing the mass spectral studies on the Schiff bases, separation of the traces of impurities from the chief component was achieved by gas chromatography. Mass spectra of the Schiff bases were recorded using QP 2010

model Shimadzu GCMS at a source temperature of 300^0C.

NMR spectra

^{1}Hnmr and ^{13}Cnmr Spectral Studies of ligands and chelates were recorded in dmso-d_6 solvent using the instrument BRUKER AVANCE III HD**.**

CHAPTER 3

STUDIES ON SCHIFF BASES DERIVED FROM 3-ACETYLPYRIDINE AND THEIR TRANSITION METAL COMPLEXES

Three heterocyclic Schiff bases namely (E)-2-(1-(pyridin-3-yl)ethylidene)hydrazinecarbothioamide (or *3-acetylpyridine thiosemicarbazone*) (APTSC), (E)-2-(1-(pyridin-3-yl)ethylidene)hydrazinecarboxamide (or *3-acetylpyridine semicarbazone*) (APSC) and (E)-3-(1-(2-phenylhydrazono)ethyl) pyridine (or *3-acetylpyridine phenylhydrazone*) (APPH) were synthesized and characterized by various methods such as mass, NMR, IR and UV-visible spectroscopic methods and elemental analysis. The complexing ability of the newly synthesized Schiff bases were exploited by synthesizing transition metal complexes of VO(II), Cr(III), Ni(II), Cu(II), Cd(II) and Ag(I) ions. These metal complexes were characterized by elemental analysis, NMR, IR and UV-visible spectroscopic methods, magnetic moment measurements and molar conductance studies. The details of synthesis and characterization of metallic complexes of these three Schiff bases are discussed as separate three sections in this chapter.

Synthesis and Characterization of the Schiff Base, 3-Acetylpyridine Thiosemicarbazone

The Schiff base 3-acetylpyridine thiosemicarbazone (APTSC) was synthesized by the condensation reaction between equimolar mixture of 3-acetylpyridine and thiosemicarbazide in ethanol medium. The reaction mixture was refluxed for 3 hours in a water bath. Evaporated and cooled the mixture to obtain pale yellow coloured solid. Yield of the product was 79%. M. P= 205^0C.

The elemental data of the compound is given in Table 1.4. Results showed that good agreement exists between the theoretical and experimental values.
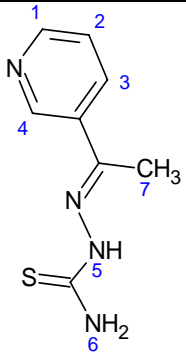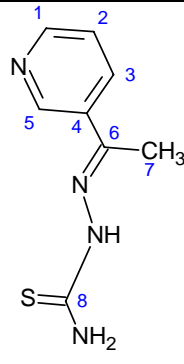
NMR spectral studies

^{1}Hnmr and ^{1}H-^{1}H correlation spectrum (COSY) of the ligand APTSC are provided in the Figures 1.3 and 1.4 respectively. The ^{1}Hnmr spectrum exhibited eight clear peaks for hydrogen atoms in different environments. The singlet appeared at 2.34δ was due to the methyl protons. A broad peak observed at 3.37 was assigned to the terminal NH_2 protons. The NH proton of the molecule gave a signal at 8.09δ. The two peaks (having multiplicity-dd) appeared at 8.34δ and 8.57δ respectively, a doublet at 9.12δ and a sextet displayed at 7.41δ can be assigned to the four hydrogen atoms of the pyridine ring. An additional strong peak displayed at 10.3δ was due to the SH proton, which was emerged due to the tautomerism in the molecule. The COSY spectrum of APTSC displayed five diagonal contours in the region 7.0-9.5δ, which was due to the labeled protons 2,5,3 and 1. Absence of off-diagonal peaks between H1 and H4 suggesting that no coupling occur between these protons, since these protons bearing carbon atoms are connected through the N atom of pyridine ring. Off-diagonal contours correspond to the meta coupling between H3 and H4 of the ring appeared in the COSY spectrum. A strong ortho coupling was confirmed in the molecule between H1& H2 and H2 & H3 and the corresponding intense off-diagonal contours appeared in the spectrum. A weak H1-H3 meta coupling is likely in the molecule and was verified by the appearance of less intense off-diagonal contours. A long range coupling between H3 and H5 atoms (W- coupling) also came into view in

the correlation spectrum. The correct assignment of the ^{1}Hnmr signals of APTSC is displayed in the Table 1.1.

The ^{13}Cnmr spectrum (Figure 1.5) of the Schiff base showed eight clear peaks for eight carbon atoms. The signal for the only sp^3 hybridized carbon atom of the molecule APTSC appeared at 13.72ppm. The signals for the carbon atoms in the pyridine ring resonated in the range 123.23-149.67ppm. The peak displayed at 145.55ppm was due to the azomethine carbon atom. The carbon atom bearing the sulphur atom displayed a signal at 179.08ppm. In the DEPT 135 spectrum of APTSC, the peaks corresponds to the labelled carbon atoms 4 and 6 were absent, but their signals were appeared in the ^{13}Cnmr spectrum at 133.24 and 145.55ppm respectively. This is due to the fact that the DEPT spectrum will not give any signals for quaternary carbon atoms. Since no inverse peaks were appeared in the DEPT spectrum, one can assure the absence of methylene carbon atoms in the molecular structure. The DEPT spectrum of this molecule is provided in Figure 1.6. The assignment of ^{13}Cnmr signals are listed in Table 1.1.

On close examination of HMQC spectrum of APTSC (Figure 1.7), it is evident that there is no corresponding contour for the ^{1}Hnmr peak at 3.37δ, which establishes that this proton is not attached on the carbon atom and therefore can be confirmed to be NH$_2$ protons. Similarly the peak at 8.09δ in the ^{1}Hnmr spectrum did not give any contour in HMQC spectrum, confirming that this signal is due to the NH proton. The corresponding contour lines were appeared for all other protons in HMQC spectrum, suggesting that these protons are bounded to carbon atoms in the molecule.

Table 1.1 ^{1}Hnmr and ^{13}Cnmr spectral data of Schiff base, APTSC

^{1}Hnmr			^{13}Cnmr		
	δ value	Assignment/ Labelled	δ value	Assignment/ Labelled	
	10.30(s,1H)	SH	13.72	7	
	9.12(d,1H)	4	123.23	2	
	8.57(dd,1H)	1	133.23	4	
	8.34(dd,1H)	3	133.94	3	
	8.09(s,1H)	5 (NH)	145.55	6	
	7.41(s_{br},1H)	2	147.74	5	
	3.37(s_{br},2H)	6 (NH$_2$)	149.67	1	
	2.34(s,3H)	7 (CH$_3$)	179.08	8	
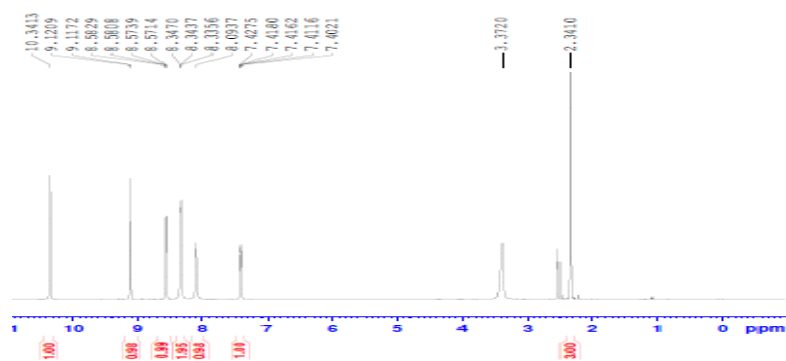
Fig. 1.3 ^{1}Hnmr spectrum of the Schiff base APTSC
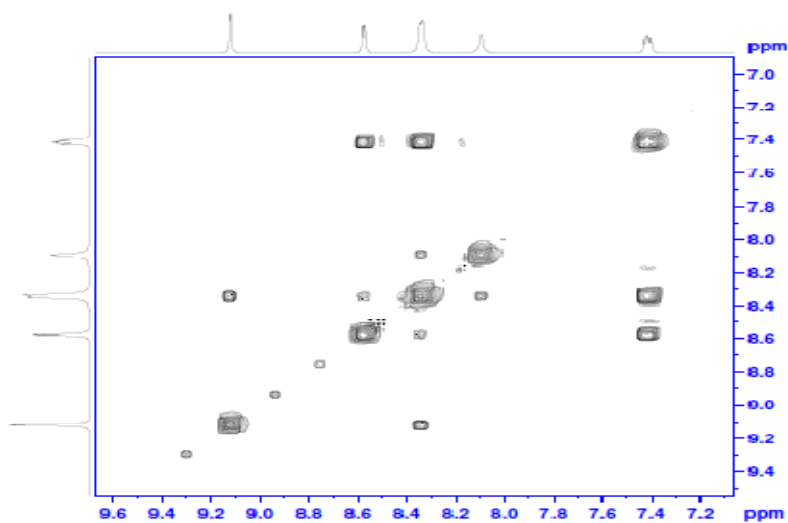
Fig. 1.4 COSY spectrum of the Schiff base APTSC
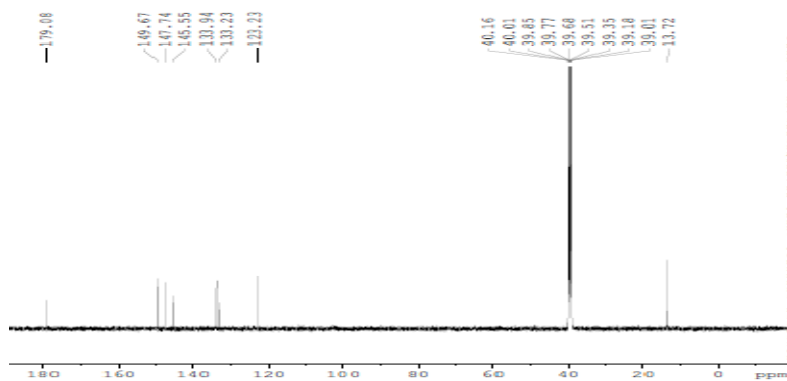
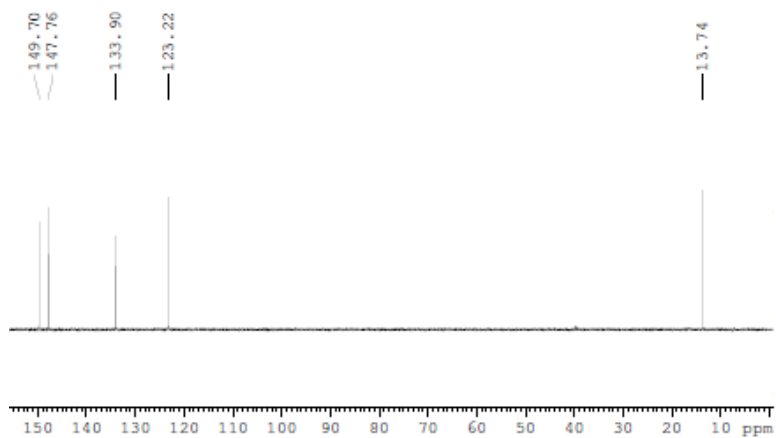**Fig. 1.5** ^{13}Cnmr spectrum of the Schiff base APTSC

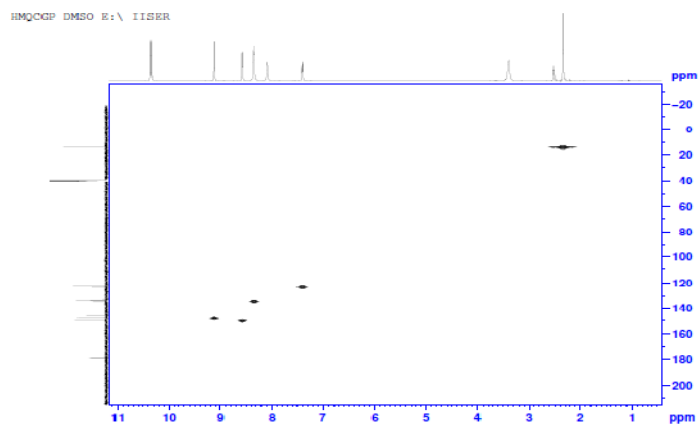**Fig. 1.6** DEPT 135 spectrum of the Schiff base APTSC

Fig. 1.7 HMQC spectrum of the Schiff base APTSC

Mass spectral studies

Figure 1.8 show mass spectrum of the Schiff base APTSC. It is evident from the spectrum that molecular ion peak having m/z 194 is the base peak, which indicate the stability of the molecule. The M+1 peak appeared at m/z 195 and the ratio between the M^+ and M+ 1 peak was 25:2. This clearly establishes the number of carbon atoms present in the molecule ie, 8. The appearance of the M+2 peak in the spectrum (m/z 196) is due to the presence of S atom in the molecule. The loss of CH_3 group from the molecular ion resulted in the fragment $[C_7H_7N_4S]^+$ (m/z 179). The peak displayed at m/z 161 was due the loss of SH moiety from the molecule which produced the fragment $[C_8H_9N_4]^+$. The other prominent peaks observed at m/z 134, 120, 104 and 93 can be assigned to the fragments $[C_7H_8N_3]^+$, $[C_7H_8N_2]^+$, $[C_7H_6N]^+$ and $[C_6H_7N]^+$ respectively. The intense peak observed at m/z 78 is due to the stable pyridine moiety $[C_5H_4N]^+$. The fragment $[CSNH_2]^+$ was displayed at m/z 60 in the mass spectrum of APTSC. The loss of acetylenic moiety from the pyridine segment ended in the fragment $[C_4H_3]^+$.
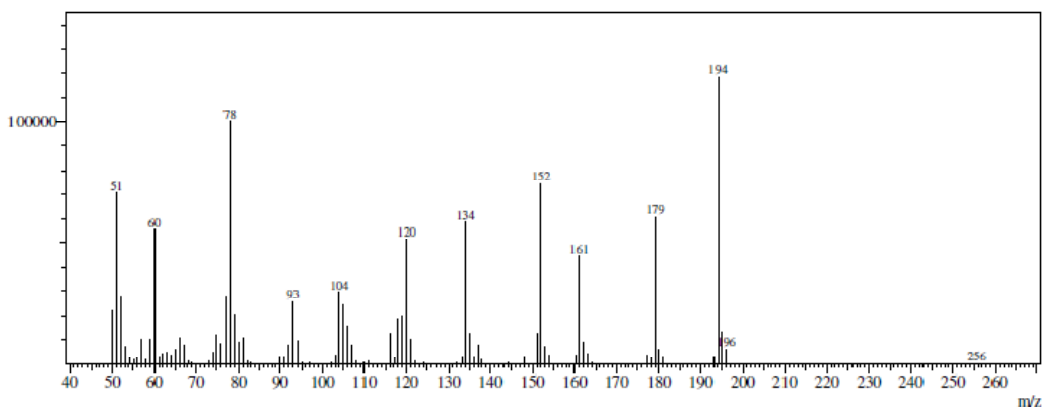

Fig. 1.8 Mass spectrum of the Schiff base APTSC

IR spectral studies

FTIR spectrum of the Schiff base APTSC exhibited characteristic stretching frequencies for various bonds. Asymmetric and symmetrical stretching frequencies of the terminal amino group observed at 3385 and 3246cm^{-1} respectively. A medium band observed at 3201cm^{-1} is due to the stretching vibration of N-H group. A very weak band at 2466cm^{-1} is assignable to the vibration of S-H bond, which arises due to the tautomerism of the Schiff base (thioenol form). The very weak nature of this characteristic band is due to the trace amount of the tautomeric form in the solid state. The stretching frequency of the azometine group appeared at 1612cm^{-1} and C=S gave its characteristic signal at 880cm^{-1}.

Electronic spectral studies

The UV-visible spectrum of the Schiff base exhibited two peaks at 31948cm^{-1} and 31347cm^{-1} which can be assigned to $\pi \to \pi^*$ and $n \to \pi^*$ transitions respectively.

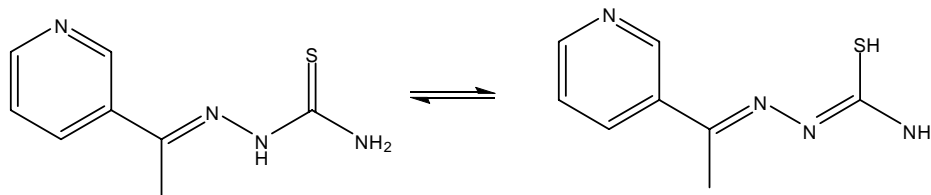From the foregoing discussions the structure can be assigned to the Schiff base APTSC as shown in Figure 1.9.

Fig. 1.9 Structure of APTSC and thioketo-thioenol tautomerism

Synthesis and Characterization of the Schiff Base, 3-Acetylpyridine Semicarbazone

Equimolar amount of 3-acetylpyridine and semicarbazide hydrochloride were dissolved in ethanol and ethanol/water mixture (3:1) respectively. These solutions were thoroughly mixed and refluxed for 3 hours in a water bath. The reaction mixture was evaporated to reduce the volume and cooled. The white coloured solid was then filtered, washed with small quantity of ethanol and dried and recrystallised from ethanol. Yield 70%. M.P= 200^0C. Elemental analysis data of the molecule is provided in Table 1.6.
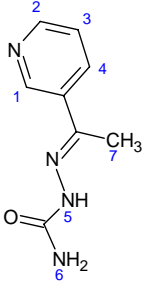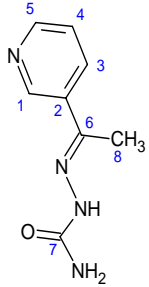
NMR spectral studies

The ^{1}Hnmr spectrum of the Schiff base showed a singlet at 2.26δ, assignable to the protons of the methyl group. A broad signal appeared at 3.56δ is due to the protons of the terminal –NH_2 group of the amino part. A very weak and broad peak exhibited at 7.7δ can be attributed to the –OH proton, which originates in the molecule due to tautomerism (Figure 1.16). All other protons of pyridine, gave their signals in the range 8.9-9.8δ. The ^{1}Hnmr and COSY spectra of the Schiff base are provided in the Figures 1.10 and 1.11. The correct assignment of protons is provided in Table 1.2. In the COSY spectrum of APSC, five diagonal contours appeared in the range 7.9-9.8δ was due to the labeled protons 3, 2, 4, 1 and 5. There were no off-diagonal contours appeared corresponds to H1-H2 interaction, indicating that no coupling occurs between these protons. Meta coupling occurs between H1 and H4 of the pyridine ring and the corresponding off signal contours appeared in the COSY spectrum. A strong ortho coupling between H2-H3 and H3-H4 occurs in the molecule which was confirmed by

appearance of the intense off-diagonal contours in the spectrum. A weak meta coupling is also possible between H2 and H4 and the corresponding signal also appeared in the correlation spectrum.

The [13]Cnmr and DEPT spectra of the Schiff base APSC are exhibited in Figures 1.12 and 1.13. Eight distinct peaks appeared in the [13]Cnmr spectrum, corresponds to eight carbon atoms. The carbon atoms and their exact signals are shown in Table 1.2. The carbon atom of the methyl group showed its signal at 12.86ppm. The oxygen bearing carbon atom displayed the signal (156.87ppm) in the low field region of the spectrum. All other carbon atoms present in the pyridine ring resonated in the range 126-145ppm. DEPT 135 spectrum was also useful to assign the exact signals for carbon atoms in [13]Cnmr. As expected in the DEPT 135 spectrum of APSC, the peaks corresponds C2 and C6 (appeared in [13]Cnmr spectrum at 137.13 and 138.76ppm respectively) were absent, since they are quaternary carbon atoms. Absence of methylene group in the compound is evident from the absence of inverse peaks in the DEPT 135 spectrum.

Table 1.2 [1]Hnmr and [13]Cnmr spectral data of Schiff base, APSC

[1]Hnmr			[13]Cnmr		
	δ value	Assignment/ Labelled No.	δ value	Assignment/ Labelled No.	
	9.80(s,1H)	5 (NH)	12.86	8	
	9.37(dd,1H)	1	126.5	4	
	8.92(d,1H)	4	137.13	2	
	8.78(m,1H)	2	138.76	6	
	7.90(dd,1H)	3	139.64	1	
	7.7(s_{br},1H)	-OH	140.55	5	
	3.56(s_{br},2H)	6 (NH$_2$)	141.40	3	
	2.26(s,3H)	7 (CH$_3$)	156.87	7	

There was no corresponding contour for the proton axis peak at 3.56δ in the HMQC spectrum of APSC. This establishes that this proton is not bearing a carbon atom and therefore it is confirmed that it is the signal due to NH$_2$ proton. Similarly the peak at 9.8δ in the ^{1}Hnmr spectrum did not give any contour in the HMQC spectrum, suggesting that it is due to the signal of NH proton. All other signals in the ^{1}Hnmr spectrum gave their corresponding contours to ^{13}C in the HMQC spectrum. The HMQC spectrum of APSC is displayed in Figure 1.14.
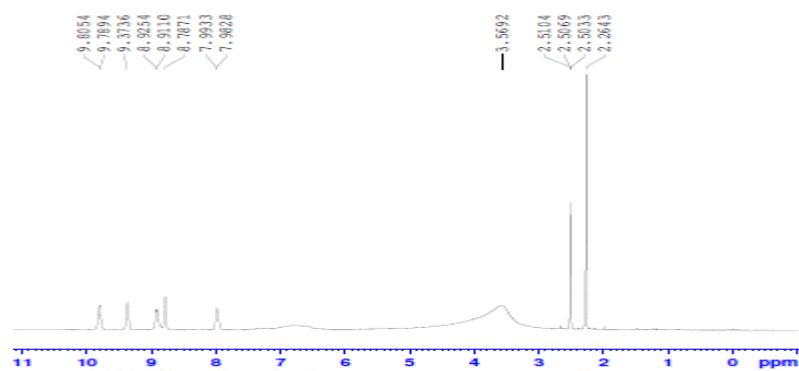

Fig. 1.10 ^{1}Hnmr spectrum of the Schiff base APSC
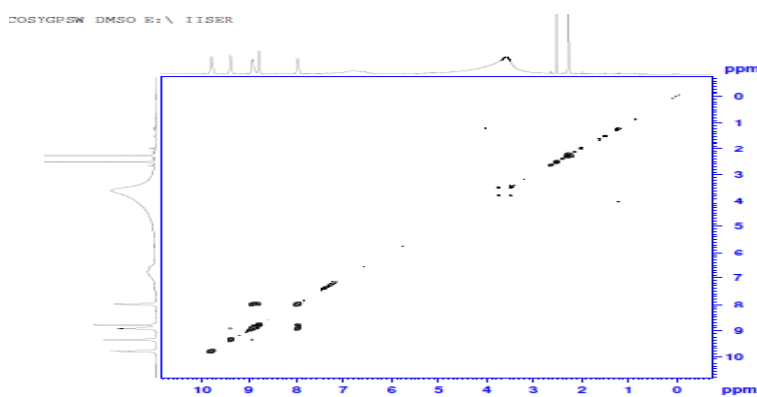

Fig. 1.11 COSY spectrum of the Schiff base APSC
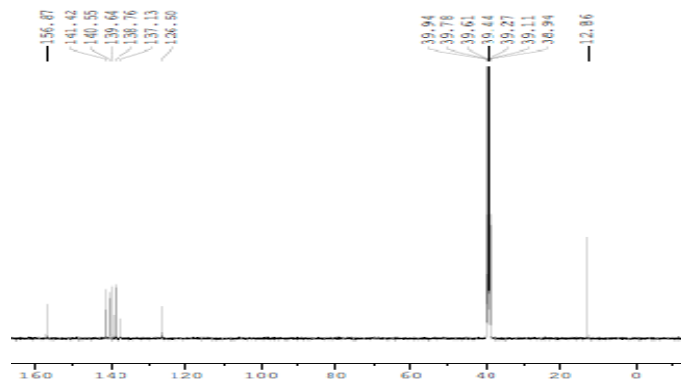
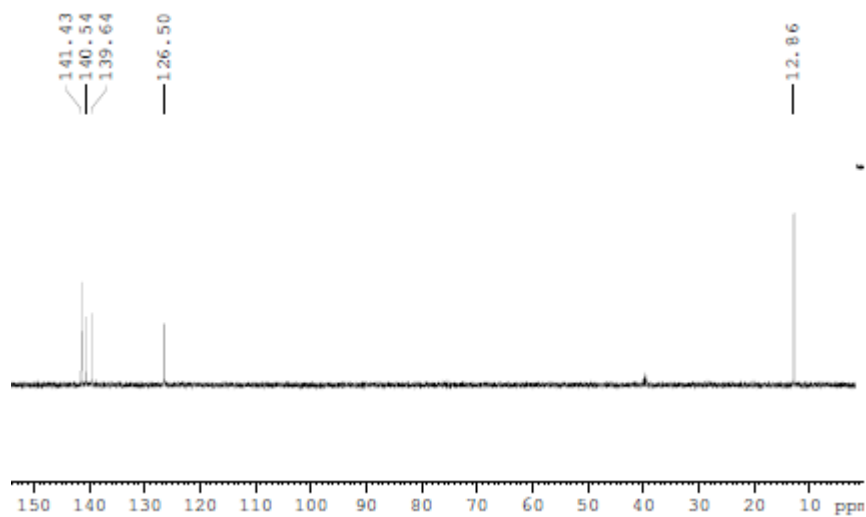**Fig. 1.12** ^{13}Cnmr spectrum of the Schiff base APSC

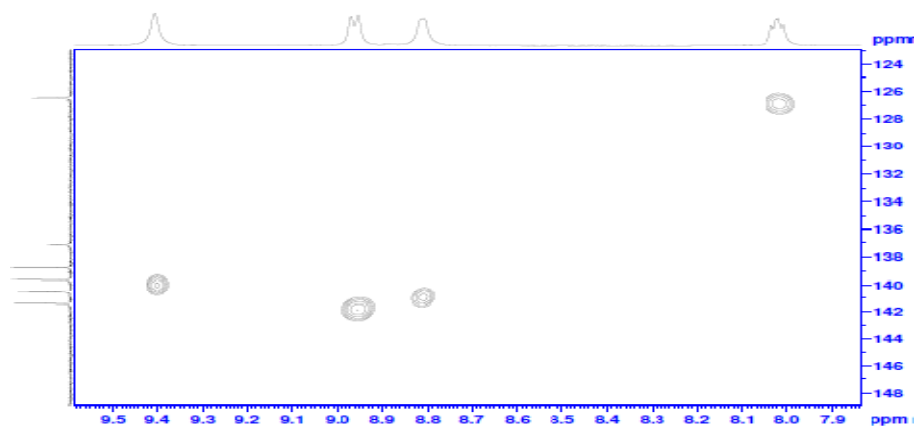**Fig. 1.13** DEPT 135 spectrum of the Schiff base APSC

Fig. 1.14 HMQC spectrum of the Schiff base APSC

Mass spectral studies

The mass spectrum of the ligand APSC is provided in Figure 1.15. In the mass spectrum, the molecular ion peak at m/z 178 was present. M+1peak was also observed at m/z 179. The base peak appeared at m/z 134 is due to the fragment $[C_7H_8N_3]^+$, which was obtained after the removal of $CONH_2$ group from the molecule. The other significant signals appeared at m/z 120, 104, 93, 78 and 51 can be assigned to the fragments $[C_7H_8N_2]^+$, $[C_7H_6N]+$, $[C_6H_7N]^+$, $[C_5H_4N]^+$ and $[C_4H_3]^+$ respectively.
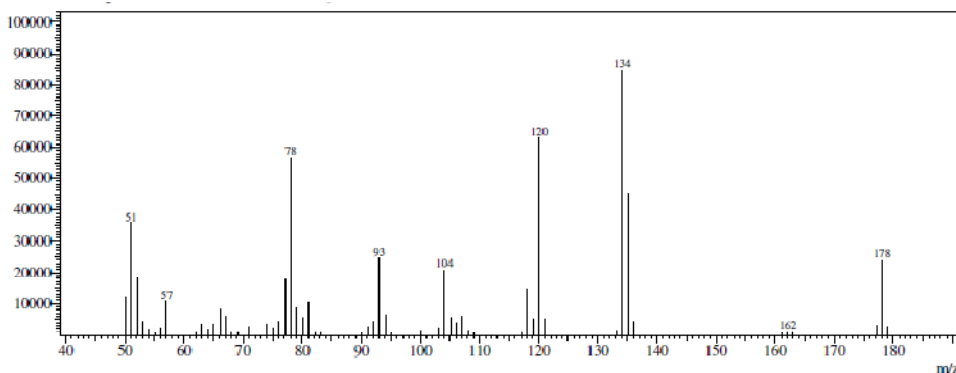
Fig. 1.15 Mass spectrum of the Schiff base APSC

IR spectral studies

Important characteristic stretching frequencies displayed in the IR spectrum of APSC are $\upsilon_{C=O}$ at $1697cm^{-1}$, and $\upsilon_{C=N}$ at $1633cm^{-1}$. The weak broad band appeared at $3415cm^{-1}$ (υ_{OH}) is an evidence for the tautometic structure of the molecule. The symmetric and asymmetric stretching vibrations of terminal $-NH_2$ group appeared at 3280 and $3454cm^{-1}$ respectively. A peak at $3201cm^{-1}$ was assignable to the stretching of N-H bond.

Electronic spectral studies

Two electronic transitions were displayed by the molecule at 33955 and 35842 cm⁻1, can be assigned to n→π* and π→π* respectively. The above discussions clearly establish the structure of APSC and it is given in Figure 1.16.

Fig. 1.16 Structure of APSC and keto-enol tautomerism

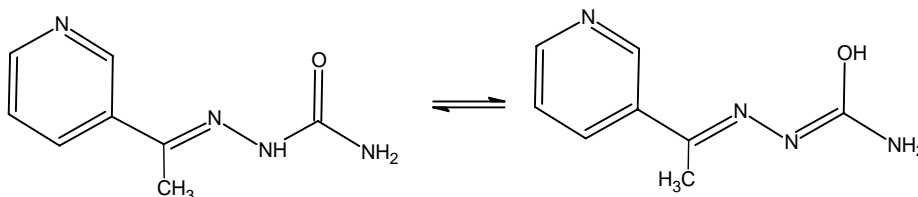**Synthesis and Characterization of the Schiff Base, 3-Acetylpyridine Phenylhydrazone**

APPH was synthesized by the condensation reaction between equimolar mixture of 3-acetylpyridine in ethanol and phenylhydrazine hydrochloride in ethanol water mixture (3:1). The reaction mixture was refluxed for four hours for the completion of the reaction. The resulting mixture was evaporated very near to dryness and allowed to cool slowly. The precipitated yellow coloured compound was filtered and washed with small quantity of ethanol. Recrystallised from ethanol and melting point was noted. Yield 81%. M. P=245^{0}C. Elemental analysis data is provided in Table 1.8.

NMR spectral studies

^{1}Hnmr spectrum (Figure 1.17) of the Schiff base APPH displayed nine signals for nine distinguished hydrogen atoms. The peak appeared at 2.28δ was due to the methyl protons. A weak but broad signal displayed at 9.86δ was assignable to the NH proton of phenylhydrazine part. The signals exhibited in the
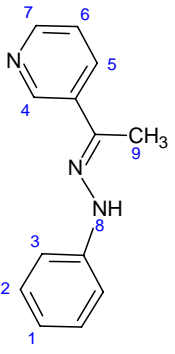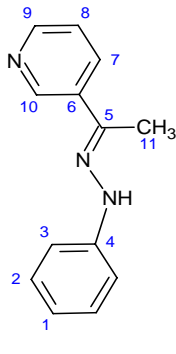
range 7.87-9.05δ were due to the protons of pyridine ring. Other three aromatic protons of the phenylhydrazine part resonated in the range 6.7-7.29δ. The signals in ^{1}Hnmr and assignments of hydrogen atoms are provided in Table 1.3. Two dimensional ^{1}H-^{1}Hnmr spectrum (COSY) was very helpful in allocating various signals to different hydrogen atoms. Nine diagonal contours appeared in the COSY spectrum, for nine different protons of the molecule. Strong off-diagonal peaks for H1-H2 & H2-H3 interactions were emerged in the COSY spectrum (Figure 1.18), which were originated by the strong ortho coupling between these protons of the benzene ring. Due to the meta coupling between the protons H5 and H4 in the pyridine ring, weak contours were appeared in the spectrum. Also strong off-diagonal contours appeared corresponds to the ortho coupling of H6-H7 and H5-H6 protons. Further it was noted that no off-diagonal contours were shown for the meta coupling between H4 and H7, indicating that these proton bearing carbon atoms are joined through the N atom.

The ^{13}Cnmr and DEPT spectrum are provided in the Figures 1.19 and 1.20 respectively. The signals appeared in ^{13}Cnmr spectrum of APPH were assigned for 11 labelled carbon atoms and given in Table 1.3. The signal for the azomethine carbon appeared at 137.99ppm in the spectrum. A peak observed at 12.53ppm was assignable to methyl carbon atom. The quaternary carbon atoms labeled 6 and 4 gave their signals at 134.88 and 145.07ppm respectively. All other labeled carbon atoms present in the pyridine ring and the aromatic ring appeared between 113-139ppm. On close observation of the molecular structure it is evident that the molecule APPH bear three quaternary carbon atoms, labeled as 4,

5 and 6. In the DEPT-135 spectrum of the molecule, the signals corresponds to these carbon atoms were totally absent, confirming that these peaks are definitely due to quaternary carbons. Since there were no methylene groups in the molecule, the DEPT 135 spectrum would not have any inverse signals.

In the HMQC spectrum of APPH, the ^{1}Hnmr signal was absent corresponds to the C4 (observed at 145.07ppm), since this carbon atom is not bearing a proton. Similarly, the corresponding ^{1}Hnmr signal was not appeared for C6 signal at ^{13}Cnmr axis. The corresponding ^{13}C contours for the proton signal appeared at 9.86δ was not present in the HMQC spectrum. This evidently establishes that this proton is not bearing a carbon atom and it is assigned for NH proton signal. The HMQC spectrum for APPH is provided in Figure 1.21.

Table 1.3 ^{1}Hnmr and ^{13}Cnmr spectral data of Schiff base, APPH

^{1}Hnmr			^{13}Cnmr		
	δ value	Assignment/ Labelled No.	δ value	Assignment/ Labelled No.	
	9.86(s$_{br}$,1H)	8 (NH)	145.07	4	
	9.05(d,1H)	4	139.92	7	
	8.72(dd,1H)	5	139.82	9	
	8.66(dd,1H)	7	138.63	10	
	7.80(m,1H)	6	137.99	5	
	7.28(d,1H)	3	134.88	6	
	7.19(m,1H)	2	128.96	2	
	6.76(m,1H)	1	126.47	8	
	2.28(s,3H)	9	120.02	1	
			113.34	3	
			12.53	11	

34

Fig. 1.17 ^{1}Hnmr spectrum of the Schiff base APPH
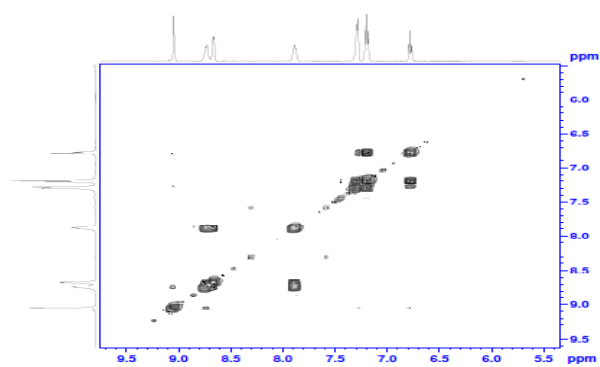
Fig. 1.18 COSY spectrum of the Schiff base APPH
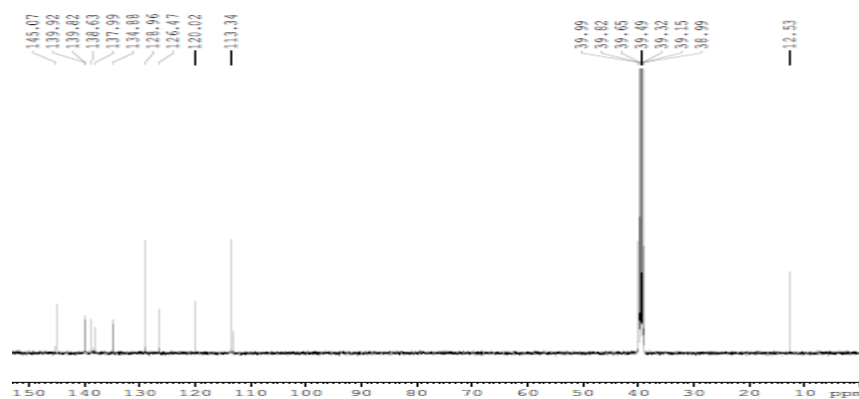
Fig. 1.19 ^{13}Cnmr spectrum of the Schiff base APPH
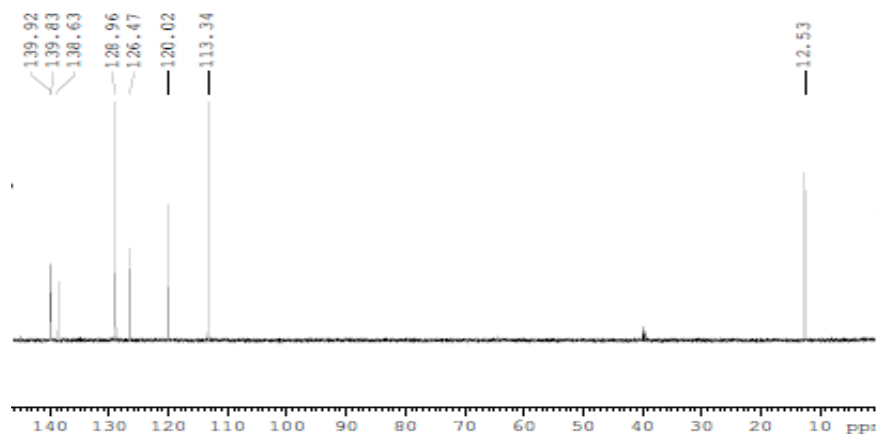
Fig. 1.20 DEPT 135 spectrum of the Schiff base APPH
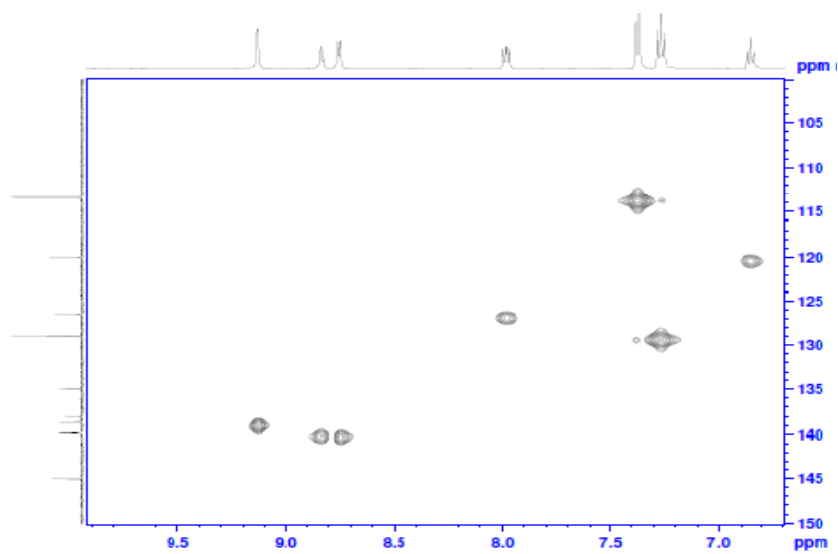
Fig. 1.21 HMQC spectrum of the Schiff base APPH

Mass spectral studies

Mass spectrum of the Schiff base is provided in the Figure 1.22. Base peak in the spectrum was observed at m/z 211, which is equal to the exact molecular mass of the compound (M+ peak). This indicates the enhanced stability of the molecule. Also a signal was obtained at m/z 212 (M+1 peak). Intense signals appeared at 92 and 78 having relative abundance 55 and 56 respectively was

clearly due to the fragments $[C_6H_6N]^+$ and $[C_5H_4N]^+$. Other peaks appeared at m/z 65 and 51 can be assigned to the secondary fragments $[C_5H_5]^+$ and $[C_4H_3]^+$ which were originated from the pyridine fragment.
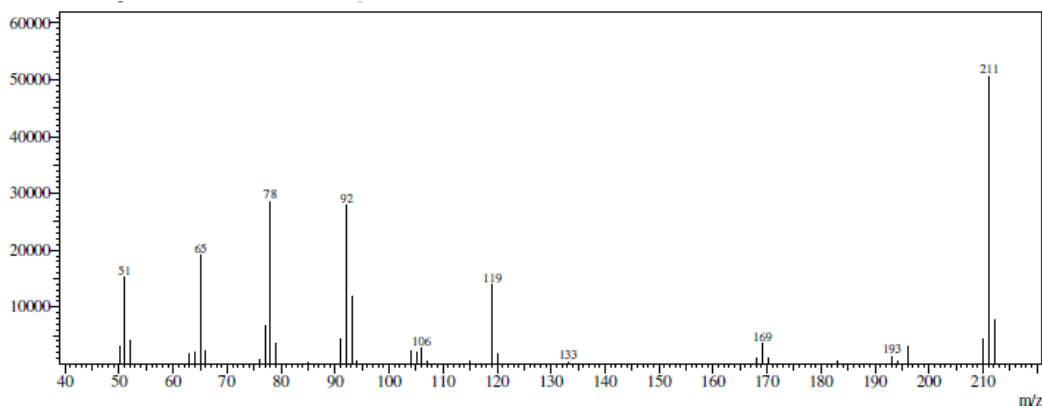
Fig. 1.22 Mass spectrum of the Schiff base APPH

IR spectral studies

The IR spectrum of the Schiff base gave characteristic frequencies for stretching and bending vibrations. An intense peak appeared at 1593cm^{-1} can be assigned to the C=N stretching vibration. A broad band displayed at 3265cm^{-1} is due to N-H frequency. The various peaks emerged in the spectrum in the range 1540-1600cm^{-1} were due to C=C vibrations of aromatic rings. υ_{C-N} was appeared at 1465cm^{-1} and C-H stretching frequencies was shown between 3030-3100cm^{-1}. The typical bands appeared at 621 and 667cm^{-1} can be considered as in-plane deformation mode of the pyridine ring.

Electronic spectral studies

The important electronic transitions occurred in the molecules were observed at 32679cm^{-1} and 29239cm^{-1}, which are attributed to $\pi\rightarrow\pi^*$ and $n\rightarrow\pi^*$

transitions respectively. From the above discussions the structure of the Schiff base APPH can be assigned and it is given in Figure 1.23.
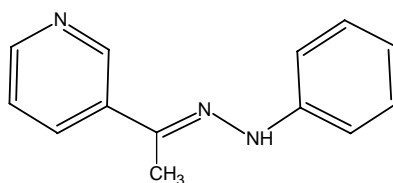
Fig. 1.23 Structure of APPH

STUDIES ON VO(II), Cr(III), Ni(II), Cu(II), Cd(II) AND Ag(I) COMPLEXES OF 3-ACETYLPYRIDINE THIOSEMICARBAZONE

Transition metal complexes of the Schiff base, 3-acetlylpyridine thiosemicarbazone (APTSC) were synthesized and characterized using elemental analysis, magnetic moment measurement studies and spectral studies. Preparation and structural derivations of these chelates are well documented in this section.

Synthesis of Complexes

3mmol solution of the ligand APTSC in ethanol water mixture (10:3) was refluxed in a water bath. To the boiling solution, 3mmol solution of the metal salt in hot ethanol was added drop wise and the reaction mixture was further refluxed for 3 hours. The mixture was then evaporated to reduce the volume and cooled. The precipitated metal complex was filtered, washed with hot water and finally with ethanol, dried and kept over an. $CaCl_2$.

Vanadyl sulphate, cadmium nitrate and silver nitrate were used for synthesizing VO(II), Cd(II) and Ag(I) chelates. All other salts were the acetates of the corresponding metals.

Characterization of Complexes

All complexes were amorphous solids and stable to light and air. They are characterized by various techniques and the details are given below.

Elemental analysis

CHNS data of metal chelates are listed in Table 1.4. Experimental data were found to agree well with the calculated values. Metal percentage data determined by various analytical procedures together with the calculated values

are also displayed in this table. Results showed that a 1:1 stoichiometry exist between the metal and ligand for Cr(III), Ni(II), Cu(II) and Ag(I) complexes, while VO(II) and Cd(II) chelates exhibited 1:2 stoichiometry.

Magnetic moment studies

Valuable information regarding the geometries of the complexes was achieved from the magnetic moment data. Results of μ_{eff} values are reported in Table 1.4. VO(II) chelate displayed effective magnetic value μ_{eff} of 1.6BM, which was in quite agreement with the value of a normal square pyramidal complex [85,86]. μ_{eff} of Cr(III) was considerably lower (2.51BM) than the μ_{eff} calculated by the spin only formula. This may be attributed to the antiferromagnetic interaction between the metal ions and hence can assume an octahedral dimeric structure to Cr(III) complex having two bridges through acetate groups [87-89]. This was further confirmed by IR spectral analysis. The Ni(II) chelate displayed μ_{eff} of 3.03 BM which indicate the octahedral geometry of the complex. The slight increase in the μ_{eff} than the theoretical value by spin only formula, can be regarded as the little orbital contribution to the magnetic moment [90]. A dimeric square planar geometry was assigned to the copper complex due to its low μ_{eff} value (1.13BM). A significant lowering of μ_{eff} from 1.73BM (d^9) can be attributed to the antiferromagnetic interaction between the copper ions [91-93]. As expected, the Cd(II) and Ag(I) chelates were diamagnetic in nature due the absence unpaired electrons and thus tetrahedral geometries were assigned to these complexes [94-97].

Molar conductance measurements

Molar conductance of the metal chelates in DMSO was determined and reported in Table 1.4. It is evident from the table that all chelates displayed poor values of conductance in DMSO ranging from 10 to 41 $\Omega^{-1}cm^2mol^{-1}$, which shows the non electrolytic nature of the complexes. This is another supporting evidence for the structure of metal chelates, in the view that absence of counter ions outside the coordination sphere makes a complex, non electrolyte.

IR spectra of complexes

Significant IR absorption frequencies of ligand and complexes were reported and compared in Table 1.5. On close examination of the spectral bands of ligand and chelates valuable information regarding the chelation sites of the ligand on the metal ion could predict. A considerable decrease in the stretching frequencies of the azomethine linkage in complexes were noted (from $1612cm^{-1}$), suggesting that one of the coordination site of the ligand APTSC is the azomethine nitrogen atom [98-102]. The characteristic stretching frequency of C=S group in the ligand at $880cm^{-1}$ was absent in the chelates. Moreover new bands were appeared in the range $700-760cm^{-1}$, suggesting that the ligand APTSC make the second coordination bond to the metal ion through the sulphur atom [103,104]. This happens by the tautomerization of Schiff base followed by the removal of proton. In addition to this, the disappearance of the band at $2466cm^{-1}$ (υ_{S-H}) indicates the coordination through S atom. Evidently the band appeared in the range $700-760cm^{-1}$ in the spectrum of metal chelates is due to the stretching vibration of C-S bond [105]. The additional broad band exhibited in the spectrum

at about 3400cm^{-1} of Cr(III), Ni(II) and Ag(I) chelates strongly support the presence of water molecules inside the coordination sphere. IR spectrum of Cr(III), Ni(II) and Cu(II) complexes displayed asymmetric and symmetric stretching frequencies   C-O bond of acetate ion at around 1600 and 1450cm^{-1} respectively, showing a difference of about 150cm^{-1} which indicate the monodentate behaviour of acetate. But in addition to this some additional bands near to the above range but having a difference less than 120cm^{-1} appeared in complexes of Cr(III) and Cu(II), emphasizing the bridging of two metal ions through acetate ion. Moreover, emergence of new peaks in the IR spectrum of complexes in the range 477-490cm^{-1} and 443-474cm^{-1} respectively is a clear evidence for the formation of M-N bond and M-S bond. Appearance of a band at 972cm^{-1} in the IR spectrum of VO(II) complex is due to the stretching vibration of V=O bond [106,107].

Electronic spectra of complexes

Metal chelates displayed electronic transitions corresponds to the intra ligand electronic transitions (ILT) and d-d transitions. The intra ligand transitions in every complexes exhibited red shifts, indicating the complexation to the metal ion. Some ILT bands overlapped with d-d transitions to get a broad band. For VO(II) complex, two bands are displayed at 20800 and 29640cm^{-1} can be assigned to $^2B_2 \rightarrow ^2B_1$ and $^2B_2 \rightarrow ^2A_1$ electronic transitions in the square pyramidal field. The expected third transition namely $^2B \rightarrow ^2E$ was merged with the intra ligand transitions. In the octahedral field, the three spin allowed electronic transitions for Cr(III) complex (d^3) are $^4A_2(F) \rightarrow ^4T_2$, $^4A_2(F) \rightarrow ^4T_2(F)$ and

$^4A_2 \rightarrow {}^4T_1(P)$ which appeared in the electronic spectrum at17845, 19560 and 26314 cm^{-1} respectively. Three bands showed by the Ni(II) complex at 32721 and 38461 and 39601cm^{-1} are assignable to the $^3A_2 \rightarrow {}^3T_2$, $^3A_2 \rightarrow {}^3T_1(F)$ and $^3A_2 \rightarrow {}^3T_1(P)$ electronic transitions, which confirms the octahedral geometry of the complex [108,109]. The electronic spectrum of Cu(II) chelate (d^9) exhibited two peaks at 28610 and 29345cm^{-1} are due to the transitions $^2B_1 \rightarrow {}^2A_1$ and $^2B_1 \rightarrow {}^2B_2$ respectively in the square planar geometry. The optical absorption bands observed for Zn(II) and Ag(I) complexes at 26980 and 30082cm^{-1}were due to the L→M charge transfer transitions.

From the elemental, spectroscopic, magnetic and conductance analyses, geometries of these complexes were assigned and showed in Figure 1.24.
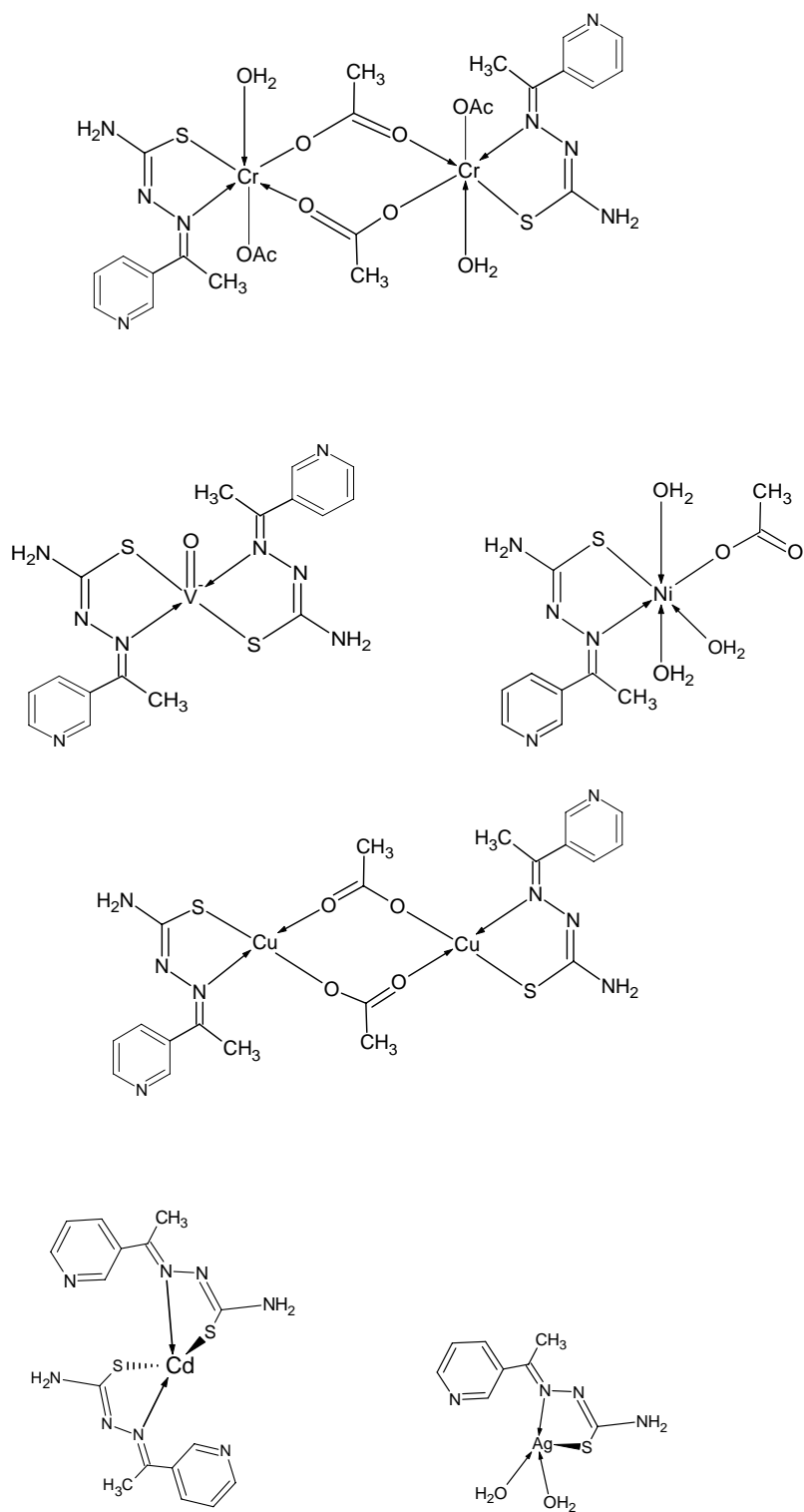
Fig. 1.24 Structures of the metal complexes of APTSC

Table 1.4 Microanalytical, maganetic and conductance data of the ligand APTSC and its transition metal chelates

Complex	Colour	Yield (%)	Mol. Wt.	M.P (^{0}C)	Metal% Found (Calculated)	C % Found (Calculated)	H % Found (Calculated)	N % Found (Calculated)	S % Found (Calculated)	μ_{eff} (BM)	Molar Conductance ($\Omega^{-1}cm^2mol^{-1}$)	Geometry
APTSC (LH)	Pale Yellow	70	194	205	-	48.55 (49.49)	4.99 (5.15)	29.22 (28.9)	16.82 (16.49)	-	-	-
[(VO)L$_2$]	Green	65	453	288	10.80 (11.25)	40.89 (42.39)	3.53 (3.97)	23.67 (24.70)	14.56 (14.13)	1.6	41	Square pyramidal
[CrLAc$_2$(H$_2$O)]$_2$	Pale Green	68	762	290	12.97 (13.65)	36.21 (37.80)	3.99 (4.46)	15.11 (14.70)	8.88 (8.40)	2.51	32	Octahedral
[NiLAc(H$_2$O)$_3$]	Pale Green	77	365	>300	16.88 (16.09)	30.59 (32.90)	4.71 (4.94)	14.85 (15.40)	7.71 (8.77)	3.03	10	Octahedral
[CuLAc]$_2$	Green	83	631	259	21.02 (20.14)	38.86 (38.03)	3.29 (3.80)	17.91 (17.70)	9.97 (10.14)	1.13	30	Square planar
[CdL$_2$]	White	60	498	>300	21.99 (22.55)	37.93 (38.52)	3.22 (3.61)	21.64 (22.50)	12.72 (12.84)	D	27	Tetrahedral
[AgL(H$_2$O)$_2$]	Grey	71	337	>300	33.22 (32.02)	27.66 (28.49)	3.37 (3.86)	15.95 (16.60)	9.62 (9.50)	D	34	Tetrahedral

Ac: Acetate, D: Diamagnetic

Table 1.5 Characteristic infrared absorption frequencies of APTSC and its transition metal complexes

Complex	υ_{OH}	υ_{N-H}	$\upsilon_{COO}(asym)$	$\upsilon_{C=N}$	$\upsilon_{COO}(sym)$	υ_{C-S}	υ_{M-N}	υ_{M-S}
APTSC (LH)	-	3264	-	1612	-	701	-	-
[(VO)L$_2$]	-	3263	-	1597	-	700	490	474
[Cr LAc$_2$(H$_2$O)]$_2$	3456	3261	1635	1610	1419	702	491	452
[NiLAc(H$_2$O)$_3$]	3417	3275	1624	1593	1423	724	477	443
[CuLAc]$_2$	-	3286	1619	1597	1479	762	485	460
[CdL$_2$]	-	3255	-	1598	-	698	488	473
[AgL(H$_2$O)$_2$]	3400	3289	-	1604	-	704	490	468

STUDIES ON VO(II), Cr(III), Ni(II), Cu(II), Cd(II) AND Ag(I) COMPLEXES OF 3-ACETYLPYRIDINE SEMICARBAZONE

The chelating efficiency of 3-acetylpyridine semicarbazone (APSC) was explored by preparing six transition metal chelates of APSC. These complexes were subjected to elemental, spectral, magnetic moment and molar conductance studies to determine their exact stoichiometries and geometries. The details are reported in this section.

Synthesis of Complexes

The metal salt (3mmol) was dissolved in hot ethanol and slowly added into a hot boiling solution of the Schiff base in ethanol water mixture (3:1) and refluxed the reaction mixture for 3 hours. It was then evaporated and cooled. The precipitated complex was filtered, washed with ethanol and hot water, dried and kept over an. $CaCl_2$. Nitrates of Cd and Ag and vanadyl sulphate were used as metal salts, while acetates of other metals were employed for the synthesis.

Characterization of Complexes

Exact stoichiometry and geometries of the chelates were determined by elemental analyses. Geometries of the complexes were derived with the help of magnetic and spectral studies. Details are reported in the following paragraphs.

Elemental analysis

To determine the correct stoichiometry of chelates, CHN analysis were performed. The data is provided in Table 1.6. The experimental data was found in good agreement with the calculated values. Data analysis showed that 1:1

stoichiometry exist between the metal and ligand for Cr(III), Ni(II), Cu(II) and Ag(I) complexes, while VO(II) and Cd(II) chelates exhibited 1:2 stoichiometry.

Magnetic moment studies

Results of magnetic moment studies are reported in Table 1.6. Vanadyl complex exhibited μ_{eff} of 1.71BM, which suggests square pyramidal geometry. The lowering of magnetic moment of Cr(III) chelate from its normal value (d^3 configuration) suggested that considerable Cr-Cr interaction exists in the complex and can assign an μ-acetato octahedral dimeric geometry. Proof for μ-acetato complex was further obtained from IR spectral analysis. The Ni(II) chelate displayed μ_{eff} of 3.13 BM which indicate the octahedral geometry of the complex. A slight enhancement from the normal value (d^8) is an indication of orbital contribution. The expected μ_{eff} calculated by the spin only formula is 1.73BM for Cu(II) ion (d^9 system). A significant lowering of μ_{eff} of Cu(II) chelate (1.01BM) from the theoretical value suggests, antiferromagnetic interaction between the metal ions and can assign (μ-acetato) dimeric square planar geometry. Due to the absence of unpaired electrons in d orbitals, the Cd(II) and Ag(I) chelates displayed diamagnetism and thus tetrahedral geometries were assigned to these complexes.

Molar conductance studies

All the metal chelates were subjected to the molar conductance measurements and the data is tabulated in Table 1.6. Results show that the metal complexes displayed molar conductance in the range 9-60 $\Omega^{-1}cm^2mol^{-1}$. The low value of conductance in DMSO medium was the clear evidence for the non

electrolytic behaviour of the metal chelates. These values also suggest the absence of any counter ions outside the coordination sphere of complexes.

IR spectra of complexes

The correct sites of coordination could predict with the aid of IR spectral data. On comparing the IR frequencies of Schiff bases and complexes, it is evident that a significant lowering in the C=N stretching frequencies happened in all metal chelates. This is a clear proof for the coordination of APSC through the azomethine nitrogen. Secondly, the disappearance of the band due to C=O from the IR spectra of chelates and the appearance of new peaks corresponds to C-O suggesting that the second binding site of APSC ligand is oxygen atom. This happens only after the tautomerisation of the ligand followed by the removal of one proton. Also strong evidence in this regard, is the disappearance of weak broad band occurred in the IR spectrum of APSC, which was due to the O-H stretching vibration due to the tautomeric structure. The additional bands exhibited in the spectrum at about $3400cm^{-1}$ of Cr(III), Ni(II) and Ag(I) chelates strongly support the presence of water molecules inside the coordination sphere. IR spectrum of Cr(III), Ni(II) and Cu(II) complexes displayed asymmetric and symmetric stretching frequencies COO bond of acetate ion in the range 1600 and $1450cm^{-1}$ respectively showing a difference of about $150cm^{-1}$, indicate the monodentate behaviour of acetate. Certain new bands appeared in the range 1550-$1400cm^{-1}$ and having a difference less than $120cm^{-1}$ appeared in complexes of Cr(III) and Cu(II), can be attributed to the bridging of two metal ions through acetate ion (μ-acetato complexes). Displaying of additional peaks in the range

460-490cm^{-1} and 600-630cm^{-1} respectively is a clear evidence for the formation of M-N bond and M-O bond. Vanadyl complex exhibited an additional band at 914cm^{-1} is due to the stretching vibration of V=O bond. The significant IR frequencies of Schiff base APSC and complexes are reported in Table 1.7.

Electronic spectra of complexes

In all metal chelates the intra ligand electronic transitions namely n→π* and π→π*, shifted to longer wavelength region suggesting the occurrence of complexation. The additional bands appeared in the vanadyl complex of APSC at 38759 and 39520cm^{-1} can be regarded as $^2B_2$→$^2B_1$ and $^2B_2$→$^2A_1$ electronic transitions. This suggests a square pyramidal geometry to this complex. The optical absorption bands observed in the spectrum of Cr(III) chelate was at 19342, 20140, 31277 and cm^{-1}, which are assignable to $^4A_2(F)$→$^4T_2$, $^4A_2(F)$→$^4T_2(F)$ and $^4A_2$→$^4T_1(P)$ electronic transitions in the octahedral field. The two bands displayed by the Ni(II) complex at 26199, 29161 and 31241cm^{-1} are assignable to the $^3A_2$→$^3T_2$, $^3A_2$→$^3T_1(F)$ and $^3A_2$→$^3T_1(P)$ electronic transitions, which confirms the octahedral geometry of the complex. A square planar geometry to Cu(II) chelate was assigned since the optical absorption spectrum gave two bands at 27786 and 29432cm^{-1} which are due to the transitions $^2B_1$→$^2A_1$ and $^2B_1$→$^2B_2$ respectively. Charge transfer bands were displayed by Cd(II) and Ag(I) chelates at 24332 and 27845cm^{-1} respectively and tetrahedral geometry was assigned to these complexes.

From the elemental, spectroscopic, electrical and magnetic moment analyses, proper geometries were assigned to these chelates and represented in Figure 1.25.
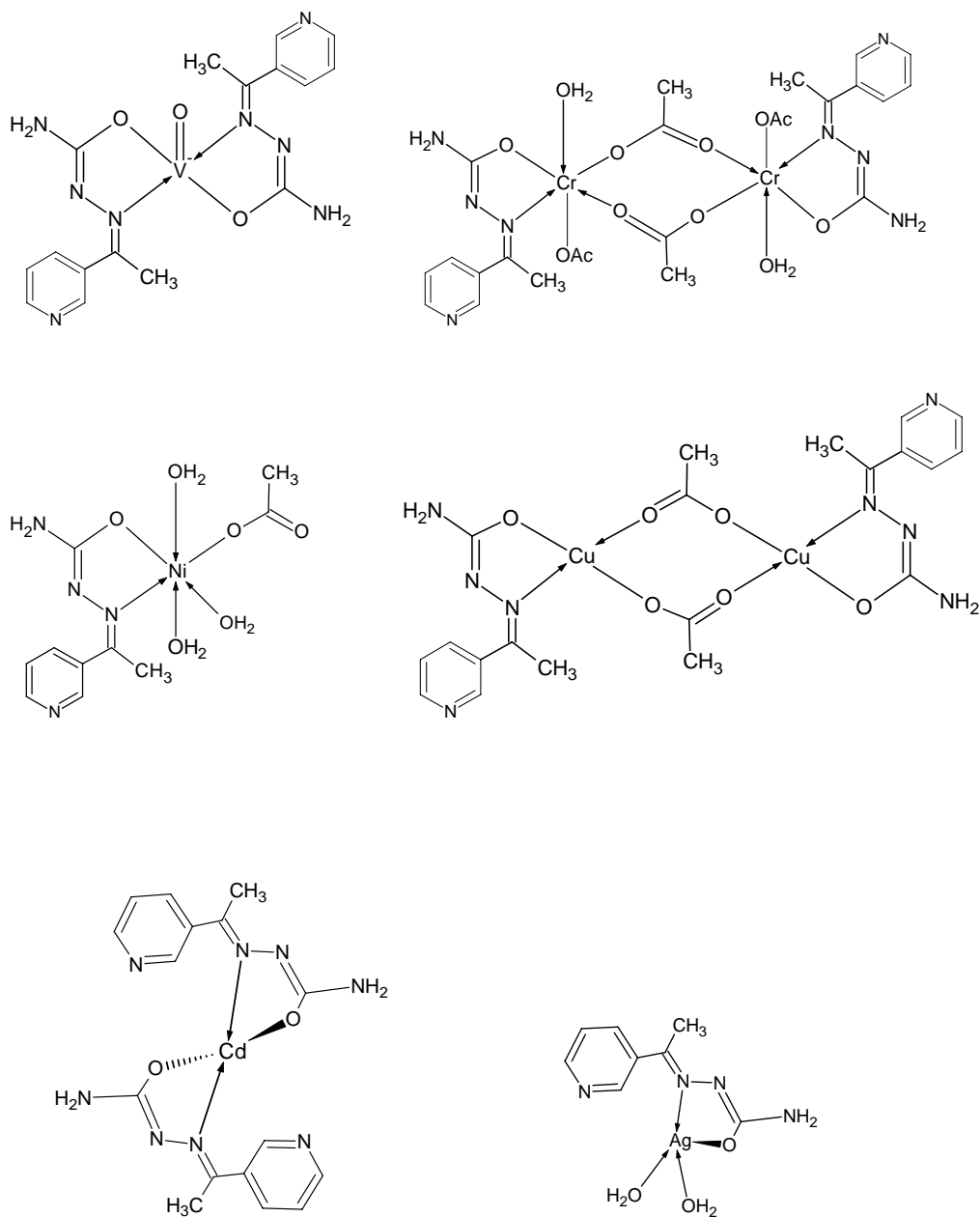

Fig. 1.25 Structures of the metal complexes of APSC

Table 1.6 Microanalytical, magnetic and conductance data of the ligand APSC and its transition metal chelates

Complex	Colour	Yield (%)	Mol. Wt.	M.P (^{0}C)	Metal% Found (Calculated)	C % Found (Calculated)	H % Found (Calculated)	N % Found (Calculated)	μ_{eff} (BM)	Molar Conductance ($\Omega^{-1}cm^2mol^{-1}$)	Geometry
APSC (LH)	Pale Yellow	80	178	218	-	52.89 (53.90)	5.91 (5.60)	30.88 (31.40)	-	-	-
[(VO)L$_2$]	Light green	65	421	283	12.81 (12.1)	44.45 (45.60)	4.88 (4.27)	26.15 (26.60)	1.71	60	Square pyramidal
[CrLAc$_2$(H$_2$O)]$_2$	Green	72	730	>300	13.99 (14.24)	39.21 (39.45)	4.92 (4.65)	15.33 (15.34)	2.2	26	Octahedral
[NiLAc(H$_2$O)$_3$]	Pale Green	73	349	>300	16.26 (16.83)	33.88 (34.41)	4.71 (5.16)	15.86 (16.05)	3.13	33	Octahedral
[CuLAc]$_2$	Green	80	599	>300	20.96 (21.21)	39.92 (40.06)	4.27 (4.0)	18.03 (18.69)	1.01	35	Square planar
[CdL$_2$]	Off white	67	466	276	25.81 (24.10)	40.98 (41.16)	4.01 (3.85)	23.69 (24.00)	D	50	Tetrahedral
[AgL(H$_2$O)$_2$]	Off white	72	321	>300	34.10 (33.62)	29.43 (29.91)	4.13 (4.05)	17.01 (17.45)	D	9	Tetrahedral

Ac: Acetate, D: Diamagnetic

Table 1.7 Characteristic infrared absorption frequencies of APSC and its transition metal complexes

Complex	$\upsilon_{OH/H2O}$	υ_{N-H}	$\upsilon_{COO}(asym)$	$\upsilon_{C=N}$	$\upsilon_{C=O}$	$\upsilon_{COO}(sym)$	υ_{C-O}	υ_{M-O}	υ_{M-N}
APSC (LH)	3454	3280	-	1633	1697	-	1294	-	-
[(VO)L$_2$]	-	3294	-	1627	-	-	1267	621	498
[Cr LAc$_2$(H$_2$O)]$_2$	3414	3316	1654	1631	-	1438	1265	620	487
[NiLAc(H$_2$O)$_3$]	3441	3305	1685	1583	-	1413	1296	601	491
[CuLAc]$_2$	3456	3292	1687	1579	-	1458	1274	623	476
[CdL$_2$]	-	3286	-	1573	-	-	1253	632	462
[AgL(H$_2$O)$_2$]	3415	3311	-	1597	-	-	1299	620	471

SECTION III

**STUDIES ON VO(II), Cr(III), Ni(II), Cu(II), Cd(II) AND Ag(I)
COMPLEXES OF 3-ACETYLPYRIDINE PHENYLHYDRAZONE**

The chelating ability of the heterocyclic Schiff base 3-acetylpyridine phenylhydrazone (APPH) was exploited by synthesizing transition metal complexes of VO(II), Cr(III), Ni(II), Cu(II), Cd(II) and Ag(I) metal ions. Since tautomerism was not possible in the ligand, the availability coordination site in addition to the azomethine nitrogen atom was not good as that of other Schiff bases such as APTSC and APSC and the ligand acted as a neutral one during the complexation process. The details of synthesis and characterization of metallic complexes of APPH are given in this section.

Synthesis of Complexes

The Schiff base APPH (3mmol) was dissolved in ethanol and heated to reflux in a water bath. To the boiling solution, a hot ethanolic solution (3mmol) of metal salt was added drop wise. The resulting mixture was refluxed for 5 hours and reduced the volume by evaporation. Cooled in ice bath to precipitate the chelate and filtered. The precipitated metal chelate was washed repeatedly with hot ethanol water mixture (1:1) and dried over an. $CaCl_2$.

Characterization of Complexes

The subsequent paragraphs deals with the results and discussion of various strategies employed for the determination of stoichiometry and geometry of complexes. Metal chelates were subjected to elemental, magnetic, conductance measurements and also spectral studies such as IR and UV-visible. All complexes

were coloured, non hygroscopic and stable to light and air. The physical parameters such as colour, yield and melting points are given in Table 1.8.

Elemental analysis

Details of microanalytical data are presented in Table 1.8. The metal percentage and CHNS data revealed that, a 1:1 stoichiometry existed between the ligand and metal ion for Cr(III), Cu(II), Cd(II) and Ag(I) complexes. It was also confirmed that the vanadyl and nickel chelates displayed 1:2 stoichiometry between the metal ion and ligand. The presence of sulphur in the vanadyl complex was also established by the elemental studies. From the data it is quite clear that a good agreement between the calculated and experimental values existed for each analysis.

Magnetic moment studies

Determination of μ_{eff} values was very useful in predicting the exact geometry of complexes. The VO(II) chelate displayed an effective magnetic moment of 1.73BM, indicating square pyramidal geometry of the chelate. Apart from the normal μ_{eff} for Cr(III) octahedral complexes (d^3 system- μ_{eff} calc. 3.87BM) calculated by the spin only formula, it showed a low value of 1.88BM. This is a clear indication of the antiferromagnetic interaction between the Cr(III)-Cr(III) metal ions in the complex. Therefore a dimeric octahedral structure bridged through the acetate moiety (μ-acetato complex) was assigned to this chelate. It is obvious from the Table 1.8 that the Ni(II) chelate displayed μ_{eff} of 2.78BM. This value is in good agreement with the calculated μ_{eff} according to the spin only formula. Thus an octahedral geometry was suggested to the nickel chelate [110,111].

A square planar geometry was assigned to the Cu(II) chelate since it displayed μ_{eff} of 1.97BM (d^9 system), which was further confirmed by electronic spectroscopic studies. The slight enhancement in the μ_{eff} value may be attributed to the orbital contribution. Since the Cd(II) and Ag(I) metal ions did not contain any unpaired electrons, the metal chelates of these ions showed diamagnetic behaviour. With the help of empirical formula derived from microanalytical studies, tetrahedral geometries were assigned to these metal complexes of APPH.

Molar conductance studies

For determining the electrolytic behaviour of metal chelates in DMSO, they were subjected to molar conductance measurements. The data is provided in Table 1.8. It is obvious from the table that all chelates except VO(II) complex exhibited molar conductance in the range 10-52 $\Omega^{-1}cm^2mol^{-1}$. On examining these values one can make assumption that these chelates were behaving as non electrolytes and they do not possesses any counter ions outside the coordination sphere. The VO(II) chelate displayed a molar conductance of 118 $\Omega^{-1}cm^2mol^{-1}$. This higher value is a clear indication of the presence of counter ion outside the coordination sphere and the electrolytic nature of the complex. It was also clear from literature that if the molar conductance of a chelate greater than 110 $\Omega^{-1}cm^2mol^{-1}$, it is a strong evidence for the presence of one anionic moiety outside the coordination sphere [112,113]. Thus the formula of VO(II) chelate was assigned as [VOL$_2$]SO$_4$.

IR spectra of complexes

Interpretation of the IR spectral data was very helpful for the assignment of the correct probe of the ligand which will make coordinate bonds with the central metal ion in a chelate. The characteristic IR stretching frequencies of the Schiff bases and chelates are listed and compared in Table 1.9. The IR spectrum of the Schiff base exhibited a peak at 1593cm^{-1}, which was due to the stretching vibration of azomethine group. On close examination of the spectra of complexes, it is worthwhile to mention that the $\upsilon_{C=N}$ of all chelates lowered to the range 1590-1546cm^{-1}. This is a clear evidence for the complexation of APPH through the azomethine nitrogen atom. Since there was no easily available coordination sites (similar to APTSC and APSC) in the APPH other than the heteroatom of the pyridine ring, the molecule tried to bind the metal ion through the nitrogen atom of the hetero aromatic ring. A confirmatory evidence for this behaviour was obtained from the IR spectral data. The in-plane deformation modes of pyridine ring shown by the ligand at 621 and 667cm^{-1} respectively shifted to 630-677cm^{-1} in chelates, suggesting the coordination of the hetero aromatic nitrogen to the metal [114-117].

Appearance of new bands at 406-423 and 432-467cm^{-1} respectively, is an indication of coordination of the heteroaromatic nitrogen and azomethine nitrogen of the ligand APPH to the central metal ion. The IR spectrum of Cr(III), Ni(II) and Cu(II) complexes displayed asymmetric and symmetric stretching frequencies C-O bond of acetate ion at around 1600 and 1450cm^{-1}, respectively showing a difference of about 150cm^{-1}, indicates the monodentate behaviour of acetate.

Additional bands observed in the IR spectrum of Cr(III) chelate in the range 1570-1460cm^{-1} are assignable to the asymmetric and symmetric stretching vibrations of bridged acetate group. In Cd(II) complex, the nitrate ion behaved as a monodentate ligand. The three NO stretching bands appeared in the IR spectrum of Cd(II) chelate was at 1489[$\upsilon_{(NO2)1}$], 1373[$\upsilon_{(NO2)2}$] and 1033cm^{-1}[$\upsilon_{(NO)}$] respectively. Since the separation of two highest frequency bands was 116cm^{-1}, monodentate nature of the nitrate ion could confirm in Cd(II) chelate. The Ag(I) complex also displayed characteristic stretching frequencies for the nitrate ion in the IR spectrum at 1487 [$\upsilon_{(N=O)1}$], 1251 [$\upsilon_{(NO2)1}$] and 1026 cm^{-1} [$\upsilon_{(NO2)1}$]. In this spectrum, the difference between the highest frequencies was 236cm^{-1}, which assumes the chelating bidentate nature of the nitrate ion in Ag(I) complex. An additional band appeared at 975cm^{-1} in the IR spectrum of VO(II) chelate was the stretching vibrational frequency of V=O bond [118].

Electronic spectra of complexes

Optical absorption bands exhibited by the metal chelates were very supportive to assign the geometry of the chelates. Even though some of the bands shown by the chelates were overlapped with the intra ligand n→π* and π→π* transitions (ILT), generally one can conclude that all ILT transitions were shifted to longer wave length region. This can be taken as a solid evidence for the complexation. The geometry of the chelates was predicted with the help of additional bands displayed in the UV-visible spectrum. Vanadyl chelate displayed two bands at 35523 and 38461cm^{-1}, which are assignable to $^2B_2 \rightarrow {}^2B_1$ and $^2B_2 \rightarrow {}^2A_1$ electronic transitions in the square pyramidal geometry. The three bands

exhibited by the Cr(III) chelate in its electronic spectrum were at 29577, 30200 and 33310cm^{-1}, which are assignable to $^4A_2(F)\rightarrow^4T_2$, $^4A_2(F)\rightarrow^4T_2(F)$ and $^4A_2\rightarrow^4T_1(P)$ electronic transitions in the octahedral field. The first transition was overlapped with the n→π* ILT. Ni(II) complex exhibited two optical bands at 39116 and 40010cm^{-1}, which are due to the $^3A_2\rightarrow^3T_2$, $^3A_2\rightarrow^3T_1(F)$ electronic transitions respectively, and assigned octahedral geometry. Since the optical absorption spectrum gave two bands at 27310 and 28998cm^{-1} for Cu(II) chelate, which are due to $^2B_1\rightarrow^2A_1$ and $^2B_1\rightarrow^2B_2$ transitions respectively, a square planar geometry was proposed. No d-d transitions and charge transfer bands are appeared in the electronic spectra of Cd(II) and Ag(I) chelate in addition to the intra ligand transitions. A tetrahedral geometry was assigned for these complexes.

From the foregoing discussions the geometry of the metal chelates of APPH can be represented as in Figure 1.26.
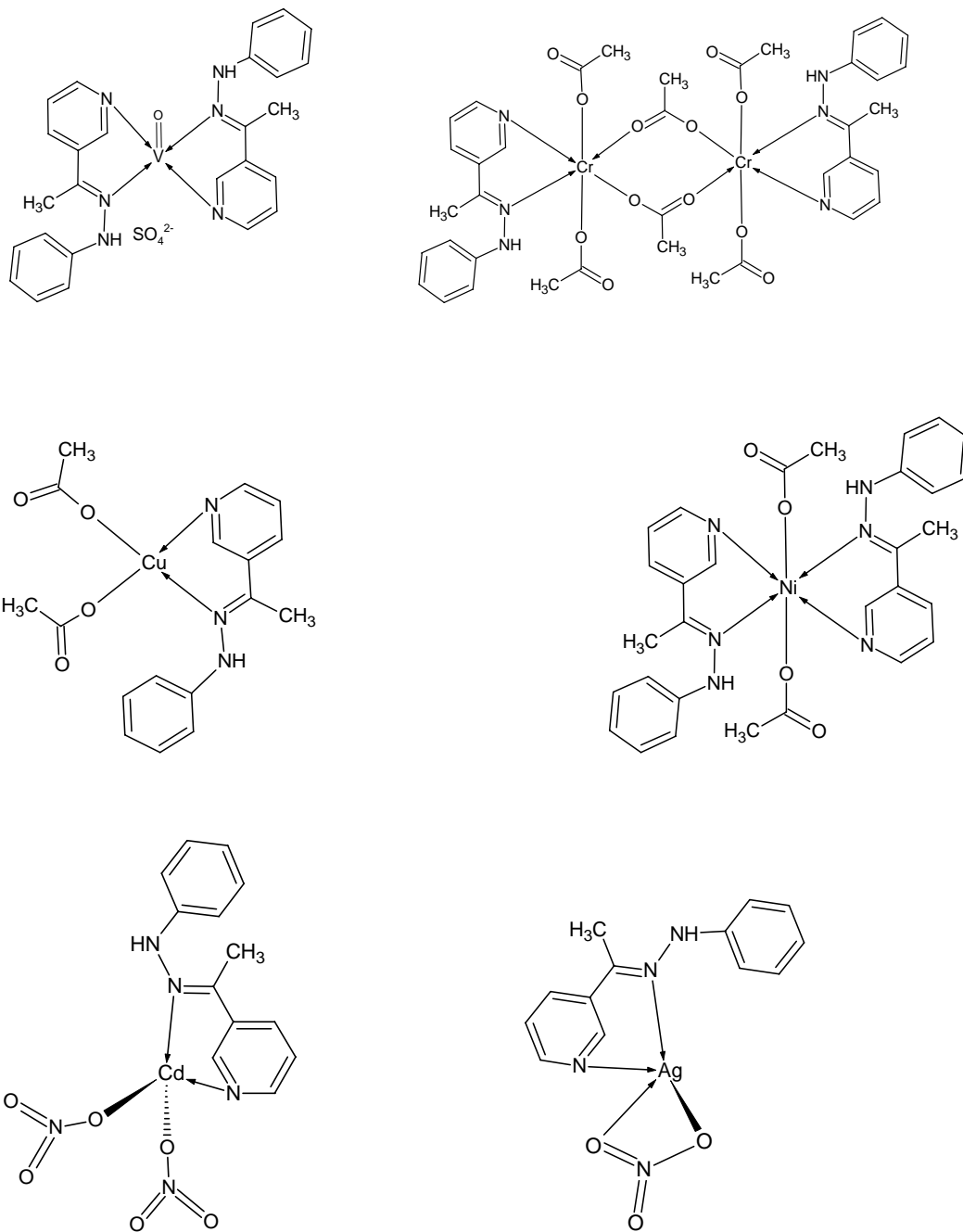
Fig. 1.26 Structures of complexes of APPH

Table 1.8 Microanalytical, magnetic and conductance data of the ligand APPH and its transition metal chelates

Complex	Colour	Yield (%)	Mol. Wt.	M.P (^{0}C)	Metal% Found (Calculated)	C % Found (Calculated)	H % Found (Calculated)	N % Found (Calculated)	S % Found (Calculated)	μ_{eff} (BM)	Molar Conductance ($\Omega^{-1}cm^2mol^{-1}$)	Geometry
APPH (L)	Yellow	82	211	245	-	72.44 (73.93)	5.99 (6.16)	19.15 (19.90)	-	-	-	-
[(VO)L$_2$]SO$_4$	Green	55	585	290	9.10 (8.70)	52.81 (53.33)	4.21 (4.94)	13.89 (14.36)	5.20 (5.47)	1.73	118	Square pyramidal
[CrLAc$_3$]$_2$	Light green	67	880	>300	11.55 (11.8)	51.20 (51.8)	4.91 (5.00)	9.28 (9.54)	-	1.88	31	Octahedral
[NiL$_2$Ac$_2$]	Pale Green	65	599	285	10.12 (9.80)	61.12 (60.12)	5.51 (5.34)	13.98 (14.03)	-	2.78	32	Octahedral
[CuLAc$_2$]	Green	75	393	>300	16.82 (16.21)	50.99 (51.96)	4.33 (4.84)	10.44 (10.69)	-	1.97	15	Square planar
[CdL(NO$_3$)$_2$]	Pale yellow	59	447	248	25.78 (25.12)	34.91 (34.86)	3.11 (2.90)	14.84 (15.64)	-	D	10	Tetrahedral
[AgLNO$_3$]	Grey	61	381	267	29.10 (28.30)	41.03 (40.95)	3.52 (3.41)	14.23 (14.70)	-	D	52	Tetrahedral

Ac: Acetate, D: Diamagnetic

Table 1.9 Characteristic infrared absorption frequencies of APPH and its transition metal complexes

Complex	υ_{N-H}	$\upsilon_{COO}(asym)$	$\upsilon_{C=N}$	$\upsilon_{COO}(sym)$	In plane deformation pyridine	υ_{NO}	$\upsilon_{M-N(C=N)}$	$\upsilon_{M-N(pyr)}$
APPH (L)	3265	-	1593	-	621,667	-	-	-
[(VO)L$_2$]SO$_4$	3250	-	1546	-	617,677	-	467	416
[CrLAc$_3$]$_2$	3394	1591	1552	1410	611,688	-	455	423
[NiL$_2$Ac$_2$]	3366	1622	1570	1422	619,692	-	449	406
[CuLAc$_2$]	3358	1597	1579	1423	625,687	-	434	411
[CdL(NO$_3$)$_2$]	3313	-	1590	-	623,686	1420,1305, 1008	432	419
[AgLNO$_3$]	3286	-	1556	-	661,692	1476,1290, 1025	444	418

CHAPTER 4

STUDIES ON SCHIFF BASES DERIVED FROM ARYLATED FURAN-2-ALDEHYDE AND THIOPHENE-2-ALDEHYDE AND THEIR TRANSITION METAL COMPLEXES

Three Schiff bases namely 4-(5-((2-carabamoylhydrazono)methyl)furan2-yl)benzoic acid (CPFASC), 4-(5-((2-carbamoylhydrazono)methyl)thiophen-2-yl) benzoic acid (CPTASC) and 4-(5-((2-phenylhydrazono) methyl)furan-2-yl)benzoic acid (CPFAPH) were synthesized and characterized using elemental and various spectroscopic techniques. Among the three Schiff bases described above, CPFASC and CPFAPH were derived from furan-2-aldehyde and CPTASC was generated from thiophene-2-aldehyde. Details of synthesis and characterization of the metal chelates of these arylated Schiff bases are given as three sections in this chapter.

The Schiff bases were synthesized in two steps. Step I was the arylation of furan-2-aldehyde/thiophene-2-aldehyde (Meerwin arylation) followed by step II i.e., the condensation reaction between the arylated product with semicarbazide or phenyl hydrazine to get the corresponding Schiff bases.

Meerwin arylation was conducted by standard method, reported [119]. 75mmol of p-aminobenzoic acid was taken in 100ml of water and dissolved by the addition 40ml conc. HCl and cooled in an ice bath to attain a temperature range of 0-5^{0}C. To this, sodium nitrite solution (91mmol in 35ml of water) was added slowly. The reaction mixture was kept for 20 minutes for the completion of diazotization. A 75mmol solution of furan-2-aldehyde or thiophene-2-aldehyde in 50ml acetone was added to the above mixture followed by 23mmol

of $CuCl_2.2H_2O$ in 25ml water with shaking. The entire reaction mixture was kept for 2 days with occasional shaking for the completion of the reaction. The precipitated yellow coloured solid was filtered, washed with copious amount of warm water and dried. Melting point of arylated furfural (CPFA) and arylated thiophene-2-aldehyde (CPTA) was 210^0C and 280^0C respectively. The scheme of step I (Meerwin arylation) is given as follows (Figure 1.27).
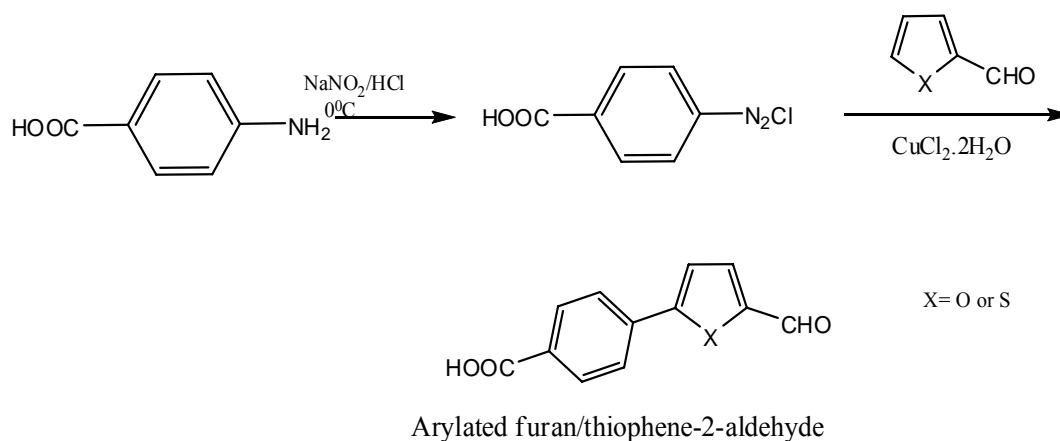

Fig. 1.27 Synthetic strategy of arylated derivative (Meerwin arylation)

Synthesis and Characterization of Schiff Base, Carboxyphenyl Furan-2-Aldehyde Semicarbazone

The arylated furfural derivative (CPFA) was dissolved in ethanol and heated to reflux in a water bath. Equimolar amount of semicarbazide hydrochloride was dissolved in ethanol water mixture (9:1) and added drop wise into the boiling solution. The reaction mixture was refluxed for 4 hours and the volume was reduced by evaporation. The mixture was kept for overnight and the precipitated compound was filtered, washed with ethanol-water mixture and dried. M.P= 290^0C. The reaction pathway is represented in the Figure 1.28.
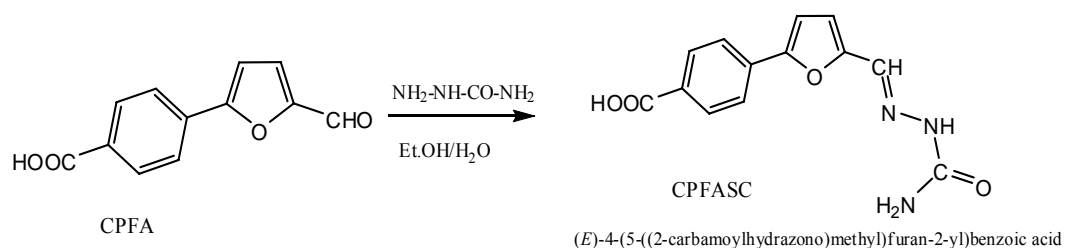
Fig. 1.28 Synthesis of CPFASC

The Schiff base CPFASC was subjected to elemental and spectroscopic analyses to establish the correct structure. CHN data (Table 1.13) revealed that the experimental values were in good agreement with the calculated values.
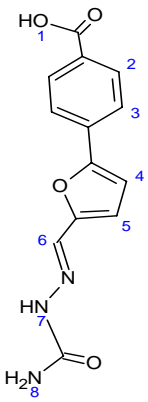
NMR spectral studies

The [1]Hnmr spectrum of the Schiff base (CPFASC), contained characteristic signals for eight different protons. The exact assignment of the protons is given in Table 1.10. The –COOH proton signal was appeared at 10.3δ. A singlet appeared at 7.73δ was due to the proton of azomethine group. A broad singlet displayed at 6.38δ was assignable to NH proton. The aromatic protons of the benzene ring resonated between 7.8-7.9δ, while protons on furfural segment exhibited its characteristic peaks between 6.9-7.2δ. A broad signal appeared at 3.27δ was assignable to NH_2 protons. Possibility of tautomerism in the molecule was confirmed by the appearance of a weak signal at 12.93δ, which was due to the enol OH. The [1]Hnmr spectrum of the Schiff base CPFASC is given in Figure 1.29.

The [13]Cnmr spectrum of the Schiff base CPFASC is provided in Figure 1.30. The eleven carbon atoms under different electronic environment in the molecule gave their characteristic signals and the exact assignments of the signals

are listed in Table 1.10. The carboxylic carbon gave its characteristic signal at 166.87ppm. A moderate signal appeared at 152.55ppm was due to the azomethine carbon atom. The carbonyl carbon of semicarbazide part showed a peak at 156.4ppm. Peaks due to other aromatic and furan carbon atoms were appeared in the ^{13}Cnmr spectrum between 113-134ppm.

Table 1.10 ^{1}Hnmr and ^{13}Cnmr spectral data of CPFASC

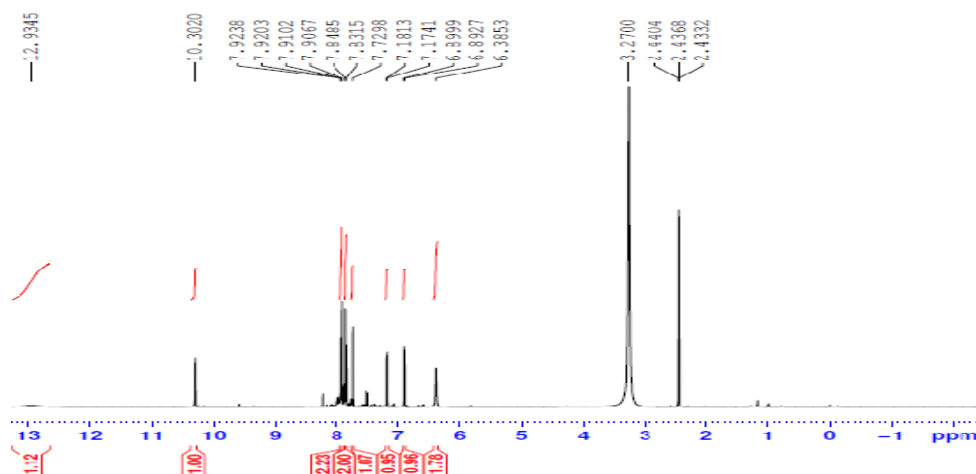|	^{1}Hnmr		^{13}Cnmr		
	δ value	Assignment/ Labelled No	δ value	Assignment/ Labelled	
	10.3(s,1H)	1(COOH)	166.87	1	
	7.91(d,1H)	2	150.55	2	
	7.83(d,1H)	3	129.95	3	
	7.73(s,1H)	6(CH)	123.59	4	
	7.18(d,1H)	5	113.32	5	
	6.89(d,1H)	4	129.18	6	
	6.38(s$_{br}$,1H)	7(NH)	110.25	7	
	3.27(s$_{br}$,2H)	8(NH$_2$)	131.12	8	
	12.93(s$_{br}$,1H)	OH(enol)	133.38	9	
			152.55	10	
			156.40	11	

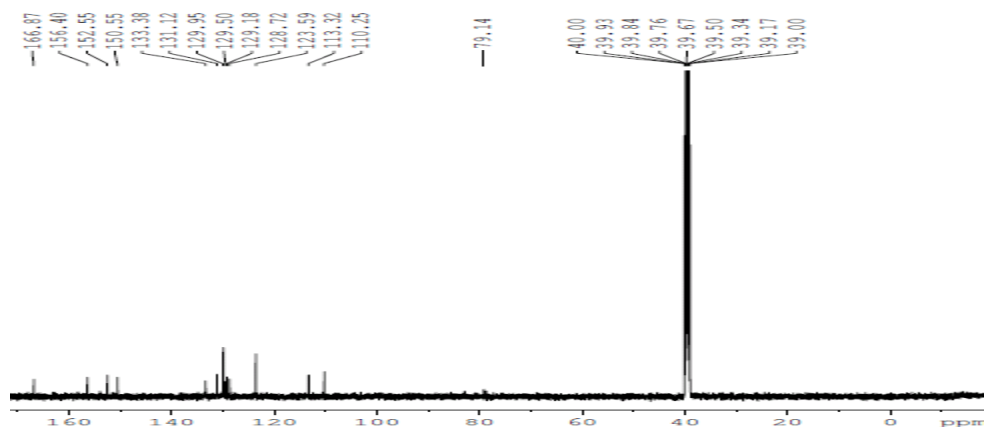**Fig. 1.29** ^{1}Hnmr spectrum of the Schiff base CPFASC

Fig. 1.30 ^{13}Cnmr spectrum of the Schiff
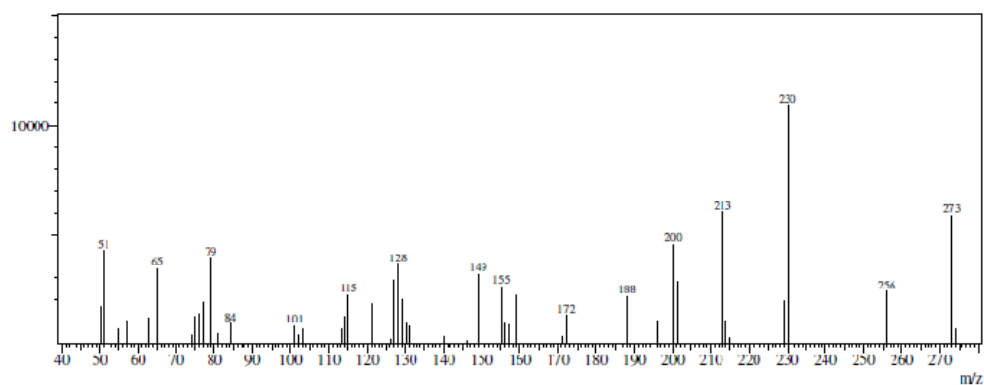
Fig. 1.31 Mass spectrum of the Schiff base CPFASC

Mass spectral studies

GCMS of the Schiff base CPFASC was recorded in order to establish the purity as well as the molecular weight of the compound. Mass Spectrum of the Schiff base is provided in the Figure 1.31. The molecular ion peak appeared at m/z 273 shows the stability of the molecule. M+1 peak was also shown by the molecule at m/z 274 with relative abundance 8.1. Loss of the OH moiety resulted in the fragment $[C_3H_{10}N_3O_3]^+$, which appeared at m/z 256. The base peak displayed in the spectrum at m/z 230 was due to the fragment $[C_{12}H_{10}N_2O_3]^+$. This fragment emerged in the mass spectrum was due to the loss of amide group from

the molecule. Other significant signals emerged at m/z 200 and 188 was due to the fragments $[C_{12}H_8O_3]^+$ and $[C_{11}H_8O_3]^+$ respectively. A medium signal displayed at m/z 115 was attributed to the fragment $[C_9H_7]^+$. The fragment of furfural part $[C_5H_3O]^+$ displayed a peak at m/z 79.

IR spectral studies

The FTIR spectrum of the Schiff base gave characteristic stretching frequencies for different bond vibrations. A sharp signal appeared at 1666cm^{-1} was due to stretching frequency of C=N. The vibrational frequency of O-H in carboxylic acid and appeared at 3477cm^{-1}. The asymmetrical and symmetrical stretching vibration of carboxylic group displayed at 1689 and 1429cm^{-1} respectively. A medium peak observed at 3400 and 3427cm^{-1} are due to the vibrations of terminal amino group. Also the N-H vibrational frequency displayed in the spectrum at 3363cm^{-1}. A weak band observed at 3401cm^{-1} can be attributed to the O-H stretching frequency of enol form which arises due to the tautomerism in the molecule.

Electronic spectral studies

The Schiff base CPFASC displayed two peaks at 27777cm^{-1} and 28490cm^{-1} in the UV-vis spectrum, are assignable to n→π* and π→π* electronic transitions.

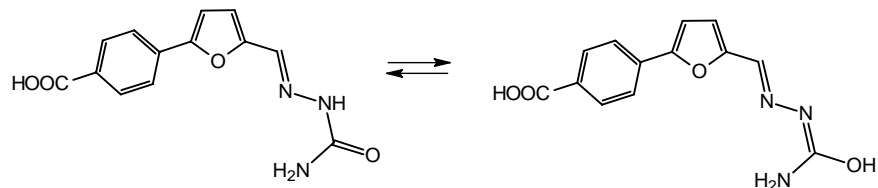The above discussion clearly establishes the structure of the Schiff base CPFASC, which is represented in Figure 1.32.

Fig. 1.32 Structure of CPFASC and keto-enol tautomerism

Synthesis and Characterization of Schiff Base, Carboxyphenyl Thiophene-2-Aldehyde Semicarbazone

To the hot ethanolic solution of arylated thione-2-aldehyde derivative (CPTA) prepared by Meerwin arylation technique, equimolar amount of semicarbazide hydrochloride in ethanol-water mixture (9:1) was added drop wise. The reaction mixture was refluxed for 7 hours. It was then evaporated, cooled and filtered. The precipitate was washed with copious amount of hot ethanol-water mixture (3:2) and dried and kept over an. $CaCl_2$. M.P=220^{0}C. Figure 1.33 represents the formation of the Schiff base CPTASC.

CPTASC

(*E*)-4-(5-((2-carbamoylhydrazono)methyl)thiophen-2-yl)benzoic acid

Fig. 1.33 Synthesis of CPTASC

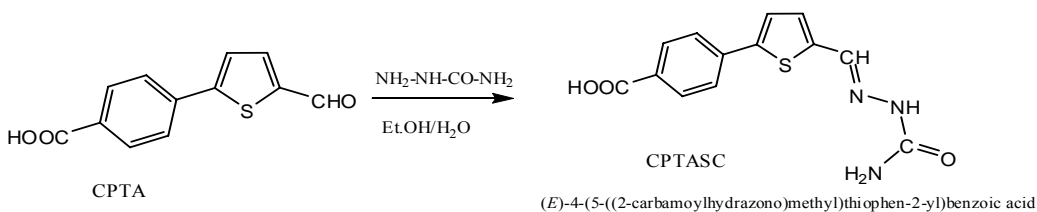The elemental analytical data (CHNS) of the Schiff base CPTASC is listed in Table 1.15. Data shows a fare agreement with the theoretical values.

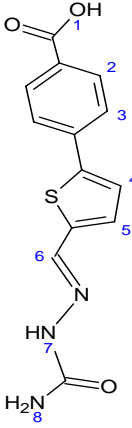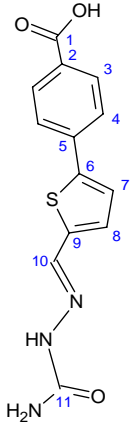### NMR spectral studies

The ^{1}Hnmr spectrum of the Schiff base CPTASC gave signals due to eight hydrogen atoms in different environments. The –COOH proton of the molecule appeared at 10.37δ as a singlet. Broad singlets observed at 6.34δ and 3.37δ were

due to the NH and NH$_2$ protons respectively. The azomethine proton peak appeared at 7.93δ. Table 1.11 shows the exact assignment of the labeled protons of CPTASC. ^{1}Hnmr spectrum of CPTASC is provided in Figure 1.34.

^{13}Cnmr spectrum of CPTASC exhibited characteristic signals due to eleven carbon atoms in different fields. The highly deshielded carboxylic carbon and carbonyl carbon of the amino part appeared at 179 and 173ppm respectively. A signal at 156.8ppm in ^{13}Cnmr spectrum was assigned to the azomethine carbon atom. Other signals appeared between 149-93ppm could assign to the benzenoid and thiophene carbon atoms. The ^{13}Cnmr spectrum of the Schiff base CPTASC and the assignment of signals for the labeled carbon atoms are given in Figure 1.35 and Table 1.11 respectively.

Table 1.11 ^{1}Hnmr and ^{13}Cnmr spectral data of CPTASC

^{1}Hnmr			^{13}Cnmr		
	δ value	Assignment	δ value	Assignment/ Labelled No.	
	12.99(s$_{br}$,1H)	OH (enol)	179.08	1	
	10.37(s,1H)	1(COOH)	173.81	11	
	8.01(d,1H)	2	156.87	10	
	7.93(s,1H)	6(CH=N)	149.67	2	
	7.64(d,1H)	5	147.74	3	
	7.24(d,1H)	4	132.03	4	
	7.63(dd,1H)	3	128.38	6	
	6.34(s$_{br}$,1H)	7(NH)	120.76	7	
	3.37(s$_{br}$,2H)	8(NH$_2$)	113.34	9	
			105.17	8	
			93.59	5	

Fig. 1.34 ^{1}Hnmr spectrum of the Schiff base CPTASC
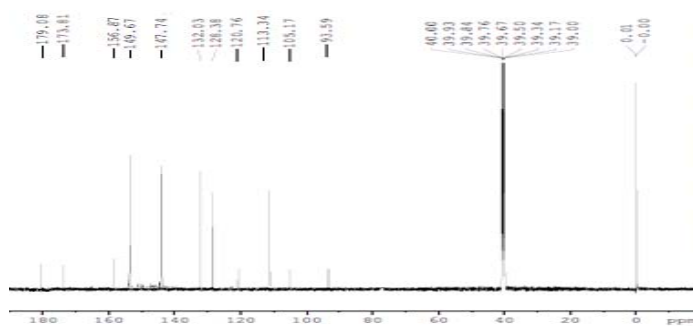
Fig. 1.35 ^{13}Cnmr spectrum of the Schiff base CPTASC

Mass spectral studies

The molecular ion peak was absent in the GCMS of CPTASC. The base peak appeared in the spectrum at m/z 59 is due to the fragment $[NHCONH_2]^+$. The rest of the molecular fragment $[C_{12}H_7NO_2S]^+$ displayed a signal at m/z 229. The peak due to the fragment $[C_{12}H_6NOS]^+$ emerged in the spectrum at m/z 212. The thiophene moiety $[C_4H_4S]^+$ showed a signal at m/z 84. Mass Spectrum of CPTASC is depicted in Figures 1.36.
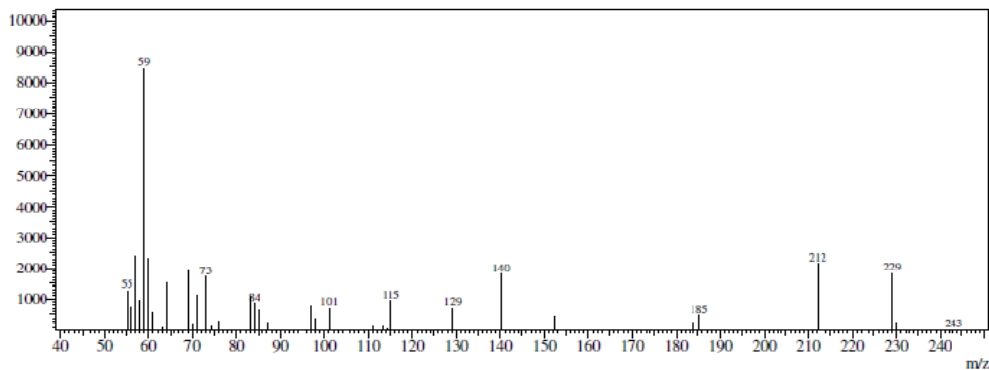
Fig. 1.36 Mass spectrum of the Schiff base CPTASC

IR spectral studies

Fourier transform infrared spectrum of the ligand CPTASC exhibited stretching frequencies at 1597, 1689cm^{-1} was due to $\upsilon_{C=N}$ and $\upsilon_{C=O}$ respectively. The broad band appeared in the range 3000-3400cm^{-1} was the stretching frequencies of NH and NH$_2$. The carboxylic OH stretching vibration was supposed to merge with this broad band. The asymmetric and symmetric vibrations of the carboxylic group displayed their characteristic signals at 1689 and 1421cm^{-1} respectively.

Electronic spectral studies

The two important peaks showed by the Schiff base CPTASC, in the UV-visible spectrum was at 28571 and 36630cm^{-1}, which are assignable to n→π* and π→π* electronic transitions. From the foregoing discussion, the structure of the Schiff base can be represented as in Figure 1.37.
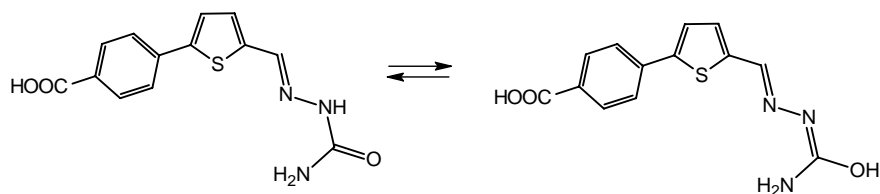
Fig. 1.37 Structure of CPTASC and keto-enol tautomerism

Synthesis and Characterization of Schiff Base, Carboxyphenyl Furan-2-Aldehyde Phenylhydrazone

Phenylhydrazine hydrochloride (3mmol) in ethanol-water mixture (9:1) was added to a boiling solution of CPFA (3mmol) under reflux. The entire mixture was further refluxed for 6 hours for the completion of the reaction. The volume of the mixture was reduced by evaporation, kept overnight and filtered. The precipitated compound was washed with ethanol water mixture (1:9) and dried. M.P=222^0C. The reaction pathway is depicted in Figure 1.38.

(*E*)-4-(5-((2-phenylhydrazono)methyl)furan-2-yl)benzoic acid
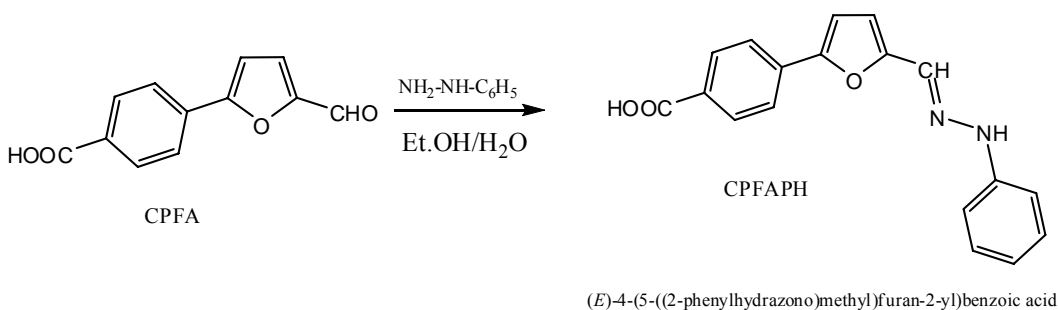
Fig. 1.38 Synthesis of CPFAPH

The compound was subjected CHN analysis and the data is reported in Table 1.17. Experimental values were found to agree with the calculated values.
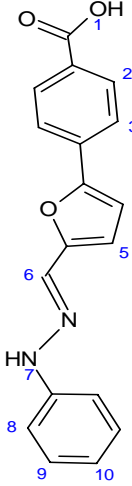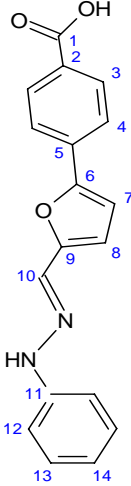
NMR spectral studies

The proton nmr spectrum of the Schiff base is given in Figure 1.39. Signals for ten nonequivalent set of hydrogen atoms at different electronic environments were appeared in the spectrum. A singlet appeared in the highly deshielded region (10.55δ) was due to the –COOH proton. A weak signal exhibited by the molecule at 8.318δ was the peak due to azomethine proton. A singlet broad peak observed at 3.47δ was assignable to the NH proton. Other aromatic protons of the benzene ring showed their characteristic signals between

6.8-7.9δ in the spectrum. The exact assignments of the various signals of ¹Hnmr are listed in Table 1.12.

The proton decoupled ¹³Cnmr spectrum of CPFAPH gave characteristic peaks for 14 different carbon atoms in different environments. The carboxylic and the azomethine carbons showed their peaks at 166.09ppm and 143.87ppm respectively. The other aromatic carbon atoms of both benzenoid and furanoid rings showed their characteristic signals between 110.50-150.83ppm. The assignments of signal for the labelled carbon atoms of the molecule are provided in Table 1.12 and the ¹³Cnmr spectrum of CPFAPH is shown in Figure 1.40.

Table 1.12 ¹Hnmr and ¹³Cnmr spectral data of CPFAPH

¹Hnmr			¹³Cnmr		
	δ value	Assignment/ Labelled No.	δ value	Assignment/ Labelled No.	
	10.55(s,1H)	1(COOH)	166.09	1	
	8.32(s,1H)	6(CH=N)	150.83	7	
	7.99(dd,1H)	2	150.75	8	
	7.85(dd,1H)	3	143.87	10	
	7.81(d,1H)	5	132.69	2	
	7.08(d,1H)	9	129.20	3	
	7.24(s,2H)	8,4	128.29	4	
	6.80(d,1H)	10	125.55	6	
	3.47(s$_{br}$,1H)	7(NH)	122.34	12	
			118.22	9	
			111.15	13	
			110.50	5,11	
			109.63	14	

Fig. 1.39 ^{1}Hnmr spectrum of the Schiff base CPFAPH
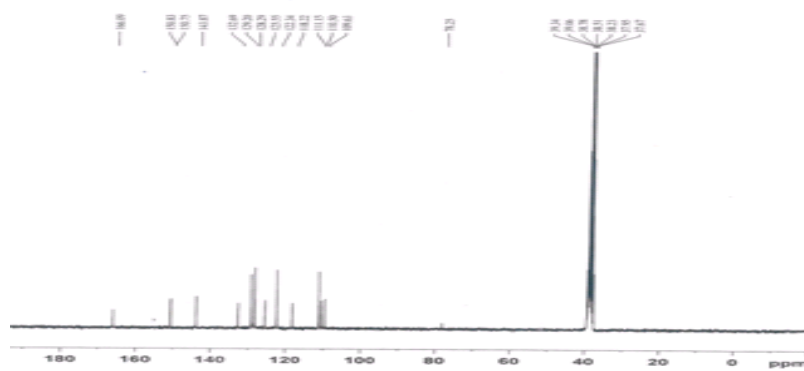
Fig. 1.40 ^{13}Cnmr spectrum of the Schiff base CPFAPH
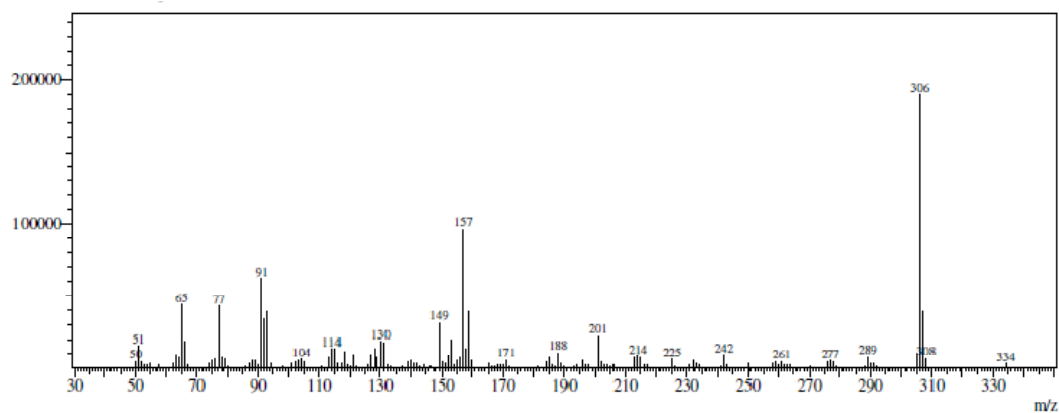
Fig. 1.41 Mass spectrum of the Schiff base CPFAPH

Mass spectral studies

The base peak appeared in the spectrum was the molecular ion peak itself at m/z 306. An intense signal displayed at m/z 157 was due to the fragment $[C_{11}H_9O]^+$. The fragment $[C_6H_5N]^+$ appeared in the spectrum at m/z 91. Other peaks appeared at m/z=65 and 51 can be assigned to the secondary fragments $[C_5H_5]^+$ and $[C_4H_3]^+$. The mass spectrum of CPFAPH is represented in Figure 1.41.

IR spectral studies

The CPFAPH Schiff base showed characteristic vibrational frequencies in the spectrum correspond to different bond stretching. An intense peak observed at 1600cm^{-1} was due to the stretching of azomethine group. Broad signals appeared at 3431 and 3307cm^{-1} was assignable to O-H and N-H bond vibrations. The symmetric and asymmetric stretching vibrations of the carboxylic group displayed at 1425 and 1668cm^{-1} respectively.

Electronic spectral studies

Electronic transitions showed by the Schiff base CPFAPH was at 24721 and 33112cm^{-1} which are assignable to n→π* and π→π* transitions.

Based on the elemental analysis and spectral studies, structure of heterocyclic Schiff base CPFAPH can be represented as given in Figure 1.42.
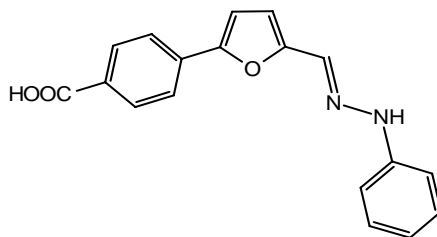
Fig. 1.42 Structure of CPFAPH

SECTION I

STUDIES ON Cr(III), Ni(II), Cu(II) AND Ag(I) COMPLEXES OF CARBOXYPHENYL FURAN-2-ALDEHYDE SEMICARBAZONE

To check the chelating efficacy of the newly synthesized Schiff base, carboxyphenyl furan-2-aldehyde semicarbazone (CPFASC), transition metal chelates were prepared and characterized. The monovalent bidentate nature of the Schiff base was established by IR and NMR spectral studies. Stoichiometry and geometry of chelates were determined by UV-visible spectroscopy, elemental, magnetic and conductance studies. The details are reported in this section.

Synthesis of Complexes

A 3mmol solution of CPFASC was prepared in 10ml of ethanol and heated in a water bath. To the hot solution, 3mmol solution of metal salts in ethanol-water mixture (10:1) was added. The whole reaction mixture was refluxed for 4 hours. The volume of the solution was reduced by evaporation, cooled and filtered. The precipitated complex was washed many times with hot ethanol and dried. Acetates of Cr(III), Ni(II) and Cu(II) was used as metal salts, while $AgNO_3$ was employed for the preparation of silver complex.

Characterization of Complexes

All complexes were coloured, amorphous solids, non hygroscopic, partially soluble in DMSO and stable to air and light. The details of elemental analysis, molar, conductance and spectral studies of the chelates are given in the subsequent paragraphs.

Elemental analysis

Exact stoichiometry of the metal chelates was achieved by performing the elemental analysis. Volumetric method was employed for the determination of metal percentage of copper and silver chelates while colorimetric and gravimetric methods were used for the estimation of chromium and nickel. CHN data of the complexes is reported in Table 1.13.   A good agreement was noticed between the theoretical and experimental values. Analyses showed that 1:2 stoichiometry exist between the metal and ligand for the chelates Cr(III) and Ni(II), while 1:1 stoichiometry was followed by Cu(II) and Ag(I) complexes.

Magnetic moment studies

The geometry of the complexes was mainly ascertained by magnetic moment studies. The Cr(III) chelate showed a μ_{eff} of 3.77 BM, which was in good agreement with the calculated value for d^3 configuration using spin only formula and hence octahedral geometry was suggested to this chelate. Similarly a distorted octahedral geometry was assigned to the Ni(II) chelate, since it displayed μ_{eff} of 3.25BM. A slight increase in the μ_{eff} value from the theoretical value was noted and this may be due to the contribution from orbital motion to the effective magnetic moment. Copper complex exhibited μ_{eff} 1.91BM and a square planar geometry was assigned. This was further verified by electronic spectral data. Diamagnetic behaviour was shown by the Ag(I) chelate and assumed tetrahedral geometry. The magnetic moment values of different complexes are listed in Table 1.13.

Molar conductance studies

To verify the electrolytic behaviour of metal chelates, these were subjected to molar conductance studies in DMSO medium. All chelates showed molar conductance in the range 14-32 $\Omega^{-1}cm^2mol^{-1}$, which shows the non-electrolytic behaviour of the chelates. The absence of any counter ions outside the coordination sphere was also confirmed by this investigation. The data is represented in Table 1.13.

IR spectra of complexes

FTIR spectral data of the ligand and metal chelates are displayed in Table 1.14. In comparison with the spectrum of ligand CPFASC, the IR spectra of all complexes showed considerable differences in the vibrational frequencies. The azomethine stretching vibration of the ligand was shifted to lower frequencies, suggesting that one of the coordination site of CPFASC is the nitrogen atom of C=N group. The weak band appeared in the infrared spectrum of CPFASC at 3401cm^{-1} was due to the tautomeric enol OH stretching frequency. This band was totally absent in all complexes, which indicates that the ligand was coordinated through the enol oxygen after deprotonation. In addition to this, appearance of new medium bands at 518-530cm^{-1} was due to the M-O vibrations. A very broad signal appeared in the spectrum of all chelates at about 3500cm^{-1} was due to the presence of coordinated water molecules. Since the O-H stretching frequency of the carboxylic group attached to the benzene ring did not change appreciably in all complexes compared to that of ligand, it was assumed that this group is not participating in the coordination process. The symmetric and asymmetric

stretching frequencies of the acetate ion and the carboxylic group also displayed their characteristic stretching frequencies in complexes.

^{1}Hnmr spectra of complexes

To confirm the exact coordination site of the ligand CPFASC on the metal ion, ^{1}Hnmr spectrum was very helpful. Generally all proton signals appeared in the ^{1}Hnmr spectrum of the ligand showed a down field shift is an indication of complexation. In addition to this, one can see three significant features in the ^{1}Hnmr spectral studies of complexes when compared to that of ligand. The proton signal appeared at 10.3δ in the ^{1}Hnmr of CPFASC, remain unaltered in all complexes. This is a strong evidence for the non-participation of –COOH group in complexation. Secondly, the disappearance of a weak broad singlet at 12.93δ (due to enolic OH) in the spectrum of chelates, suggest that the ligand was attached to the metal ions definitely after deprotonation of the enolic form. Thirdly, the disappearance of the peak due to the NH proton at 6.38δ also strongly supports binding of deprotonated tautomeric form with the metal ion. It is also worthwhile to note that the azomethine proton signals of all chelates appeared in the range 7.9-8.3δ which is a clear evidence for the complexation of CPFASC through C=N linkage.

Electronic spectra of complexes

In addition to the intra ligand electronic transitions (ILT), complexes exhibited additional bands due to d-d transitions and charge transfer processes. All ILT bands shifted to longer wavelength region, indicating the complex formation. Cr(III) chelate exhibited three d-d transitions at 26455, 31347 and

37313cm^{-1}, which are assignable to $^4A_2(F)\rightarrow^4T_2$, $^4A_2(F)\rightarrow^4T_2(F)$ and $^4A_2\rightarrow^4T_1(P)$ transitions respectively in the octahedral field. Two bands displayed by the Ni(II) complex at 31325 and 33662cm^{-1} are owed to the $^3A_2\rightarrow^3T_2$ and $^3A_2\rightarrow^3T_1(F)$ electronic transitions, which confirms the octahedral geometry. A square planar geometry to Cu(II) chelate was assigned since the optical absorption spectrum gave two bands at 29169 and 39215cm^{-1}, which are due to the transitions $^2B_1\rightarrow^2A_1$ and $^2B_1\rightarrow^2B_2$ respectively. Charge transfer bands was displayed by Ag(I) chelate in addition to ILT, at 31897cm^{-1} and tetrahedral geometry was assigned to this complex.

Discussions clearly establish the structure of metal chelates of CPFASC and it is given in the Figure 1.43.
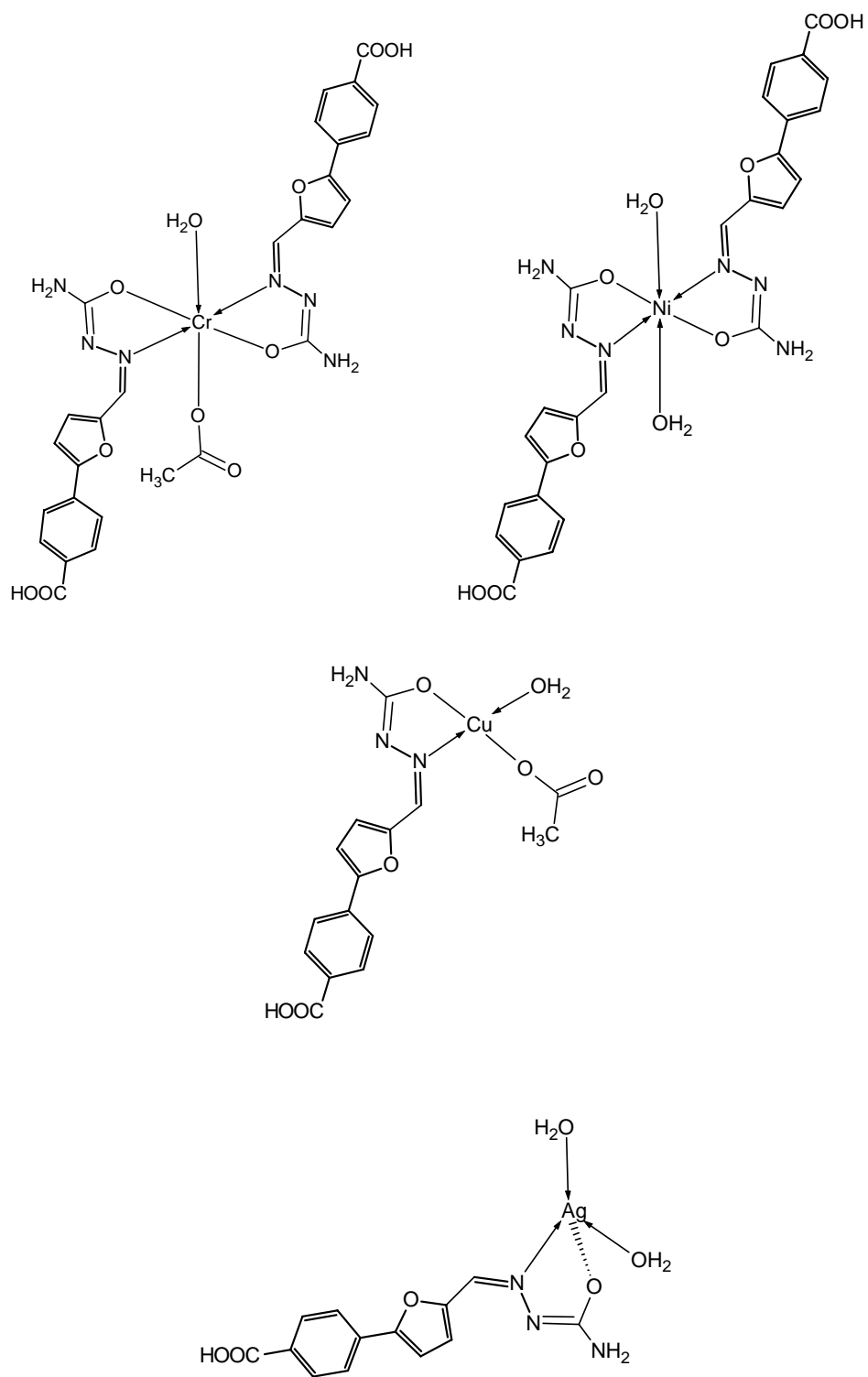
Fig. 1.43 Structures of complexes of CPFASC

Table 1.13 Microanalytical, magnetic and conductance data of the ligand CPFASC and its transition metal chelate

Complex	Colour	Yield (%)	Mol. Wt.	M.P (^{0}C)	Metal % Found (Calculated)	C % Found (Calculated)	H % Found (Calculated)	N % Found (Calculated)	μ_{eff} (BM)	Molar Conductance ($\Omega^{-1}cm^2mol^{-1}$)	Geometry
CPFASC (LH)	Yellow	82	273	290	-	55.85 (57.14)	4.14 (4.03)	14.44 (15.38)	-	-	-
[CrL$_2$Ac(H$_2$O)]	Pale green	72	673	>300	7.98 (7.73)	48.64 (49.93)	3.88 (3.71)	11.87 (12.48)	3.77	28	Octahedral
[NiL$_2$(H$_2$O)$_2$]	Pale Green	71	639	279	9.67 (9.19)	47.87 (48.84)	3.92 (3.75)	12.95 (13.15)	3.25	22	Octahedral
[CuLAc(H$_2$O)]	Green	74	413	>300	14.99 (15.40)	42.74 (43.63)	3.73 (3.63)	9.84 (10.18)	1.91	14	Square planar
[AgL(H$_2$O)$_2$]	Ash	69	416	269	26.31 (25.93)	36.22 (37.51)	3.67 (3.37)	11.13 (10.09)	D	32	Tetrahedral

Ac: Acetate, D: Diamagnetic

Table 1.14 Characteristic infrared absorption frequencies of CPFASC and its transition metal complexes

Complex	$\upsilon_{COOH/H2O}$	υ_{N-H}	$\upsilon_{COO}(asym)$	$\upsilon_{C=N}$	$\upsilon_{COO}(sym)$	υ_{C-O}	υ_{M-O}	υ_{M-N}
CPFASC (LH)	3477	3363	1689	1666	1429	1286	-	-
[CrL$_2$Ac(H$_2$O)]	3475,3515	3309	1688	1583	1421	1282	530	449
[NiL$_2$(H$_2$O)$_2$]	3473,3501	3215	1660	1582	1415	1280	518	467
[CuLAc(H$_2$O)]	3475,3499	3209	1672	1585	1423	1288	528	465
[AgL(H$_2$O)$_2$]	3480,3490	3340	1672	1589	1427	1239	529	475

SECTION II

STUDIES ON Cr(III), Fe(III), Ni(II), Cu(II), Zn(II) AND Cd(II) COMPLEXES OF CARBOXYPHENYL THIOPHENE-2-ALDEHYDE SEMICARBAZONE

Metal chelates of the Schiff base carboxyphenyl thiophene-2-aldehyde semicarbazone (CPTASC) were synthesized and characterized. Investigations showed that 1:2 stoichiometry existed between metal and ligand for Cr(III), Fe(III) and Ni(II) complexes, while 1:1 stoichiometry was shown by Zn(II) and Cd(II) complexes. The details of synthesis and structural evaluation of the metal chelates by various techniques are given in this section.

Synthesis of Complexes

The Schiff base CPTASC (3mmol) was dissolved in 10ml of ethanol and heated in a water bath. To the hot solution, 3mmol metal salt solution in ethanol was added drop wise. The reaction mixture was refluxed for 5 hours. pH of the solution was adjusted (pH 7-8) by adding few drops of saturated CH_3COONa solution. Volume of the mixture was reduced by evaporation, cooled in an ice bath, filtered and dried over an. $CaCl_2$.

Characterization of Complexes

Stoichiometry of metal chelates was achieved by the CHNS and metal percentage estimations. Complexes were insoluble in ethanol, but showed appreciable solubility in DMSO and DMF. All complexes were amorphous solids and stable to air and light. Details of characterization of complexes are given in this section.

Elemental analysis

The metal percentage and CHNS data are provided in Table 1.15. The theoretical values are also showed in parenthesis. Experimental values were in good agreement with the theoretical values. Analyses clearly ascertained that 1:2 stoichiometry was found between metal and ligand for Cr(III), Fe(III) and Ni(II) complexes, but 1:1 stoichiometry was exhibited by Zn(II) and Cd(II) complexes.

Magnetic moment studies

Chromium complex displayed μ_{eff} of 3.99BM, which suggests an octahedral geometry to the complex. For Fe(III) chelate, octahedral geometry was assigned, since it exhibited an effective magnetic moment of 5.41BM. This value showed a close agreement with the calculated value for d^5 configuration, using spin only formula. The nickel chelate showed μ_{eff} of 3.1BM, indicating octahedral geometry. A distorted square planar geometry was given for Cu(II) chelate (d^9 system), because it exhibited 2.01BM for effective magnetic moment. As expected Zn(II) and Cd(II) chelates were diamagnetic in nature due to the absence of unpaired electrons. Tetrahedral geometry was the fit one for these complexes, which was proposed mainly by elemental studies. The results are summarized in table 1.15.

Molar conductance studies

The non electrolytic nature of the metal chelates was confirmed by molar conductance studies. Poor values of molar conductance ranging between 18-33 $\Omega^{-1}cm^2mol^{-1}$ in DMSO showed by these chelates emphasized that they are acting

as non electrolytes. Absence of any counter ions outside the coordination sphere was also confirmed by these studies.

IR spectra of complexes

The azomethine stretching vibration of the CPTASC was shifted to lower frequencies, suggesting that one of the coordination site of CPTASC is the nitrogen atom of C=N group. Presence of coordinated water molecules in all chelates was assured by the emergence of very broad signals between 3300-3500cm^{-1}. Since the stretching frequency of O-H of carboxylic group (3454cm^{-1}) attached to the benzene ring did not change appreciably in complexes, we can assume that this group is not participating in the coordination process. Though the symmetric and asymmetric stretching frequencies of the acetate ion and the carboxylic group displayed in the spectrum of complexes, their exact assignment was difficult due to the overlapping of peaks. The OH stretching vibration of enolic group which appeared in the IR spectrum of ligand at 3224cm^{-1} was absent in the spectra of all chelates, indicating that the metal ion was coordinated through the oxygen atom after deprotonation. The appearance of additional bands in the spectra of chelates at about 520-540cm^{-1} was due the M-O vibrations. Moreover the vanishing of C=O vibrations from the IR spectrum of chelates also indicate the coordination through the oxygen atom. The details of IR spectral data of the ligand and complexes are provided in Table 1.16.

^{1}Hnmr spectra of complexes

In ^{1}Hnmr spectra of complexes, all peaks were found to shift to downfield region in comparison with the spectrum of ligand, indicating that complexation

was occurred between metal and CPTASC. The non involvement of the –COOH group in coordination was confirmed by the appearance of signal at 10.37δ in all complexes. A broad singlet appeared in the ^{1}Hnmr spectrum of CPTASC at 12.99δ was due to the enolic proton and this signal was totally disappeared in all chelates, suggesting that deprotonated ligand (after tautomerization) was attached to the metal ion during complexation. Also, disappearing of the broad singlet due to NH proton at 6.34δ from the spectra of chelates clearly supports the above argument. Moreover, the azomethine proton signal of CPTASC shifted to downfield region in all chelates, approving that the one of the coordination site of the ligand was C=N group.

Electronic spectra of complexes

The complexation of the ligand was further verified by the shifting of intra ligand electronic transitions to longer wavelength. Other optical absorption bands due to d-d transitions were also displayed by the metal chelates. Cr(III) chelate exhibited three d-d transitions at 22597, 29444 and 31267 cm^{-1} which are assignable to $^{4}A_{2}(F)\rightarrow^{4}T_{2}$, $^{4}A_{2}(F)\rightarrow^{4}T_{2}(F)$ and $^{4}A_{2}\rightarrow^{4}T_{1}(P)$ transitions respectively in the octahedral field. Ni(II) complex displayed two d-d transition at 32600 and 37409cm^{-1}, assignable to the $^{3}A_{2}\rightarrow^{3}T_{2}$ and $^{3}A_{2}\rightarrow^{3}T_{1}(F)$ electronic transitions, which confirms the octahedral geometry. A strong L→M charge transfer band also appeared at 25370cm^{-1}. Iron complex exhibited two LMCT transitions in addition to ILT at 39370 and 40899cm^{-1} respectively. Signals appeared in the electronic spectrum of Cu(II) chelate at 26420cm^{-1} and 30303cm^{-1} respectively were regarded as the transitions $^{2}B_{1}\rightarrow^{2}A_{1}$ and $^{2}B_{1}\rightarrow^{2}B_{2}$ in the square

planar geometry. An intense peak appeared at 26730cm^{-1} in the electronic spectrum of Zn(II) chelate can be assigned to ligand to metal CT band. No additional CT transitions in addition to ILT were observed in the optical absorption spectrum of Cd(II) chelate. Foregoing results and discussion established the structure and geometry of metal chelates of CPTASC and they are depicted in Figure 1.44.
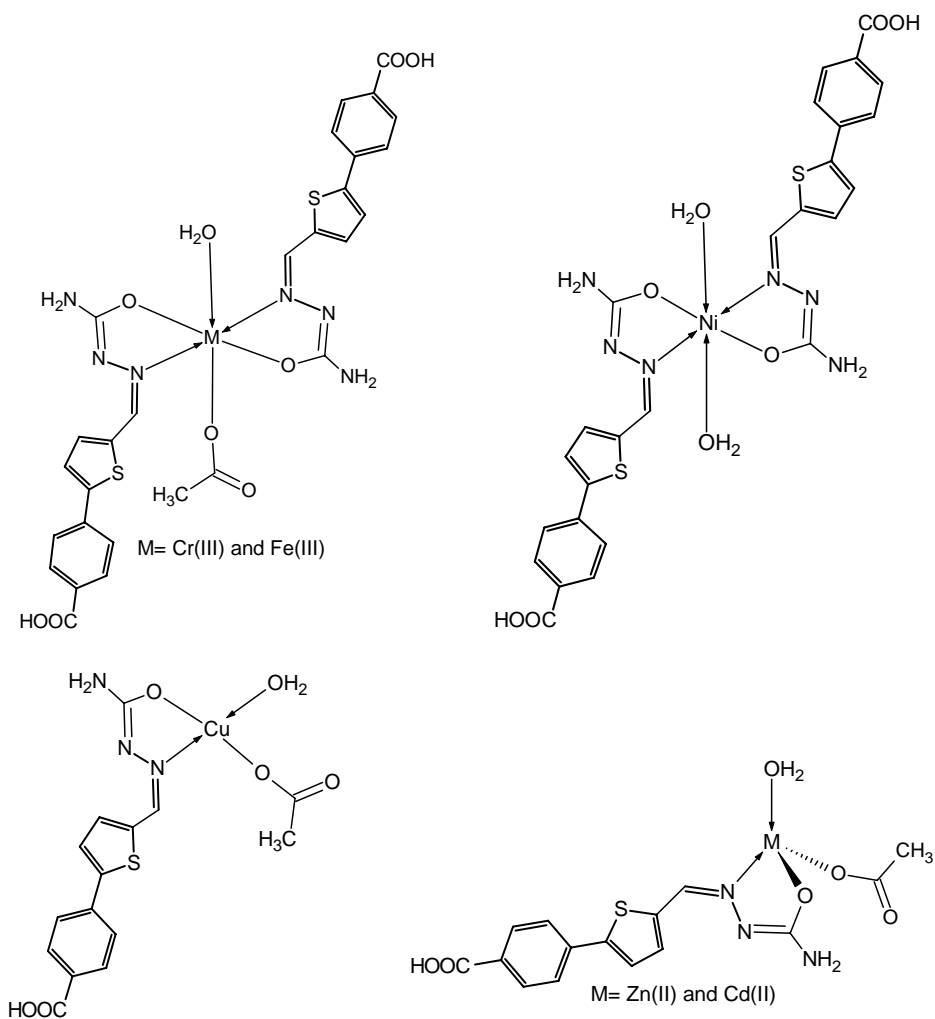
Fig. 1.44 Structures of complexes of CPTASC

Table 1.15 Microanalytical, magnetic and conductance data of the ligand CPTASC and its transition metal chelates

Complex	Colour	Yield (%)	Mol. Wt.	M.P (^{0}C)	Metal % Found (Calculated)	C % Found (Calculated)	H % Found (Calculated)	N % Found (Calculated)	S % Found (Calculated)	μ_{eff} (BM)	Molar Conductance ($\Omega^{-1}cm^2mol^{-1}$)	Geometry
CPTASC (LH)	Yellow	79	289	220	-	53.66 (53.97)	3.97 (3.80)	15.10 (14.53)	10.98 (11.07)	-	-	-
[CrL$_2$Ac(H$_2$O)]	Pale blue	72	705	>300	7.88 (7.37)	46.91 (47.65)	4.01 (3.54)	11.21 (11.91)	8.36 (9.07)	3.99	18	Octahedral
[FeL$_2$Ac(H$_2$O)]	yellow	67	709	>300	8.02 (7.87)	47.21 (47.40)	3.93 (3.52)	10.78 (11.85)	8.73 (9.02)	5.41	33	Octahedral
[NiL$_2$(H$_2$O)$_2$]	Pale Green	73	671	267	8.34 (8.75)	45.99 (46.51)	3.81 (3.57)	12.66 (12.52)	8.99 (9.54)	3.1	26	Octahedral
[CuLAc(H$_2$O)]	Green	79	429	>300	14.98 (14.82)	41.67 (42.00)	4.07 (3.50)	10.02 (9.80)	6.89 (7.46)	2.01	22	Square planar
[ZnLAc(H$_2$O)]	Off white	69	430	289	15.88 (15.19)	40.86 (41.82)	4.11 (3.48)	9.22 (9.75)	7.00 (7.43)	D	27	Tetrahedral
[CdLAc(H$_2$O)]	White	67	477	298	22.81 (23.54)	36.44 (37.70)	3.88 (3.14)	9.03 (8.79)	6.47 (6.70)	D	19	Tetrahedral

Ac: Acetate, D: Diamagnetic

Table 1.16 Characteristic infrared absorption frequencies of CPTASC and its transition metal complexes

Complex	$\upsilon_{COOH/H2O}$	υ_{N-H}	$\upsilon_{COO}(asym)$	$\upsilon_{C=N}$	$\upsilon_{COO}(sym)$	υ_{C-O}	υ_{M-O}	υ_{M-N}
CPTASC (LH)	3454	3377	1689	1597	1421	1286	-	-
[CrL$_2$Ac(H$_2$O)]	3457,3396	3318	1666	1596	1420	1279	529	492
[FeL$_2$Ac(H$_2$O)]	3456,3377	3346	1668	1590	1421	1291	555	510
[NiL$_2$(H$_2$O)$_2$]	3458,3265	3349	1687	1595	1417	1284	520	490
[CuLAc(H$_2$O)]	3462,3275	3356	1643	1589	1408	1298	513	489
[ZnLAc(H$_2$O)]	3460,3398	3336	1633	1556	1412	1282	540	488
[CdLAc(H$_2$O)]	3456,3271	3391	1690	1596	1421	1286	523	482

SECTION III

STUDIES ON Co(II), Cu(II) AND Zn(II) COMPLEXES OF CARBOXYPHENYL FURAN-2-ALDEHYDE PHENYLHYDRAZONE

By exploiting the chelating ability of the Schiff base carboxyphenyl furan-2-aldehyde phenylhydrazone (CPFAPH) transition metal complexes were synthesized. The details of synthesis and structural evaluation of the metal chelates are reported and discussed in this section.

Synthesis of Complexes

To a hot ethanolic solution of Schiff base CPFAPH (3mmmol), equimolar amount of metal salt in ethanol-water mixture (9:1) was added the reaction mixture was refluxed for 4 hours in a water bath. The pH of the solution was adjusted by adding few drops of saturated solution of CH_3COONa. The solution was evaporated to reduce the volume, cooled in ice bath and the precipitated product was filtered out. Washed with copious amount of ethanol-water mixture (1:1) and dried.

The chelating ability of the Schiff base CPFAPH was lower than that of the arylated heterocyclic carbonyl derived Schiff bases namely CPFASC and CPTASC and only three transition metal chelates such as Co(II), Cu(II) and Zn(II) could prepare with this ligand. The yields of the chelates were poorer than the complexes of other two Schiff bases.

Characterization of Complexes

Complexes were amorphous and non-hygroscopic solids. Poor solubility was noted in ethanol but exhibited appreciable solubility in DMSO.

Elemental analysis

The CHN and the metal percentage data of the three chelates are represented in Table 1.17. Studies clearly revealed that a 1:1 stoichiometry exist between the ligand and metal in all chelates. The experimental values were found to be in fare agreement with the calculated values.

Magnetic moment studies

The Co(II) chelate displayed magnetic moment of 3.52BM, which showed that the most probable geometry of this complex was octahedral. Copper chelate exhibited a higher magnetic moment of 2.4BM than calculated value by spin only formula (d^9 configuration), which is an indication of octahedral geometry and it was further verified by the optical absorption studies. Diamagnetism was shown by the Zn(II) chelate and tetrahedral geometry was assigned to it. The magnetic moment data is given in Table 1.17.

Molar conductance studies

The Co(II), Cu(II) and Zn(II) chelates of CPFAPH exhibited molar conductance 21, 36 and 15 $\Omega^{-1}cm^2mol^{-1}$ respectively in DMSO at a concentration of $10^{-3}M$ (Table 1.17). These low values suggest that these chelates were behaving as non-electrolytes in DMSO and non ionic nature.

IR spectra of complexes

Interpretation of FTIR spectral bands was useful in predicting the exact coordination site of the ligand. The azomethine stretching frequency of Schiff base, CPFAPH, lowered considerably in all complexes, which ascertain that one of the coordination sites of CPFAPH is definitely the nitrogen atom of azomethine

group. Other possible coordination sites of CPFAPH were the carboxylic group on benzene ring and the hetero atom oxygen. It was difficult to assign the exact stretching frequencies corresponds to –OH vibrations of carboxylic group, since these frequencies were overlapped with the stretching frequencies of coordinated water molecules and the NH bond. However, compared to the ligand spectrum, in the IR spectrum of Zn(II) complex, υ_{COOH} was not altered and hence can assume that the –COOH group is not participating in chelation process. Valuable information regarding the non involvement of –COOH group was obtained by [1]Hnmr spectrum analysis. Above discussion clearly point out that the second coordination site of CPFAPH was the oxygen atom of the furan ring.

On close examination of the spectrum of ligand and complexes it was understandable that medium to sharp bands, due to υ(C-O-C) stretching vibration of furan, appeared at 1263cm^{-1} in the ligand was shifted to 1219-1261cm^{-1} in metal complexes. These shifts refer to the coordination through a furan O atom [120,121]. Appearance of the additional peaks in the IR spectrum of chelates at about 500 and 450cm^{-1} respectively can be regarded as the stretching vibrations of newly formed M-O and M-N bonds, which acts as supporting evidence to the above arguments. Characteristic IR frequencies of ligand CPFAPH and its metal chelates are represented in Table 1.18.

[1]Hnmr spectra of complexes

On comparing the [1]Hnmr spectra of ligand and chelates, one can reach into two major conclusions. The proton signal (appeared in CPFAPH at 10.55δ) corresponds to the –COOH proton in chelates did not alter significantly,

suggesting the non participation of this group in coordination. Moreover the signal due to the azomethine protons in chelates moved to downfield region from 8.32δ, which is a clear indication of coordination through the imine nitrogen. Other relevant peaks corresponds to various aromatic protons were also displayed in the ^{1}Hnmr spectrum of chelates.

Electronic spectra of complexes

Under octahedral environment, the ground state of the d^7 metal ion splits into three states. The possible electronic transitions of Co(II) chelate in octahedral environment are $^4T_1(F)\rightarrow^4T_2$, $^4T_1(F)\rightarrow^4A_2$ and $^4T_1(F)\rightarrow^4T_1(P)$. These transitions in the electronic spectrum appeared at 18524, 25220 and 32573cm^{-1} respectively. The copper chelate displayed two electronic transitions at 12936 and 14326cm^{-1} in addition to the intra ligand transitions. This can be assigned to $^2E\rightarrow T_2$ d-d transition of d^9 system and charge transfer band respectively. Distorted octahedral geometry was suggested to Cu(II) chelate. The Zn(II) chelate exhibited only two ILT bands and charge transfer transitions were totally absent in the electronic spectrum.

The above results and discussion conclude that 1:1 stoichiometry exists between the metal and ligand in all chelates. Octahedral geometry was suggested for Co(II) and Cu(II) chelates and tetrahedral geometry was assigned to Zn(II) complex. The structures of the chelates are depicted in Figure 1.45.
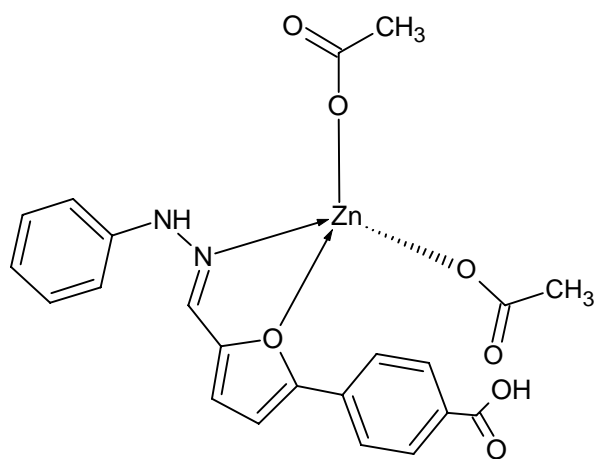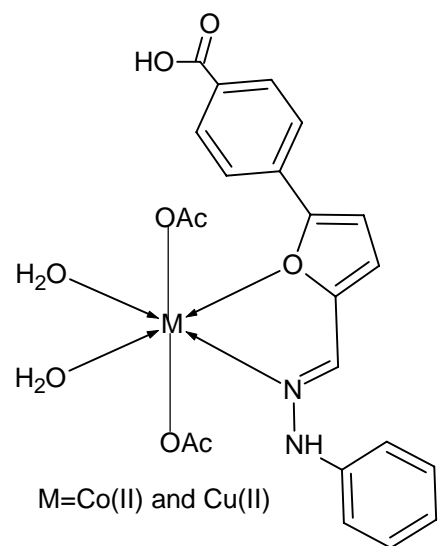
M=Co(II) and Cu(II)

Fig. 1.45 Structures of complexes of CPFAPH

Table 1.17 Microanalytical, magnetic and conductance data of the ligand CPFAPH and its transition metal chelates

Complex	Colour	Yield (%)	Mol. Wt.	M.P (^{0}C)	Metal % Found (Calculated)	C % Found (Calculated)	H % Found (Calculated)	N % Found (Calculated)	μ_{eff} (BM)	Molar Conductance ($\Omega^{-1}cm^2mol^{-1}$)	Geometry
CPFAPH (L)	Yellow	75	306	222	-	69.87 (70.58)	4.86 (4.57)	8.92 (9.15)	-	-	-
[CoLAc$_2$(H$_2$O)$_2$]	Light blue	61	519	>300	11.76 (11.35)	49.98 (50.87)	4.01 (4.62)	5.04 (5.39)	3.52	21	Octahedral
[CuLAc$_2$(H$_2$O)$_2$]	Green	58	524	>300	11.98 (12.13)	49.78 (50.42)	4.93 (4.58)	4.99 (5.34)	2.4	36	Octahedral
[ZnLAc$_2$]	Pale yellow	59	489	285	13.81 (13.35)	52.91 (53.94)	4.65 (4.08)	5.41 (5.72)	D	15	Tetrahedral

Ac: Acetate, D: Diamagnetic

Table 1.18 Characteristic infrared absorption frequencies of CPFAPH and its transition metal complexes

Complex	$\upsilon_{OH(water)}$	$\upsilon_{COOH}/\upsilon_{NH}$	$\upsilon_{COO}(asym)$	$\upsilon_{C=N}$	$\upsilon_{COO}(sym)$	υ_{C-O-C}	υ_{M-O}	υ_{M-N}
CPFAPH (L)	-	3431	1668	1600	1425	1263	-	-
[CoLAc$_2$(H$_2$O)$_2$]	3589	3406	1654	1521	1399	1261	518	470
[CuLAc$_2$(H$_2$O)$_2$]	3558	3369	1668	1589	1419	1219	545	462
[ZnLAc$_2$]	-	3430	1600	1531	1425	1259	509	445

CHAPTER 5

STUDIES ON SCHIFF BASE FURAN-2-ALDEHYDE-3-AMINOBENZOIC ACID AND ITS TRANSITION METAL COMPLEXES

The Schiff base furan-2-aldehyde-3-aminobenzoic acid (FAABA) and its transition metal chelates such as VO(II), Cr(III), Mn(II), Fe(III), Co(II), Ni(II), Cu(II), Zn(II), Cd(II) and Ag(I) were synthesized and characterized. The details are reported in this chapter. The chelating ability of FAABA was significantly higher than any other ligands studied in this research work. Moreover, the yields of the synthesized metal chelates were very appreciable when compared to chelates of other ligands.

Synthesis of Schiff Base, Furan-2-Aldehyde-3-Aminobenzoic Acid

5mmol of furan-2-aldehye was dissolved in 10ml of ethanol. To this, 5mmol ethanolic solution of 3-aminobenzoic acid (10ml) was added drop wise with constant stirring. The reaction mixture was continuously stirred for 3 hours at 40^0C. It was then slowly evaporated nearly to dryness at this temperature. The mixture was cooled and added 10ml of ethanol again. The precipitated violet coloured product was filtered, washed with ethanol and dried. M.P =197^0C.
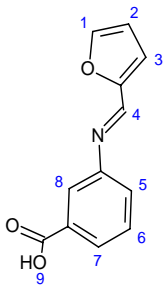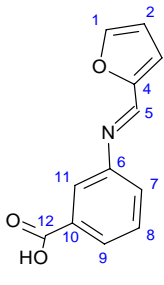
Characterization of Schiff Base, Furan-2-Aldehyde-3-Aminobenzoic Acid

The Schiff base FAABA was characterized by elemental analysis and FTIR, mass, NMR, UV-visible spectral studies. The details are given in the succeeding paragraphs.

NMR spectral studies

The [1]Hnmr spectrum of FAABA (Figure 1.46) showed nine characteristic signals for nine different types protons in the compound. Presence of a broad singlet signal at 12.25δ was due to the highly deshielded –COOH proton. The azomethine proton gave its signal at 7.27δ. Aromatic protons on the benzene ring appeared between 6.68-7.18δ and the protons of the furan ring displayed their peaks between 7.55-7.76δ.

Table 1.19 [1]Hnmr and [13]Cnmr Spectral data of FAABA

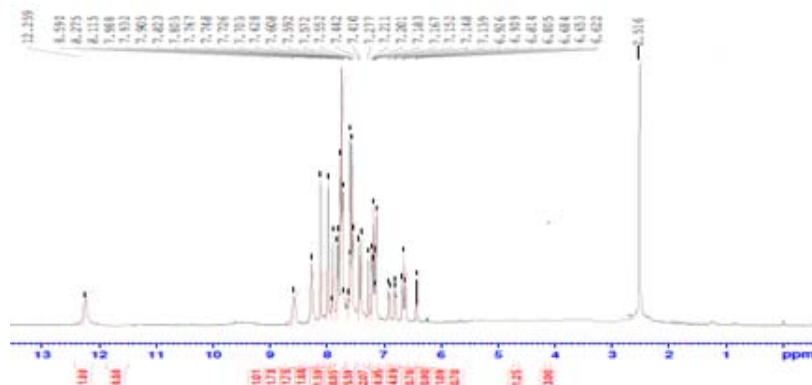| [1]Hnmr			[13]Cnmr		
	δ value	Assignment/ Labelled No.	δ value	Assignment/ Labelled	
	12.25(s,1H)	9(COOH)	166.66	12	
	7.76(dd,1H)	1	153.13	4	
	7.703(dd,1H)	2	147.96	1	
	7.57(dd,1H)	3	147.42	6	
	7.28(s,1H)	4(CH=N)	143.01	5	
	7.21(s,1H)	8	139.13	10	
	7.18(dd,1H)	7	132.33	7	
	7.13(dd,1H)	6	132.14	8	
	6.68(m.1H)	5	131.57	9	
			131.33	11	
			130.05	2	
			129.94	3	

Fig. 1.46 [1]Hnmr spectrum of the Schiff base FAABA
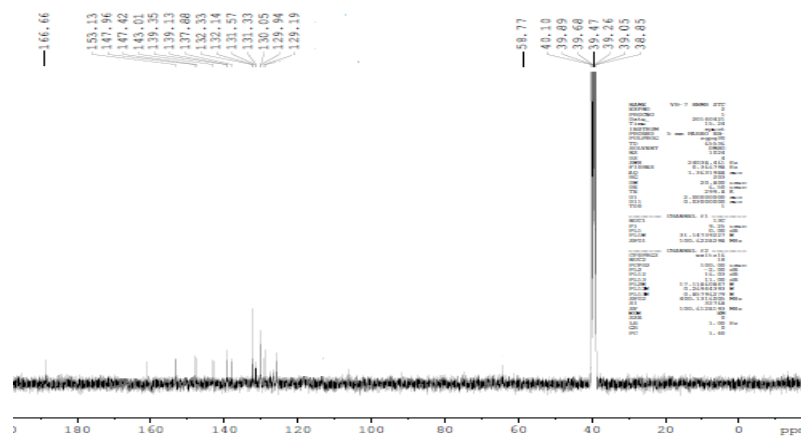
Fig. 1.47 ^{13}Cnmr spectrum of the Schiff base FAABA

Twelve distinct peaks were appeared in the proton decoupled ^{13}Cnmr spectrum of FAABA, corresponds to twelve different carbon atoms. The positions of the peaks and the assignment of labeled carbon atoms are provided in Table 1.19. The highly deshielded carbon atom of the carboxylic group showed its signal at 166.66ppm. A sharp peak appeared at 143.01ppm was due to the azomethine carbon atom. The ortho carbon atoms of furan rings showed their signals at 153.13 and 147.96ppm respectively. Aromatic carbon atoms of the benzene ring resonated in the range 139-131ppm. The ^{13}Cnmr spectrum of FAABA is given in Figure 1.47.

Mass spectral studies

The separation of the ligand was ascertained by the appearance of a single signal in the gas chromatogram. The high resolution mass spectrum of the Schiff base FAABA is given in Figure 1.48. Molecular ion signal was absent in the spectrum, indicates the instability of the compound. The base peak appeared at m/z 137 was due to the fragment $[C_7H_7O_2N]^+$, originated from amino part of the molecule. An intense peak appeared at m/z 120 was assignable to the fragment

100

$[C_7H_4O_2]^+$. The additional important signals appeared at m/z 92 and 65 were due to the fragments $[C_5H_2NO]^+$ and $[C_4HO]^+$ respectively.
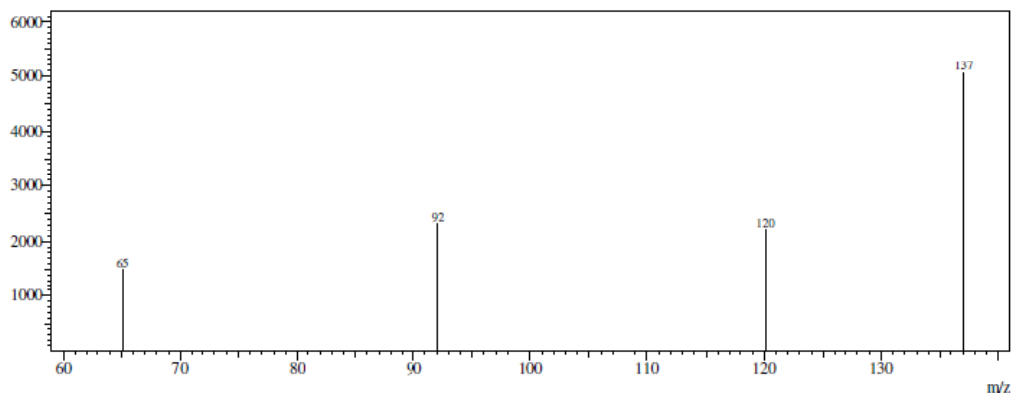
Fig. 1.48 Mass spectrum of FAABA

IR spectral studies

Vibrational spectrum of the Schiff base FAABA displayed characteristic frequencies for stretching and bending vibrations. $\upsilon_{C=N}$ exhibited by the Schiff base was at $1633cm^{-1}$. A broad peak appeared at $3340cm^{-1}$ was due to the –OH stretching vibration. A medium peak displayed at $1168cm^{-1}$ can be assigned to the breathing vibration of furan ring. υ_{C-O-C} vibration of the furan ring was appeared at $1234cm^{-1}$ in the IR spectrum [122-124].The asymmetric and symmetric stretching frequencies of carboxylic group emerged at 1612 and $1382cm^{-1}$ respectively. Table 1.21 represents the vibrational frequencies of FFABA and its complexes.

Electronic spectral studies

The UV-visible spectrum of the Schiff base exhibited two pronounced electronic transitions namely n→π* and π→π* transitions appeared at 30211 and $38986cm^{-1}$ respectively.

The elemental analytical data of FAABA is provided in Table 1.20. The experimental values were in good agreement with the calculated values.

The above results and discussions were sufficient to establish the structure of the Schiff base which is given in Figure 1.49.
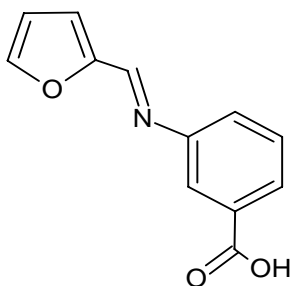
Fig. 1.49 Structure of FAABA

Synthesis of Complexes of FAABA

Due to the instability of the Schiff base in solution phase and tendency to get polymerized, the complexes were prepared by *in situ* method. To the ethanolic solution of furan-2-adehyde (3mmol), equimolar amount of m-aminobenzoic acid in ethanol was added drop wise with constant stirring at 40^0C for 3hours. To this mixture, 3mmol of metal salt in ethanol was added and continued the stirring for additional 2 hours at a higher temperature range of $60\text{-}70^0$C. The total volume of the mixture was not exceeded above 15ml. The pH of the reaction mixture was adjusted by adding few drops of saturated sodium acetate solution. The precipitated complex was filtered, washed with alcohol and warm water and finally dried.

Characterization of Complexes of FAABA

The metallic complexes of FFABA were characterized by elemental and spectral studies. The denticity of the ligand was established by IR and [1]Hnmr

spectral studies. All the complexes were amorphous powder and stable to air and light. Partial solubility in DMSO was noted for all complexes. The following paragraphs represent the structural evaluation of the metal chelates.

Elemental analysis

The percentage of metal estimated by various techniques and the elemental analysis data are provided in Table 1.20. From the table, it is evident that the experimental values are in good agreement with the calculated values. The elemental analysis revealed the correct stoichiometry of metal chelates. This analysis also helped to reach into the appropriate conclusion regarding the molecular formulae of complexes. It was noticed that all chelates of FAABA obeyed a 1:1 stoichiometry between the metal and ligand.

Magnetic moment measurements

Magnetic moment value of the newly synthesized chelates was a power tool for elucidating the exact geometry. The μ_{eff} data of complexes are provided in Table 1.20. The VO(II) chelate displayed a magnetic moment of 1.48BM which suggest a square pyramidal geometry to this complex. Octahedral dimeric geometry was assigned to Cr(III) and Fe(III) complexes, since they exhibited considerably low value of μ_{eff} from the calculated value corresponds to d^3 and d^5 systems using spin only formula. They exhibited respectively μ_{eff} values 2.1 and 3.2BM, suggesting that a strong antiferromagnetic interaction occurs between the metal ions in these complexes. Distorted octahedral geometries were specified to Mn(II), Co(II) and Ni(II) chelates, because they showed μ_{eff} values of 5.22, 3.32 and 2.91BM respectively [125-128].These values were in good agreement with

the calculated values (5.47, 3.87 and 2.82BM) using spin only formula. Copper complex exhibited μ_{eff} of 1.72BM and hence assigned square planar geometry [129]. Diamagnetism was shown by Zn(II), Cd(II) and Ag(I) chelates due to their d^{10} configurations. Tetrahedral geometry was assigned to these chelates with the help of elemental analyses [130].

Molar conductance studies

The non electrolytic nature of all chelates was proved by performing the molar conductance measurements in DMSO. The transition metal complexes of FAABA showed the molar conductance values in the range 3-31$\Omega^{-1}cm^{2}mol^{-1}$ which are represented in Table 1.20.

IR spectra of complexes

The monovalent tridentate nature of the Schiff base FAABA was established by examining and comparing the vibrational frequencies of the ligand and complexes. Four major conclusions can be drawn out from the IR spectrum analyses. The frequencies correspond to the azomethine stretching vibrations of FAABA considerably lowered in all complexes from 1633cm^{-1} (shown by the free ligand). This substantiates the complexation of the Schiff base through C=N group. Secondly the disappearance of OH stretching frequency from the IR spectrum of chelates was a strong evidence for the coordination of the Schiff through carboxylic group, after deprotonation. Thus the monovalent nature of the ligand was established. If the symmetric and asymmetric stretching frequency of carboxylate group differ greater than or equal to 150cm^{-1}, it indicates that the carboxylate groups attached to the metal ion in a monodentate manner, and if it is

less than or equal to 120cm^{-1}, it shows a bidentate character. Therefore in all the present complexes the carboxylate groups existed as a monodentate moiety [131].

On close comparison between the IR spectra of ligand and complexes, one can understand that the breathing frequency corresponds to the furfural ring system showed differences up to 60cm^{-1} in ligand and complexes, suggesting that the third site of coordination is the hetero oxygen atom. The υ_{C-O-C} vibrations of the furan ring system also shifted after complexation, which ensure that the hetero oxygen atom is participating in complexation. In addition to these significant changes, the appearance additional bands corresponds to υ_{M-N} and υ_{M-O} frequencies also supported that the Schiff base FAABA was acting as monobasic tridentate ligand. The emergence of broad peaks at 3300-3400cm^{-1}, in the IR spectra of Mn(II), Co(II), Ni(II) and Ag(I) chelates indicates the presence of coordinated water molecules. Characteristic vibrational stretching frequencies of ligand and complexes are listed in Table 1.21.

^{1}Hnmr spectra of complexes

The ^{1}Hnmr spectra of chelates were very useful to confirm the complexation and to assign the binding probes of ligand. All the peaks were slightly changed to low field region, which indicates the complexation. The peak due to the carboxylic proton was totally disappeared from the ^{1}Hnmr spectrum (12.25δ) is a clear indication of coordination the ligand through carboxylic group after deprotonation. In addition to this, a considerable alteration of signals due to azomethine proton to downfield region suggested that one of the coordination probes of the ligand FAABA was C=N group.

Electronic spectra of complexes

Majority of the chelates displayed peaks due to intra ligand electronic transitions (ILT) and d-d transitions in the optical absorption spectrum. The ILT bands were showed red shifts in the electronic spectrum of complexes, indicating complexation. VO(II) chelate displayed two additional peaks at 28011 and 31456cm^{-1} which are assignable to $^2B_2 \rightarrow ^2B_1$ and $^2B_2 \rightarrow ^2A_1$ electronic transitions in the square pyramidal field. Cr(III) chelate displayed two higher energy bands at 390625 and 41152cm^{-1}, which are attributed to $^4A_2(F) \rightarrow ^4T_2(F)$ and $^4A_2 \rightarrow ^4T_1(P)$ transitions respectively. The third transition corresponds to d^3 configuration in octahedral environment, was not appeared in the electronic spectrum. Mn(II) chelate exhibited intense peaks at 28818 and 29325cm^{-1} respectively which can be regarded as L$\rightarrow$M charge transfer spectra. A charge transfer band was also displayed by Fe(III) chelate in addition to ligand transitions at 34461cm^{-1}. The three electronic transitions for a d^7 system is $^4T_1(F) \rightarrow ^4T_2$, $^4T_1(F) \rightarrow ^4A_2$ and $^4T_1(F) \rightarrow ^4T_1(P)$ and electronic spectrum of Co(II) chelate exhibited these transitions respectively at 29670, 32416 and 35621cm^{-1}. Optical absorption bands shown by Ni(II) chelates were at 29218 and 34239 cm^{-1}, which was assignable to $^3A_2 \rightarrow ^3T_2$ and $^3A_2 \rightarrow ^3T(F)$ electronic transitions in octahedral environment. A square planar geometry to Cu(II) chelate was assigned since the optical absorption spectrum gave two bands at 40650 and 42256cm^{-1}, which are due to the transitions $^2B_1 \rightarrow ^2A_1$ and $^2B_1 \rightarrow ^2B_2$ respectively. Zn(II) and Ag(I) chelates didn't show CT bands in addition to the intra ligand transitions, while Cd(II) complex demonstrated LMCT band at 41152cm^{-1}.

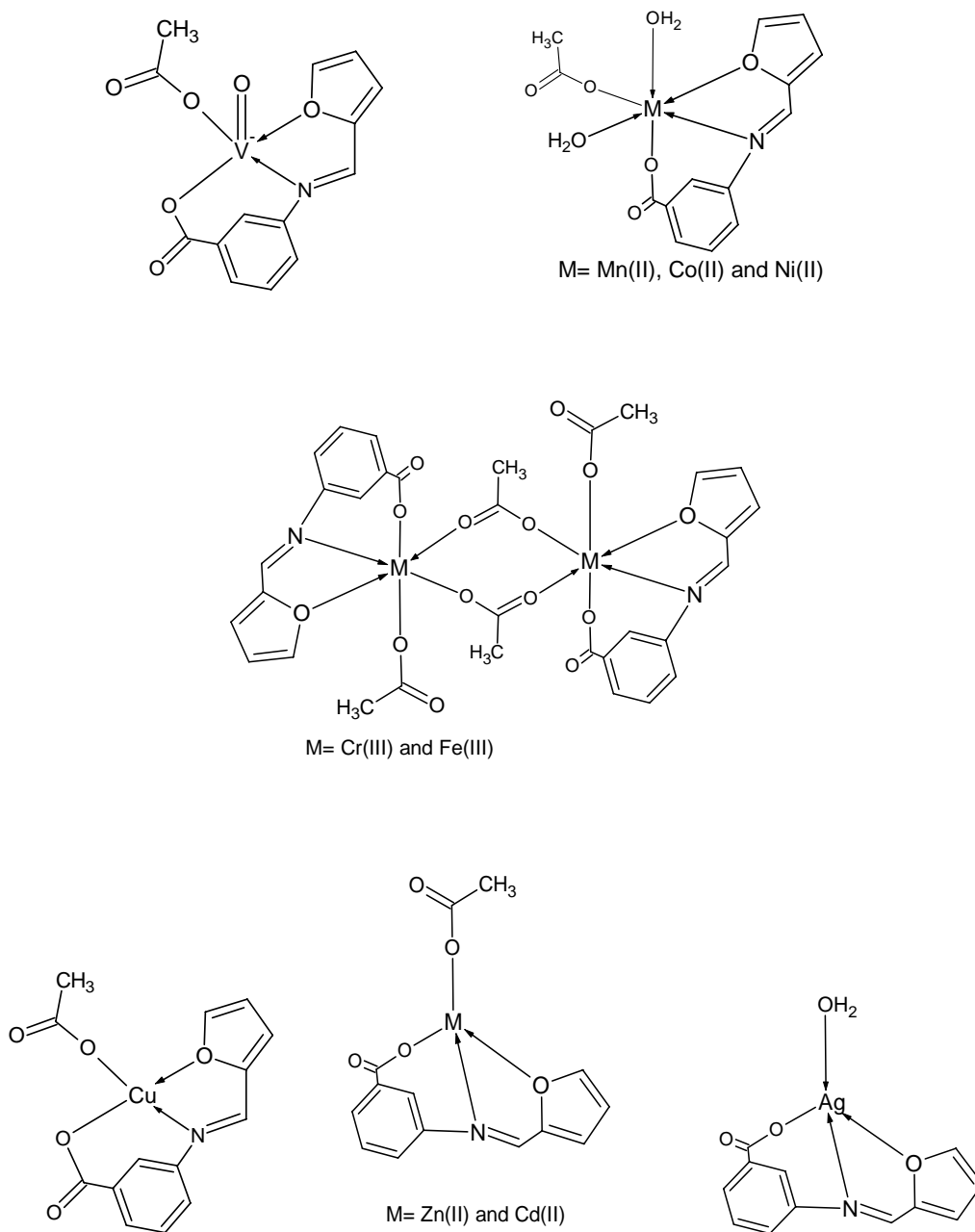The structures of metal chelates were assigned based on the above discussions and displayed in Figure 1.50.

M= Mn(II), Co(II) and Ni(II)

M= Cr(III) and Fe(III)

M= Zn(II) and Cd(II)

Fig. 1.50 Structures of metal complexes of FAABA

Table 1.20 Microanalytical, magnetic and conductance data of the ligand FAABA and its transition metal chelates

Complex	Colour	Yield (%)	Mol. Wt.	M.P (^{0}C)	Metal % Found (Calculated)	C % Found (Calculated)	H % Found (Calculated)	N % Found (Calculated)	μ_{eff} (BM)	Molar Conductance ($\Omega^{-1}cm^2mol^{-1}$)	Geometry
FAABA (LH)	Yellow	72	215	197	-	65.23 (66.97)	4.47 (4.18)	6.45 (6.51)	-	-	-
[VOLAc]	Green	75	340	288	14.66 (14.98)	47.97 (49.42)	3.76 (3.23)	4.219 (4.11)	1.48	20	Square pyramidal
[CrLAc$_2$]$_2$	Pale green	83	768	>300	12.96 (13.54)	49.75 (50)	3.79 (3.64)	3.48 (3.64)	2.1	2	Octahedral
[MnLAc(H$_2$O)$_2$]	Brown	81	364	>300	15.75 (15.09)	45.85 (46.16)	4.86 (4.12)	3.91 (3.84)	5.22	5	Octahedral
[FeLAc$_2$]$_2$	Yellow	84	776	>300	14.51 (14.39)	48.82 (49.50)	3.94 (3.60)	3.67 (3.60)	3.2	4	Octahedral
[CoLAc(H$_2$O)$_2$]	Brown	79	368	256	16.48 (16.01)	44.87 (45.66)	4.12 (4.07)	3.43 (3.80)	3.32	10	Octahedral
[NiLAc(H$_2$O)$_2$]	Pale Green	80	368	283	16.07 (15.96)	45.93 (45.68)	4.02 (4.07)	3.65 (3.80)	2.91	20	Octahedral
[CuLAc]	Green	86	337	>300	19.21 (18.88)	48.16 (49.91)	3.29 (3.26)	4.44 (4.15)	1.72	14	Square planar
[ZnLAc]	Grey	76	338	276	19.66 (19.32)	48.45 (49.64)	3.72 (3.25)	4.34 (4.13)	D	16	Tetrahedral
[CdLAc]	White	74	385	>300	29.49 (29.16)	44.17 (43.59)	3.03 (2.85)	3.78 (3.63)	D	3	Tetrahedral
[AgL(H$_2$O)]	Grey	70	340	259	30.97 (31.73)	41.75 (42.36)	3.12 (2.94)	4.27 (4.11)	D	31	Tetrahedral

Ac: Acetate, D: Diamagnetic

Table 1.21 Characteristic infrared absorption frequencies of FAABA and its transition metal complexes

Complex	$\upsilon_{OH/H2O}$	$\upsilon_{COO}(asym)$	$\upsilon_{C=N}$	$\upsilon_{COO}(sym)$	υ_{C-O-C}	υ_{breath}	υ_{M-O}	υ_{M-N}
FAABA (LH)	3340	1612	1633	1382	1234	1168	-	-
[VOLAc]	-	1583	1573	1379	1344	1118	560	498
[CrLAc$_2$]$_2$	-	1591	1539	1384	1276	1118	600	490
[MnLAc(H$_2$O)$_2$]	3371	1588	1554	1396	1282	1127	620	487
[FeLAc$_2$]$_2$	-	1603	1548	1323	1249	1108	613	467
[CoLAc(H$_2$O)$_2$]	3373	1581	1558	1394	1165	1138	619	481
[NiLAc(H$_2$O)$_2$]	3365	1574	1557	1394	1321	1113	618	491
[CuLAc]	-	1600	1554	1390	1286	1169	601	489
[ZnLAc]	-	1593	1562	1396	1297	1161	608	501
[CdLAc]	-	1565	1553	1392	1163	1128	601	496
[AgL(H$_2$O)]	3425	1595	1556	1381	1159	1122	614	497

SUMMARY

Heterocyclic Schiff bases (derived from 3-acetylpyridine, furan-2-aldehyde and thiophene-2-aldehyde) such as 3-acetylpyridine thiosemicarbazone (APTSC), 3-acetylpyridine semicarbazone (APSC), 3-acetylpyridine phenylhydrazone (APPH), carboxyphenyl furan-2-aldehyde semicarbazone (CPFASC), carboxyphenyl thiophene-2-aldehyde semicarbazone (CPTASC), carboxyphenyl furan-2-aldehyde phenylhydrazone (CPFAPH) and furan-2-aldehyde-3-aminobenzoic acid (FAABA) have been synthesized and characterized using CHNS analysis and spectral studies such as NMR, mass, FTIR and UV-visible. Two dimensional NMR spectroscopic methods like COSY and HMQC and ^{13}CDEPT 135 techniques were very useful in predicting the exact assignment of protons and carbons in the molecules. The chelating ability of these heterocyclic Schiff bases was checked by synthesizing transition metal complexes. The exact geometries and stoichiometries of these complexes were evaluated by elemental, magnetic, conductance, IR, UV-visible and ^{1}Hnmr spectral studies. The results are summarized and well discussed in this part.

The chelating efficacy of the imines derived from 3-acetylpyridine was fair and six metal chelates of each ligand were prepared by combining with VO(II), Cr(III), Ni(II), Cu(II), Cd(II) and Ag(I) ions. Schiff bases, APTSC and APSC, were behaved as monobasic bidentate ligand, while APPH acted as neutral bidentate ligand during complexation. Octahedral geometry was shown by the chromium and nickel complexes, while tetrahedral geometry was followed by Cd(II) and Ag(I) complexes. Square planar geometry was assigned to Cu(II)

complex. Elemental and magnetic studies of Cr(III) and Cu(II) chelates of APTSC and APSC, revealed that these complexes owned dimeric bridge structures. The electrolytic nature of vanadyl complex of APPH was confirmed by the molar conductance studies. In addition to the azomethine linkage, the hetero nitrogen atom of the pyridine ring participated in complexation of APPH, which was verified by FTIR spectral studies.

Three Schiff bases namely CPFASC, CPTASC and CPFAPH were synthesized in two steps. First one was the arylation step followed by the condensation reaction with amines. Though the chelating ability of these imines was relatively low, may be due to the bulky nature of the molecules, a total of twelve metal complexes could prepare with these ligands. Tautomerization was possible in the Schiff bases, CPFASC and CPTASC, which was verified by NMR and IR spectral studies. These Schiff bases acted as monovalent bidentate ligands during complexation. The exact coordination probes of these ligands were established by [1]Hnmr and FTIR spectral studies of metal chelates. Elemental studies revealed that 1:2 stoichiometry was followed by the Cr(III) and Ni(II) chelates, while Cu(II), Zn(II), Cd(II) and Ag(I) chelates showed 1:1 stoichiometry between the metal and ligand. The Schiff base CPFAPH was behaved as neutral bidentate ligand and the involvement of hetero oxygen atom in addition to imine moiety was verified by FTIR studies.

Ten transition metal chelates of the Schiff base FAABA were synthesized and characterized. Investigations showed that this Schiff base behaved as monobasic tridentate ligand in all chelates. All metal complexes exhibited 1:1

stoichiometry between the metal and ligand. Magnetic moment and UV-visible spectral studies revealed that Cr(III), Mn(II), Fe(III), Co(II) and Ni(II) complexes possess octahedral geometry. Tetrahedral geometry was followed by Zn(II), Cd(II) and Ag(I) complexes.

To conclude, seven novel potential Schiff base ligands derived from 3-acetylpyridine, furan-2-aldehyde and thiophene-2-aldehyde and various amines such as semicarbazide, thiosemicarbazide, phenylhydrazine and 3-aminobenzoic acid and their forty one transition metal chelates were synthesized and characterized using most modern analytical techniques and described in detail in this part.

REFERENCES

1. R. Grewe, R. Hamann, G. Jacobsen, E. Nolte, K. Riecke, *Ann. Chem.*, 581(1953) 85

2. Y. Zheng, K. Ma, H. Li, J. Li, J. He, X. Sun., *Catal. Lett.,* 3 (2009) 465

3. J. F Geldard, F. Lions, *Inorg. Chem.*, 4 (1965) 414

4. R. B. Moffett, N. Rabjohn, *"Organic Syntheses"*, John Wiley & Sons, Inc., New York 4 (1963) 605

5. K. Taguchi, F. H. Westheimer, *J. Org. Chem.*, 36 (1971) 1570

6. B. E. Love, J. Ren, *J. Org. Chem.*, 58 (1993) 5556

7. G. C. Look, M. M. Murphy, D. A. Campbell, M. A. Gallop, *Tetrahedron Lett.*, 36 (1995) 2937

8. J. H. Billman, K. M. Tai, *J. Org. Chem.,* 23 (1958) 535

9. P. Panneerselvam, R. R. Nair, G. Vijayalakshmi, E. H. Subramanian, S. K. Sridhar, *Eur. J. Med. Chem.*, 40 (2) (2005) 225

10. A. Kulkarni, S. A. Patil, P. S. Badami, *Eur. J. Med. Chem.*, 44 (7) (2009) 2904

11. J. D. Armstrong, C. N. Wolfe, J. L. Keller, *Tetrahedron Lett.*, 38 (9) (1997) 1531

12. A. K. Chakraborti, S. Bhagat, S. Rudrawar, *Tetrahedron Lett.*, 45 (2004) 7641

13. H. Naeimi, F. Salimi, K. Rabiei, *J. Mol. Catal. A. Chem.*, 260 (1) (2006) 100

14. G. Liu, D. A. Cogan, T. D. Owens, T. P. Tang, J. A. Ellman, *J. Org. Chem.*, 64 (4) (1999) 1278

15. J. S. M. Samec, J. E. Backvall, *Eur. J. Chem*., 8 (2002) 2955

16. N. Baricordi, S. Benetti, G. Biondini, C. de Risi, G. P. Pollini, *Tetrahedron Lett.,* 45 (2004) 1373

17. N. F. Curtis, *Coord. Chem. Rev.,* 3 (1968) 3

18. M. S. Niasari, M. Bazarganipour, M. R. Ganjali, P. Norouzi, *Transition Met. Chem.,* 32 (2007) 9

19. M. S. Niasari, F. Davar, *Inorg. Chem. Commun*., 9 (2006) 175

20. D. Singh, K. Kumari, R. Kumari, J. Singh, *J. Serb. Chem. Soc., 75* (2) (2010) 217

21. A. Prakash, B. K. Singh, N. Bhojak, D. Adhikari, *Spectrochim. Acta,* 76 (2010) 356

22. K. S. Siddiqi, R. I. Kureshy,N. H. Khan, S. Tabassum, S. Zaidi, *Inorg. Chem. Acta*, 151 (1988) 95

23. D. A. Laidler, D. J. Miller, *J. Organomet. Chem.*, 270 (1984) 121

24. L. Zhu, H. Li. Chen n, F. Song, X. Zhu, *Hua. Shif. Dax. Xue. Zirank.*, 37 (2003) 499

25. B. Dash, P. K. Mahapatra, D. Panda, J. M. Patnaik, *J. Indian Chem. Soc.*, 61 (1984) 1061

26. N. R. Rao, P. V. Rao, G. V. Reddy, M. C. Ganorkar, *Indian J. Chem.*, 26A (1987) 887

27. P. Mishra, P. N. Gupta, A. K. Shakaya, *J. Indian Chem. Soc.*, 68 (1991) 539

28. V. Srinivasa, S. K. Srivastava, A. P. Mishra, *J. Indian Chem. Soc.*,72 (1995) 47

29. R. Dhakrey, G. Saxena, *J. Indian Chem. Soc.*, 64 (1987) 685

30. C. Rîmbu, R. Danac, A. Pui, *Chem. Pharm. Bull.*, 62 (1) (2014) 12

31. O. Nakamoto, Hidaka, *Delta J. Sci.*, 15 (1991) 47

32. Z. A. Malik, S. Alam, *J. Pure Appl. Sci.*, 17 (1984) 69

33. Z. H. Cohan, M. Praveen, A. Ghaffar, *Met. Based Drugs*, 4 (1997) 267

34. K. T. Joshi,A. M. Pancholi, *Oriental. J. Chem.*, 16 (2000) 287

35. K. Singh, M. S. Barwa, *Eur. J. Med. Chem.,* 41 (2006) 147

36. D. M. Kar, S. K. Sahu, D. Pradhan, G. K. Dash, P. K. Misra, *J. Tech. Res. Chem.*, 10 (2003) 20

37. V. K. Patel, C. R. Jejurkar, *Oriental J. Chem* 10 (1995) 44857

38. J. Csaszar, J. Morvay, *Acta Phys. Chem.*, 31 (1985) 717

39. P. G. More, R. B. Bhalvankar, S. C. Pattar, *J. Indian Chem. Soc.*, 78 (2001) 474

40. T. Jeewoth, M. G. Bhowon, H. Wah, K. Li, *Trans Met. Chem.*, 24 (1999) 445

41. M. E. Hossain, M. A. Alam, M. A. Ali, *Polyhedron*, 15 (1996) 973

42. L. Hadjipavlu, J. Dimitra, Gerronikaki, A. Athina, *Drugs Discovery*, 15 (1998) 199

43. X. Luo, J. Zhao, Y. Ling, Z. Liu, *Chem. Res. Chinese Univ.*, 18 (2002) 287

44. Z. Gou, R. Xing, S. Liu, H. Yu, P. Wang, C. Li, P. C. Li, *Bio-or. Med. Chem. letters*, 14 (2005) 4600

45. K. P. Latha, V. P. Vaidya, J. Keshavayya, *J. Tech. Res. Chem.,* 11 (2004) 39

46. J. Thomas, G. Parameswaran, *Asian J. Chem.*, 14 (3-4) (2002) 1354

47. V. E. Kuz'min, V. P. Lozitsky,G. L. Kamalov, R. N. Lozitskaya, A. I. Zheltvay, A. S. Fedtchouk, *Acta Biochim. Pol.,*47 (3) (2000) 867

48. A. A. Osowole, I. Ott, O. M. Ogunlana, *Int. J. Inorg. Chem.* 2012 (2012), Article ID 206417, 6 pages

49. A. Obeid, A. El-Shekeil, S. Al-Aghbari, *J. Coord. Chem.,*65 (15) (2012) 336

50. J. Thomas, G. Parameswaran, *Asian J. Chem.*, 14 (3-4) (2002) 1370

51. A. Nishinaga, T. Yamada, H. Fujisawa, K. Ishaizaki*, J. Mol. Catal.* 48 (1998) 249

52. Z. Xi, W. Liu, G. Cao, W. Du, J. Huang, K. Cai, H. Guo, *C. Xuebao*, 7 (1986) 357

53. S. Förster, A. Rieker, *J. Org. Chem.*, 61 (10) (1996) 3320

54. M. X. Liu, T. B. Wei, Q. Lin, Y. M. Zhang, *Spectrochim. Acta (A) Mol. Biomol. Spectrosc.*, 79 (5) (2011) 1837

55. E. Toyota, H. Sekizaki, Y. U. Takahashi, K. Itoh, K. Tanizawa, *Chem. Pharm. Bull.*, 53(1) (2005) 22

56. A. Fakhari, Khorrami, R. Afshin, H. Naeim, *Talanta*, 66 (2005) 813

57. R. J. Young, G. W. Cooper, *J. Reprod. Fertil.*, 69 (1983)1

58. Y. Hamada,T. Sano, M. Fujita, T. Fujii,Y. Nishio,K. Shibata, *Japan. J. Appl. Phys.*, 32 (1993) 511

59. Z. H. Chohan, M. Praveen, A. Ghaffar, *Synth. React. Inorg. Met. Org. Chem.*, 28 (1998) 1673

60. N. S. Gwaram , H. M. Ali, H. Khaledi, M. A. Abdulla, H. A. Hadi, T. Kwai, C. L. Ching, C. L. Ooi, *Molecules,* 17 (2012) 5952

61. R.H. Prince, D.A. Stotter, *Inorg. Chim. Acta,* 10 (1974) 89

62. N. A. Nawar, *Trans. Met. Chem.*, 26 (1-2) (2001) 180

63. N. M. Hosny, F. I. El-Dossoki, *J. Chem. Eng. Data*, 53 (11) (2008) 2567

64. N. M. Hosny, *J. Coord. Chem.*, 60 (24) (2007) 2755

65. A. A. Alhadi, S. A. Shaker, N. G. Suleiman, W. A. Yehye, H. M. Ali, *J. Chil. Chem. Soc.*, 57 (3) (2012) 1283

66. R. Manikandan, R. Karthiga, P. Viswanathamurthi, *Chem. Res. Letters*, 1(2) (2012) 62

67. V. R. Souza, H. R. Rechenberg, J. A. Bonacin, H. E. Toma, *Spectrochim. Acta, (A) Mol. Biomol. Spectrosc.*, 71 (4) (2008) 1296

68. A. Angel, R. Despaigne, B. Fernanda, *Polyhedron,* 38 (2012) 285

69. F. Esmadia, O. F. Khabourb, A. I. Albarqawib, M. Ababneha, M. Al-Talib, *Jord. J. Chem.*, 8 (1) (2013) 31

70. D. Wang Bo, *Trans. Met. Chem.*, 18 (1) (1993) 101

71. P. Mittal, S. Joshi, V. Panwar, V.Uma, *Int. J. Chem. Tech. Res.*, (1) (2) (2009) 225

72. M. A. Ali, *Polyhedron*, 3 (5) (1984) 517

73. M. S. Suresh, V. Prakash, E-*J. Chem.*, 8 (3) (2011) 1408

74. Y. Harinath, D. H. K. Reddy, B. N. Kumar, C. H. Apparao, K. Seshaiah, *Spectrochim. Acta (A) Mol. Biomol. Spectrosc.*, 101 (2013) 264

75. *Vogel's Quantitative Inorganic Analysis*, 7th edn, Prentice Hall (2010)

76. A. F. Gilman, *"A laboratory Outline for Determination in Quantitative Chemical Analysis"* Chemical Publishing company (1908)

77. H. A Fales, F. J. Kenny, D. Appleton, *"Inorganic Quantitative Analysis"*, Centuary company (1939)

78. F. Wohler, Walton, Mabrely, *" Hand Book of Inorganic Analysis"* (1854)

79. D. Pavia, G. Lampman, G. Kriz, J. Vyvyari, *"An Introduction to Spectroscopy"* 4th edn (2009)

80. M. Bruch, *"NMR Spectroscopic Techniques"* 2nd edn (1996)

81. G. Clayton Bassler, R. M. Silverstein, *"Spectroscopic Identification of Organic Compounds"* (1963)

82. L. Coury, *Conductance Measurements Part 1: Theory. Current Separations*, 18 (1999) 91

83. B. N. Figgis, J. Lewis, *"Modern Coordination Chemistry"*, Eds, Interscience, New York (1958)

84. P. W. Selwood, *"Magnetochemistry"*, Interscience, New York (1958)

85. N. M. El-Metwally, G. A. Al-Hazmi, *Spectrochim. Acta (A) Mol. Biomol Spectrosc.*, 107 (2013) 289

86. N. Ramana, L. Mitub, A. Sakthivela, M. S. S. Pandia, *J. Iranian Chem. Soc.*, 6 (2009) 738

87. Soleimani, Esmaiel, *J. Therm. Anal. Calorimetry*, 111 (1) (2013) 129

88. M. F. Alias, M. O. Hamza, T. A. Kareem, *J. Al-Nahrain Univ.,*14 (2) (2011) 10

89. V. Ciornea, S. Shova, Gh. Novitchi, D. Ganzhu, O. N. Kazheva, A. Gulea, Yu. A. Simonov, *Russ. J. Coord. Chem.,* 35 (11) (2009) 817

90. T. Rosu, M. Negoiu, S. Pasculescu, E. Pahontu, D. Poirier, A. Gulea, *Eur. J. Med. Chem.*, 45 (2) (2010) 774

91. E. Ruiz, P. Alemany, S. Alvarez, J. Cano, *Inorg. Chem.*, *36* (17) (1997) 3683

92. N.S. Biradar, B. R. Havinale, *Inorg. Chim. Acta,* 17 (1976) 1570

93. R. B. Coles, C. M. Harris, E. Sinn, *Inorg. Chem.*, 8 (12) (1969) 2607

94. S. J. Berners-Price, R. K. Johnson, A. J. Giovenella, L. F. Faucette, C. K. Mirabelli, P. J. Sadler, *Inorg. Biochem*., 33(4) (1988) 285

95. L. G. Wang, *Acta Cryst.,*63 (2007) 479

96. S. Paulo*, J. Braz. Chem. Soc.,* 19 (3) (2008) 845

97. T. H. Al-Noor, A. T. AL- Jeboori, R. L. Sadaw, *Chem. Process Engg. Res.*, 13 (2013) 112

98. A. A. R. Despaigne, J. G. Da Silva, A.C. M. Do Carmo, O. E. Piro,   E. E. Castellano,   H. Beraldo, *Inorg. Chim. Acta*., 362 (2009) 2117

99. A. A. R. Despaigne, J.G. Da Silva, A. C. M. Do Carmo, O. E. Piro,   E. E. Castellano, H. Beraldo, *J. Mol. Struct*., 920 (2009) 97

100. A. A. R. Despaigne, J. G. Da Silva, A. C. M. Do Carmo, F. Sives, O.E. Piro, E. E. Castellano, H. Beraldo , *Polyhedron* 28 (2009) 3797

101. G. L. Parrilha, R. P. Vieira, A. P. Rebolledo, I. C. Mendes, L. M. Lima, E. J. Barreiro, O. E. Piro, E. E. Castellano, H. Beraldo, *Polyhedron,* 30 (2011) 1891

102. A. A. Soliman, W. Linert, *Thermochim. Acta*, 333 (1999) 67

103. D. X. West, A. M. Stark, G.A. Bain, A. E. Liberta, *Trans. Met. Chem.*, 21 (1996) 289

104. M. M. Moustafa, *J. Thermal Anal.*, 50 (1997) 463

105. R. Samanta, B. Mondal, P. Manchi, G.K. Lahiraj, *J. Chem. Soc.*, *Dalton Trans*, 12 (2001) 1827

106. B. Stuart, *"Infrared Spectroscopy: Fundamentals and Applications"*, John Wiley & Sons, Ltd (2004)

107. N. N. Greenwood, A. Earnshaw, *"Chemistry of Elements"*, 2nd edn. Prigman Press (1998)

108. R. Prasad, P. P. Thankachan, M. T. Thomas, R. Pathak, *J. Ind. Chem. Soc.*, 78 (2001) 28

109. M. S. Masoud, A. M. Hindawy, A. S. Soayed, *Trans. Met. Chem.*, 16 (1991) 372

110. F. A. Cotton, G. Wilkinson, C. A. Murillo, M. Bochmann, *"Advanced Inorganic Chemistry"*, 6th edn. Wiley, New York (1999)

111. M. S. Refat, *J. Mol. Struct.*, 842 (2007) 24

112. M. S. Refat, I. M. El-Deen, M. A. Zein, A. M. A. Adam, M. I. Kobeasy, *Int. J. Electrochem. Sci.*, 8 (2013)

113. N. Mahalingam, F. R. Chitrapriya, K. Fronczek, Natarajan, *Polyhedron* 27 (2008) 1917

114. I. C. Mendes, J. P. Moreira, A. S. Mangrich, S. P. Balena, B. L. Rodrigues, H. Beraldo, *Polyhedron,* 26 (2007) 3263

115. I. C. Mendes, J. P. Moreira, N. L. Speziali, A. S. Mangrich, J. A. Takahashi, H. Beraldo, *J. Braz. Chem. Soc*., 17 (2006) 1571

116. A. A. Recio- Despaigne, F. B. Da Costa, O. E. Piro, E. E. Castellano, S. R. W. Louro, H. Beraldo, *Polyhedron*, 38 (2012) 285

117. K. Nakamoto *"Infrared and Raman Spectra of Inorganic and Coordination Compounds"*, 5th edn., Wiely- Interscience publication (2000)

118. V. Malik, G. Solanki, V. Singh, *Orient. J. Chem.*, 25 (4) (2009) 1041

119. L. Racane, V. T. Kulenovic, D. W. Boykin, G. Karminski-Zamola , *Molecules*, 8 (2003) 342

120. A. Kriza, M. Voiculescu, A. Nicolae, *Analele Universitatii Bucuresti. Chimie*, 11 (2002) 197

121. J. K. Nag, D. Das, B. B. De, C. Sinha, *J. Indian Chem. Soc*., 75 (1998) 496

122. K. Arora, D. Kumar, K. Burman, S. Agnihotri, B. Singh, *J. Saudi Chem. Soc*., 15 (2) (2011) 161

123. D. Lin-Vien, *"Hand book of Infrared and Raman Characteristic Frequencies of Organic Molecules"*, Academic Press Limited (1991)

124. M. M. Omar, G. G. Mohamed, A. M. M. Hindy, *J. Therm. Anal. Cal*., 86 (2006) 315

125. N. Mondal, D. K. Dey, S. Mitra, K. M. A. Malik, *Polyhedron*, 19 (2000) 2707

126. J. Kohout, M. Hvastijova, J. Kozisek, J.G. Diaz, M. Valko, L. Jager, I. Svoboda, *Inorg. Chim. Acta*, 287 (1999) 186

127. A. Bury, A. E. Underhill, D. R. Kemp, N. J. O'Shea, J. P. Smith, P. S. Gomm, F. Hallway, *Inorg. Chim. Acta*, 138 (1987) 85

128. N. R. S. Kumar, M. Nethiji, K. C. Patil, *Polyhedron*, 10 (1991) 365

129. N. H. Al-Shaalan, *Molecules*, 16 (2011) 8629

130. G. G. Mohammed, M. M. Omar, A. M. Hindy, *Turk. J. Chem*., 30 (2006) 361

131. Z. F. Dawood, M. W. Ibrahim, *Natl. J. Chem*., 30 (2008) 330